MOLECULAR MEDIATORS OF ALVEOLARIZATION

JENS-CHRISTIAN WOLFF

INAUGURAL DISSERTATION
submitted to the Faculty of Medicine
in partial fulfillment of the requirements
for the PhD-Degree of the Faculties
of Veterinary Medicine and Medicine
of the Justus Liebig University Giessen

édition scientifique
VVB LAUFERSWEILER VERLAG

1. Auflage 2010

1st Edition 2010

Printed in Germany

édition scientifique
VVB LAUFERSWEILER VERLAG

STAUFENBERGRING 15, D-35396 GIESSEN
Tel: 0641-5599888 Fax: 0641-5599890
email: redaktion@doktorverlag.de

www.doktorverlag.de

Molecular Mediators of Alveolarization

INAUGURAL DISSERTATION

submitted to the

Faculty of Medicine

in partial fulfillment of the requirements

for the PhD-Degree

of the Faculties of Veterinary Medicine and Medicine

of the Justus Liebig University Giessen

by

Jens-Christian Wolff

of Erlangen, Germany

Giessen, 2010

From the Department of Internal Medicine, Medical Clinic II
(Director: Prof. Dr. med. Werner Seeger)
of the Faculty of Medicine of the Justus Liebig University Giessen

First Supervisor and Committee Member: Prof. Dr. Werner Seeger
Second Supervisor and Committee Member: Prof. Dr. Johannes C. Schittny (Bern, CH)
Committee Members: Prof. Dr. Wolfgang Kummer
Prof. Dr. Christiane Herden

Date of Doctoral Defense: July 23rd, 2010

I Index

II List of tables and figures

A) Tables:

B) Figures:

III Abbreviations

7-AAD	7-Aminoactinomycin D
A549	human cell line
AEC(s) I / II	alveolar epithelial cell(s) type I / II
AP-1	activator protein-1
bp	base pairs
br.	bronchus / bronchi
BSA	bovine serum albumin
c-Fos	FBJ osteosarcoma oncogene
C57BL/6N	mouse strain
Ccnd1	Cyclin D1
CDH	congenital diaphragmatic hernia
Cst	Cystatin(s)
Cy3 / Cy5	labelling dyes
DIG	digoxigenin
d[N]TP	desoxynucleotide triphosphates of Adenine (dATP), Cytosine (dCTP), Guanine (dGTP) and Thymine (dTTP)
DTT	1,4-Dithiothreitol
E	in mice: embryonic day post fertilization
ECM	extracellular matrix
EDTA	ethylenediaminetetraacetic acid
Egr1	Early growth response 1
FCS	fetal calf serum
FGF	fibroblast growth factor
Fstl1	Follistatin-like 1
HBSS	Hank's Buffered Salt Solution
Hepes	4-(2-hydroxyethyl)-1-piperazineethanesulfonic acid
HIMF	Hypoxia-induced mitogenic factor
Hox	homeobox
Igf	insulin-like growth factor
kD	kiloDalton (weight unit)
LB	Luria Broth (medium)
Lcn2	lipocalin 2
LH	luteinizing hormone
Ly6a	lymphocyte antigen 6 complex, locus A
MAPK	mitogen-activated protein kinase
MHC	Major Histocompatibility Complex
min	minute(s)

MLE-12	mouse cell line
MTS	3-(4,5-dimethylthiazol-2-yl)-5-(3-carboxymethoxyphenyl)-2-(4-sulfophenyl)-2H-tetrazolium
NTM	buffer consisting of NaCl, Tris and $MgCl_2$ (s.b.)
P	in mice: postnatal day (day of birth = P0)
PAI-1	plasminogen activator inhibitor-1
PBS	phosphate-buffered saline
PBT	PBS (s.a.) with 0.1 % Tween 20
PCR	polymerase chain reaction
PFA	paraformaldehyde
RA(R)	retinoic acid (receptor)
Rras2	related RAS viral (r-ras) oncogene homolog 2
s.a. / s.b.	see above / see below
SDS-PAGE	sodium dodecylsulfate polyacrylamide gel electrophoresis
sec	second(s)
Sh[X]	post-sham surgery day X
SMC(s)	smooth muscle cell(s)
SP-[A-D]	surfactant protein [A-D]
SSC	Standard Saline Citrate
Stf	Stefin(s)
S[X]	post-pneumonectomy day X
Tcf21	transcription factor 21
TE	buffer consisting of tris and EDTA (s.a.)
TGF-beta	transforming growth factor beta
TNFα	tumour necrosis factor alpha
TTF-1	thyroid transcription factor 1
UTP(s)	Uridine triphosphate(s)
v/v	volume per volume
VEGF	vascular endothelial growth factor
w/v	weight per volume

Chemical abbreviations:

CO_2	carbon dioxide
HCl	hydrochloric acid (solution)
$MgCl_2$	magnesium chloride
N_2	nitrogen (gas)
NaCl	sodium chloride (solution)
NaOH	sodium hydroxide (solution)
NO	nitric oxide

1 Introduction

Chronic destructive lung diseases, e.g. fibrosis, emphysema and COPD, have become an increasing problem in today's pulmonary medicine. The severe alterations of the lung structure cause a continuously increasing affection of gas-exchange efficiency and an ongoing loss of quality of life. Although the number of patients is increasing, there are still very few therapeutic options for inhibiting or at least decelerating the tissue degradation and reorganization processes. Often the only "cure" is lung transplantation, with all its inherent acute and chronic complications.

Therefore, strategies to overcome pulmonary tissue damage of patients by activation of endogenous regenerative programs would be desirable. The study presented here deals with the search for suitable candidate genes in two different mouse lung growth models, namely compensatory lung growth, which regularly does not exist in humans, and normal postnatal alveolarization.

1.1 Lung functions and structure

As the experiments performed for the work presented here focused on the search for molecular mediators of alveolarization and lung growth, it is necessary to explain lung functions, structure and growth behaviour in detail first to give an overview of the regular situation and to show which elements and growth steps may be affected by disorders or may be targets for therapeutic approaches.

Being situated in the thorax, the main function of the lung is the gas exchange, meaning to supply the organism with adequate amounts of oxygen and to dispose the carbon dioxide originating from metabolic processes. Apart from this, the lung is in direct contact with microorganisms and toxins / pollution from the outer environment which either need to be eliminated - using ciliated cells supplied by coughing - or which have to be inactivated or killed, e.g. by alveolar macrophages.

Using respiratory movements of intercostal and thorax musculature as well as the diaphragm, the lung is alternatingly enlarged and down-scaled by air flowing through mouth, pharynx, trachea and the bronchial system up to the gas-exchanging alveoli and backwards. In humans, the trachea ends up with the primary bronchus and dichotomously divides into two main bronchi (bronchi (br.) principales) which themselves branch into br. lobares each supporting one lung lobe (three on the right side

of the thorax, two on the left). The latter ones again branch into br. segmentales to supply ten lung segments on the right side and nine on the left. After several further divisions and becoming cartilage-lacking bronchioli, the conducting bronchial system ends up with bronchioli terminales, which pass into the transitional zone, firstly represented by bronchioli respiratorii. These structures can be found from about the 17th generation of dichotomous divisions; they contain single alveoli and further branch to generate alveolar ducts with numerous adherent alveoli. The ducts divide into alveolar sacs which finally open up into numerous alveoli. As there are millions of these bubble-like structures, the total gas-exchanging surface of the human lung (ca. 140 m^2) roughly equals the size of a tennis court. In total, about 24 divisions are made from the end of the trachea up to the alveoli.

To enable a gas exchange, blood needs to be transported to the alveoli. For this, branches of Arteria pulmonalis coming from the right ventricle and containing blood with low oxygen and high carbon dioxide concentrations run and divide in parallel with the bronchial system and spread up into fine meshes of capillaries surrounding the alveoli. Gas exchange is performed by diffusion through a thin tissue layer consisting of alveolar epithelial cells type I (AECs I) on the alveolar side, a common basal membrane and endothelial cells on the capillary side. To be pumped into the body, the resulting oxygen-rich blood is collected in branches of the four Venae pulmonales, running to the left atrium via connective tissue and between the lung segments - and not in parallel with arteries and bronchi.

In opposite to humans, mice have four right lobes and only one on the left side, but the branching and vascularization pattern is similar. Further differences imply a comparatively wide central bronchial system facilitating a high breathing frequency and a mainly irregular, i.e. asymmetric, branching behaviour with the major branches being arranged vertically. This aspect helps to additionally function as an internal organ skeleton and fits best to the quadrupedal anatomy of the mouse. Due to the similarities with humans, rodents, which are mammals as well, are proper model animals for numerous scientific approaches. Because of that, mice, which additionally provide many genetically engineered strains for further studies, were chosen for the experiments performed in the study presented here.

1.2 Regular lung development

Descriptions given here refer to human lung development; corresponding time points and events from mice - where nearly identical procedures happen significantly quicker - are given in parentheses. **The different stages appear with some physiologic overlap.**

Prenatal development:

a) Organogenesis / embryonic period: On gestational day 26 (mouse: embryonic day (E) 8-9), the lung appears as a small, single bud on the ventral part of the foregut. While the bud enlarges and invades into the surrounding mesenchyme, it is separated from the prospective oesophagus by laryngotracheal grooves; only a small, cranial connection to the foregut is maintained, the future larynx entrance. With 4.5 weeks (E9.5), the lung anlage consists of five little saccules, generated by dichotomous divisions: three on the right-hand side and two on the left, respectively (mouse: four / one). With ongoing branching, the future bronchial tree reaches subsegmental levels at the end of week 7 (E10) [1].

b) Fetal period:

Pseudoglandular stage: In gestational weeks 5 to 17 (E10-16), the lung looks like a small, primitive gland. The whole air-conducting part, i.e. the bronchial tree, is generated in this period [2]. In vessel formation, arteries run and divide in parallel with the bronchial system, while veins branch separately. Cuboidal epithelial cells lining the distal airways contain significant amounts of glycogen serving as energy supply for later differentiation steps. Although a little controversy, today's view of the final stage of the pseudoglandular period includes the "birth of the acinus", which is defined as the respiratory unit originating from one bronchiolus terminalis [1, 3].

Canalicular stage: This period lasts from gestational week 16 to 26 (E16-18). The transition from the pseudoglandular appearance is performed by establishing gas-exchanging tissue in the future acini, and the term "canalicular" originates from the "canalization" of future parenchyma by multiple capillaries forming a network in the mesenchyme and approaching bronchial structures. While air spaces enlarge, the glycogen-rich cuboidal epithelial cells either flatten to facilitate a thin air-blood barrier and become AECs I or they differentiate into AECs II. The latter ones begin to form lamellar bodies containing surfactant components and they start to secrete small amounts of surfactant at the end of the canalicular phase - what makes this time point the earliest at which premature babies could survive [1].

Saccular stage: Lasting from 24 weeks up to term (E18 - postnatal day (P) 5), in this period a lot of gas-exchanging tissue is generated. The peripheral air spaces widen to form saccules, and more proximal parts of the acini widen and elongate. The number of distal branching generations significantly increases. Due to these processes, the volume of interstitial tissue is extremely reduced, and two layers of a capillary network are situated directly next to each other between the air spaces [1].

Alveolar stage: This period begins in the 36th week of human pregnancy; only about 15 % of all alveoli have been generated at birth. In mice, the whole process is postnatal. Due to these facts, the alveolar stage is summarized in the postnatal time.

Postnatal development:

a) Alveolar stage: Beginning in the 36th week of pregnancy, this period lasts at least up to 18 month of age, but estimations go up to even 20 years. Similarly, the calculated number of alveoli at delivery is extremely variable [3, 4]. In mice, the alveolar stage ranges from birth up to about 4 weeks.

For primary alveolarization, small ridges appear along the saccular walls. They divide the sacculi into smaller units to generate alveolar ducts and sacs as well as primary alveoli. The latter ones are immature, indicated by a double capillary layer. Within the following secondary alveolarization, additional septae fold up from the walls of primary alveoli. By this process (and microvascular maturation, see below), supported by apoptosis of interstitial cells, mature alveoli with only one capillary layer and thin air-blood barriers are generated [5]. In the origin (and later the tips) of secondary septae, Elastin fibres play an important role in guidance and elongation [1].

b) Microvascular maturation: In addition to the extreme reduction of connective tissue, the capillary network needs to be changed from its double to a single layer to ensure an optimal gas exchange. For this purpose, two principles seem to interact: Capillaries fuse, involving apoptosis of dispensable cells, and merged / “mature” areas display a preferential growth, suppressing immature structures [1, 5].

c) Adult lung: Having undergone all developmental steps described above, the mature lung is still able to grow without major structural changes; this happens in parallel with the normal growth of the body and leads to following adult dimensions: Assuming an average body weight of 74 ± 4 kg, the lung volume makes up 4,340 ± 285 ml. The alveolar surface area adds up to 143 ± 12 m^2, while the capillary surface covers only 126 ± 12 m^2 [1].

1.3 Modifyers of lung development

As normal lung development is a highly complicated process with many different cell types having to interact in an optimal temporospatial manner, there is obviously a high susceptibility for disturbances. These may result in alterations of structure and function, which may even cause the death of affected individuals. In the following chapters, examples of promoting / interfering molecules and of uncommon situations are given:

1.3.1 Varying concentrations of endogenous molecules

Glucocorticoids inhibit cell divisions in several tissues including the lung [6, 7]. Due to that, these hormones undergo a natural decrease in their concentration in the phase of septation, when a high degree of proliferation is required [8]. Another well-known effect of glucocorticoids is used in clinical practice when babies are (in danger of being) born too early: High hormone levels initiate the end of septation and accelerate the thinning of alveolar walls as well as the transition from the double-layer to the mature capillary system [9]. This results in lungs with a higher degree of maturity and improves the gas-exchange effectiveness of preterm babies. Despite the temporary advantages, glucocorticoid treatments also cause complications in later life as the inhibited septation is not spontaneously reactivated and the comparatively small number of pulmonary arteries generated under therapy tends to cause pulmonary hypertension [6, 10, 11].

Retinoic acid (RA), an active metabolite of vitamin A, is involved in embryonic development and septation. From the clinical point of view, its abilities to “rescue” septation after the application of glucocorticoids and to induce alveolar regeneration are very important [12-15]. Although having these positive effects, RA administration has to be weighed critically as a teratogenic impact of lacking as well as excess RA is known [16]. RA has an influence on the formation of alveoli by determining the distance between septae and inducing “eruptions” of primary to generate secondary septae. The length of the new septae is regulated by another mechanism (e.g. oxygen tension) as despite RA administration the total surface area of healthy test animals did not significantly change before adding hypoxic conditions [17, 18]. RA-specific effects are mediated via retinoic acid receptors (RARs): A knock-out of RAR-β, which is usually down-regulated within septation due to its exceptionally inhibitory effect, causes a preliminary, quick septation, while a constitutive expression and agonists lead to immature distal lung structures and collapsed air spaces at birth [19].

Thyroid hormones are also known to have an influence on septation, as studies proved that the concentrations of these mediators and of their receptors significantly increase before the onset of this event [20, 21]. In newborn rats not only DNA synthesis was shown to be elevated, but triiodthyronine (T_3) also accelerated the speed of septation. This resulted in more and smaller alveoli comprising a higher total gas-exchanging surface area without affecting the total lung volume [22].

TTF-1 (thyroid transcription factor 1, also known as Nkx2.1) is a growth factor downstream of the thyroid hormones. Apart from the thyroid gland and the foetal brain, it is expressed in AECs II of adult animals as well as in cells with epithelial characteristics during lung development. Its first appearance in the "respiratory tract" was detected even in the lung bud (→ **1.2**) [23]. TTF-1 is of highest importance for surfactant synthesis as it binds to and activates the promoters of SP (surfactant protein) -A, SP-B and SP-C. Knocking out the TTF-1 gene caused a non-viable phenotype of lungs with a rudimentary bronchial tree and lacking parenchyma [24].

The **TGF-beta (transforming growth factor beta) family** consists of at least 24 different cytokines, which can be modulated by RA (see above). These molecules are involved in cellular proliferation, differentiation, recognition and death; they influence extracellular matrix synthesis and epithelial cell growth and suppress the immune system [25, 26]. As a combined TGF-beta 1, 2 and 3-specific (overexpression) effect, Bragg et al. found an accumulation of alpha-smooth muscle actin as well as inhibited branching, cell proliferation and SP-C expression [27]. On the other hand, the important role of TGF-beta 3 on its own became obvious with knockout mice showing alveolar hypoplasia, lacking septation, thickened mesenchyme and not enough AECs II [28].

The **Hox (Homeobox) genes** are an RA-sensitive family of transcription factors containing a helix-turn-helix DNA binding-motif. They are arranged in four clusters (Hox a-d) on different chromosomes and they can be regarded as master regulators of developmental processes as they steer the positioning of organs [29]. In a 3' → 5' direction, the Hox genes of each cluster are sequentially arranged according to stimulatory sensitivity (decreasing RA gradients necessary for activation), localization of being operative (from rostral to caudal) and time point of activation during development (from early to later) [30]. The importance of the Hox genes becomes evident when studying for example Hox a-5 knockout mice, which die soon after birth due to lung defects [31].

Surfactant proteins [SP-(A-D)]: These molecules are of extreme importance for growth and proper function of the lung. Surfactant consists of about 90 % phospholipids and 10 % proteins; the latter ones can functionally be divided in two groups: While SP-A and SP-D are hydrophilic and play a role in defending the body from microbial intruders and in keeping the alveolar maintenance, SP-B and SP-C are hydrophobic and essential for keeping the surface tension on low levels [32]. When an individual faces disturbances in the normal surfactant composition, this often causes life-threatening conditions: SP-A knockouts live well under normal circumstances, but have severe problems in defending themselves from microbial attacks [33]. Even worse are SP-D knockouts: They have less SP-A and SP-C and a slower phosphatidyl choline metabolism causing alveolar proteinosis, dilated distal airways and higher levels of oxidants and phospholipids [34, 35]. SP-B-lacking mice showed the worst experimental outcome as they died at birth due to lacking surface tension reduction, and SP-C knockouts presented with severe interstitial lung diseases [36, 37].

1.3.2 Extrapulmonary and environmental influences

Congenital diaphragmatic hernia (CDH):

A severe abnormality causing disturbances without originating from the lung itself is the CDH, a condition in which, due to a (mostly left-sided) hole in the diaphragm, parts of abdominal organs move up into the thorax and prevent the respiratory tract from regular development. The resulting **hypoplastic lung** features a reduced number of airway branches, cardial and vascular abnormalities including less vascular generations, extremely muscularized pulmonary vessels (possible long-term effect even under therapy: pulmonary hypertension due to vasoconstriction) and surfactant deficiency [38, 39]. These conditions can cause a severe respiratory failure within hours after birth.

CDH is found in 1 of about 2,500 births with a mortality of up to 35 % of the live-borns [40, 41]. According to the aetiology, different concepts have been raised: A higher susceptibility of selected pregnant women to environmental toxins was considered as well as disturbances in RA metabolism - or simply lacking RA [42-44]. Additionally, genetic reasons were suggested, e.g. aneuploidies, structural abnormalities of chromosomes or mutations of the transcription factor Nr2f2 (nuclear receptor subfamily 2, group F, member 2), which plays a role in RA signalling [45, 46]. As long as a CDH is detected prenatally, a fetal tracheal occlusion therapy with a balloon plugging the trachea to increase the intrapulmonary pressure is helpful in some cases (→ **1.4.3**) [47].

Postnatally, the babies often need immediate intubation and ventilatory support using e.g. high frequency oscillatory ventilation; surgical interventions often become necessary very soon [48]. As more than 85 % of the affected patients are also facing (mostly pulmonary) problems in later life, one main therapeutic target is the reduction of the typical pulmonary hypertension, e.g. by inhaled NO (reduces intracellular Ca^{2+}), PDE-5 (phosphodiesterase 5) inhibitors like Sildenafil or endothelin inhibitors like Bosentan [49, 50]. Due to its importance, there is a well-established mouse model of CDH as well. The unborn animals develop the defect after administration of nitrofen, an environmental toxicant formerly used as herbicide, to the pregnant mouse [51].

Inappropriate oxygen tension:

Alveolarization processes are influenced by the amount of oxygen being present in breathing air. Excess concentrations (**hyperoxia**) as well as lacking oxygen (**hypoxia**) both cause fundamental changes in the outcome of lung formation:

For **hyperoxia**, a diminished septation could be shown by several groups; this was accompanied by less gas-exchanging surface and slower growth of the body [52-54]. In experiments, regularly using ≥ 95 % oxygen, it could not be clearly figured out whether the observed effects were due to an intentionally diminished / not enlarged surface area (because of an effective oxygenation even with few alveoli), or whether a toxic effect of oxygen itself destroyed parts of the tissue [55, 56].

From the clinical point of view, the lung initially copes with excess oxygen by generating reactive oxygen species (first three days of treatment), followed by an accumulation of inflammatory cells releasing inflammatory mediators. The subsequent affection of capillary endothelial cells causes an increased capillary permeability resulting in pericapillary oedema, which aggravates the situation as the diffusion distance for gas exchange is enlarged. In addition to that, it has been observed that AECs I are lost due to persisting hyperoxia and AECs II show a hyperplasia trying to replace the missing cells [57-59]. Becoming a chronic affection, also fibroblasts proliferate, and with an increased collagen deposition a fibrosis is generated. This condition can finally cause secondary pulmonary hypertension [59, 60].

A common medical indication for usage of high oxygen concentrations is the artificial ventilation of very preterm babies. As a main reason for the oxygen-induced damage seems to be an immature endogenous antioxidant defence, therapies using external antioxidants (e.g. superoxide dismutases) in addition to glucocorticoid, nitric oxide and surfactant administration, are helpful [61-63].

In opposite to hyperoxia, the effects of **hypoxia** / diminished oxygen tensions are relatively common, e.g. in case of people living in high altitudes. These individuals were found to have larger alveoli and a dysanaptic lung growth, i.e. a relative excess of gas-exchanging tissue compared to conducting airways [64]. Oxygen tension was found to be of highest relevance for the amount and shape of alveoli, but only in animals with postnatal septation: Sheep lungs, undergoing intrauterine septation, were not affected by high altitude conditions [65]. In opposite to that, rat lungs, performing postnatal alveolarization, had fewer and larger alveoli, as long as hypoxia was present in the critical first two postnatal weeks. In case of a hypoxia exposition beginning after this period, size and total surface area of alveoli were larger, but their number was not statistically changed [17, 66]. According to Massaro, these data suggest a hypoxia-depressible component of septation [67]. Although the need for oxygen can be regarded as the most important regulator of the surface area, early hypoxia seems to decrease the basal organismal oxygen uptake, which generally is in relatively strict linear relationship with the body mass of mammals [18]. This may happen, because the mechanism of hypoxia-driven increase in ventilation does not yet work in the early postnatal phase; apart from this, hypometabolism, resulting in a lower body temperature, is a good way to cope with (temporal) hypoxia [68, 69]. Hypoxia-exposed animals have a smaller body weight, lowering the need of oxygen uptake and by this the required alveolar surface area. To overcome the hypoxia-driven structural deficiencies, individuals develop adaptation mechanisms; good examples are guinea pigs grown up in high altitudes and presenting a smaller mean thickness of alveolar walls as well as human “highlanders” also showing an improved diffusion capacity [70, 71].

1.4 Experimental modifications of lung growth

As obviously no human alveolarization samples could be used for the study, animal experiments had to be performed. Due to many advantages including manageability, knowledge about the genome and ease of designing / available number of genetically engineered animals, mice were chosen. In order to search for genes possibly regulating alveoli formation, newborn animals were the first choice, but for a good comparison and to reduce the number of candidates by studying especially overlapping genes, at least one additional model had to be included. In the following chapters, some ways to either inhibit or to (re-) initiate lung growth are presented:

1.4.1 Glucocorticoid treatment

Glucocorticoids have a well-known inhibitory effect onto septation (→ **1.3.1**). Due to their maturity-promoting influence, these hormones are administered to very preterm babies in order to enable / ease an extra-uterine life (→ **1.3.1**). In principle, it would have been interesting to see the differences in gene expression due to glucocorticoid administration as well as after discontinuation of the therapy at defined time points during and / or after regular septation as these processes can be assumed to happen also in numerous human individuals. On the other hand, glucocorticoids have many side effects according to several organs as well as the immune system, and not all changes observed in the lung are completely opposite of what naturally happens, e.g. the initiation of maturation in later stages of alveolarization. These facts make the detected effects difficult to judge and may cause unexpected interactions / pseudo-regulations not (only) originating from the lung. This led to the decision to not preferably study glucocorticoid-treated mice at first - but future comparisons with results from more "physiological" models may help to further curtail the list of candidate genes. Additionally, Clerch et al. have published a microarray study about dexamethasone and RA-treated neonatal mice which, although only one time point for measurement was monitored, can be used as a reference for initial comparisons [72].

1.4.2 Calorie restriction and refeeding

Assuming that not only the mammalian liver, but also other organs including the lung have regenerative abilities, the group around D. Massaro performed calorie restriction and refeeding studies with mice [73]. Their idea was based on the knowledge that a) in adult mammals there is always a linear relationship between body mass and oxygen uptake / gas-exchanging surface area and b) oxygen uptake is diminished under calorie restriction what in consequence lowers the need for alveolar surface area [18, 74]. Additionally, the lung proteolysis rate was found to be doubled when food is lacking to provide substrates for gluconeogenesis and metabolism, while refeeding of starving mice leads to an increased oxygen uptake which can be met only with more gas-exchanging surface [74, 75].

In their experiments, Massaro et al. fed mice with only one third of the chow they regularly consumed and found the animals to lose about 40 % of their body weight within 15 days, while there was no significant difference in lung volume [73]. Refed mice (3 weeks of ad libitum food after the restriction period) did not show any

significant difference in body mass or lung volume compared to control animals having been fed without any limitations. Measurements in lung sections proved that the alveolar number and the gas-exchanging surface area of calorie-restricted animals was significantly lower than in all control and refed groups, while the average volume of single alveoli increased [73]. Measurements showing less lung DNA after 3 days of restriction and a return to normal levels after 3 days of subsequent ad libitum-refeeding indicated varying cell numbers to be responsible for the findings. This was underlined by increasing amounts of fragmented DNA and by far more apoptotic cells in starving as well as extremely increased numbers of proliferating cells in refed mice [73].

By this study, Massaro et al. have proven a regenerative potential of lung tissue in adult mice. Their results were extended and deepened by two further, microarray-based studies concentrating on the regulation of gene expression in different functional groups including e.g. apoptosis, proteolysis, cell replication, angiogenesis, cell motion and extracellular matrix composition [76, 77]. As these data are nicely in line with the aims of the study presented here, they are discussed later in connection with own results (→ **4.2.1**).

Although the calorie restriction and refeeding model nicely shows an interesting type of "untypical" lung growth, it was not the first choice for a comparison with the gene expression in regular alveolarization of newborn mice. One reason for subordinating this model was, as before with the glucocorticoid treatment (→ **1.4.1**), the starvation-based affection of the whole body and its potentially falsifying influences on lung gene expression. Another complicating aspect would have been how to define when exactly calorie restriction starts or ends, as regulations on RNA level not immediately change and in the beginning of starvation / refeeding numerous overlaps could be expected. Due to these points, the effects to be seen might (still) have been covered. On the other hand, waiting for too long would have possibly skipped important early regulators.

In summary: Due to non-excludable interactions with the whole body and because of expectable overlaps between growth-promoting and -inhibiting factors at the onset and the end of the restriction phase, this model was not chosen for the first studies.

1.4.3 Tracheal occlusion

Congenital diaphragmatic hernia (CDH) is a major cause of hypoplastic lungs as abdominal organs move into the thorax and prevent the lung tissue from regular growth (→ **1.3.2**). Due to the importance of this developmental disturbance, numerous attempts have been made to improve the outcome of affected babies (→ **1.3.2**) [40, 41]. A potential intrauterine therapeutic approach is the tracheal occlusion procedure established in a sheep model. This intervention is based on two observations, namely a) a physiological fluid production of foetal lungs up to some days before birth (about 4.5 ml/kg/h) and b) the finding of hyperplastic lungs in animals with laryngeal / tracheal atresia [78-81]. The idea of the model is to use an inflatable balloon (or simply a ligation) to simulate a tracheal atresia and to keep the fluid from leaving the lung [82]. By this, the intrapulmonary pressure is raised, preventing the abdominal organs from intruding into the thorax and compressing the developing lung. Studies proved the effectiveness of the treatment even in animals without CDH, as lungs significantly grew according to size, alveolar number, gas-exchanging surface, DNA and protein content etc. [82]. A major side-effect of the treatment is a loss in AEC II density (especially in case of early occlusion application) resulting in a severe surfactant deficit [83, 84]. Although these problems could mostly be overcome by applying only a temporal occlusion, the respiratory function remained critical afterwards [85].

Studying foetal rabbits undergoing tracheal ligation, de Paepe et al. found a 3-day lag-phase after treatment before accelerated distension of airspaces and proliferation became detectable [86]. Indicating preliminary maturity, architectural changes appeared earlier than regularly and numerous AECs II had transformed into AECs I [86].

Up to date, tracheal ligation is possible even in foetal mice. In different studies, it could be shown that internal pressure regulates the branching speed via the FGF10-FGFR2b-Sprouty2 pathway and that tracheal occlusion accelerates epithelial cell proliferation and mesenchymal cell apoptosis [87, 88]. As in sheep, a decrease in maturity (e.g. lacking surfactant) in parallel with the increased proliferative activity was detected [89].

The tracheal occlusion model was not suitable for the intended microarray study as it just represents a change of the regular alveolarization accelerating some processes and inhibiting others, not applicable to adult individuals. As the intervention causes atypical lung structures and a potentially altered functional behaviour, it does not match the needs of a model for regular lung growth being comparable to newborn mice.

1.4.4 Compensatory lung growth

Compensatory lung growth is defined as the re-initiation of lung growth in adult individuals after surgical removal of part of the gas-exchanging tissue; it could be observed in several mammalian species, e.g. mice, rats, dogs and rabbits [90-92]. This phenomenon includes not only an emphysema-like volumetric expansion of the remaining alveolar structures as seen after cancer surgery in humans, but true alveolar growth and neo-alveolarization [93]. Compensatory growth does not mean the generation of an exact copy of the excised lobe(s), but the hyperplastic reconstitution of tissue within the remaining part(s) of the lung [94]. Fehrenbach et al. showed that about 50 % of the removed alveoli are restored, while organ volume and surface area are substituted completely; this implies an additional growth of pre-existing alveoli [93].

Usually, for induction of the process a unilateral pneumonectomy is performed. In case of mice this means the removal of the left part of the lung consisting of only one lobe and making up about 30-35 % of the total tissue (→ **2.1.1**); the compensation takes about three weeks [95].

Although compensatory lung growth globally proceeds in a conserved manner, there are some species-specific exceptions and facts to keep in mind when judging the degree of lung regeneration: In rodents, the process is easily inducible by removal of one or two lobes, and the reaction is quick and generates (at least) most of the removed tissue [95]. Due to a large physiological reserve, comparatively small changes of the volume do not always cause the expected effect in other species: In dogs more than 50 % of the tissue need to be removed for induction of effective compensatory growth [92, 96]. For these and other large mammals the maturity is also very important: In immature dogs with ongoing proliferation the regenerative growth reaction is significantly quicker than in adult animals, and in the latter ones it is generally incomplete [94, 97]. Similar data were obtained for rabbits which change from a predominant alveolar multiplication in the juvenile time to a more pronounced airspace enlargement [91]. Even in humans, compensatory growth up to an age of 15 years was detected, but this finding is controversial as another group found no age-dependent changes in the reaction to lung resection [98, 99].

An increased blood and air flow through the remaining tissue seems to be the main stimulus for regeneration. As soon as an adequate stimulation has been generated, compensatory lung growth is implemented - even under complicating circumstances: Positioning an inflated prosthesis into the thorax of a right-sided pneumonectomized

dog to prevent a mediastinal shift caused a caudal enlargement of the remaining lung, deforming the diaphragm [100].

There are two further interesting phenomenons regarding compensatory lung growth: It is possible to re-initiate this process by removing additional lobes several weeks after the first surgical intervention; in this case, the affected rats tended to show a predominantly hypertrophic growth behaviour combined with pulmonary hypertension, the latter one probably due to the low amount of remaining parenchyma [101]. In another approach, Kaza et al. showed that the growth potential not only depends on the age / maturity of the affected lobe: Transplanting a left lower lung lobe from adult pigs to (left-sided) pneumonectomized immature animals of the same species resulted in a growth reaction of the originally mature tissue. As this effect was observed significantly later than in case of an immediate compensatory growth reaction, different steering mechanisms were assumed [102].

Despite the promising potential of compensatory lung growth, one has to take into account that there are also severe side-effects which could bear a risk for later patient therapy: The susceptibility to lung tumour generation and the speed of tumour growth are significantly increased in the period of tissue regeneration [103]. Additionally, metastases seem to settle down easier in lung tissue of pneumonectomized mice [104, 105].

The compensatory lung growth model has been chosen for further experiments as there are several advantages, which could not (all) be found in the other treatments mentioned before (→ **1.4.1-3**):

- As the lung is by far the most affected organ in this model, influences from generalized effects can be widely excluded.
- Compensatory growth leads to similar structural results as seen in normal alveolarization; there is no extreme interplay of stimulating and inhibiting factors.
- In opposite to a glucocorticoid treatment, the surgical intervention has no physiological counterpart with a basic influence.
- Working with adult mice, the influence of natural growth processes, as seen in the glucocorticoid and the tracheal occlusion model, can be excluded.
- The generation of control / sham animals is relatively easy, and there is no problem in defining starting and end point of the experiment or the severity of treatment.

1.5 The present study: Intentions and technical approaches

Aim of the study presented here was to find genes being involved in lung growth, in particular the process of alveolarization. Knowing these candidates, it might be possible to influence their activity in order to reactivate growth processes. This might help to overcome the necessity of transplantation and increase the quality of life in many cases of chronic lung diseases.

The best way to screen the activity of large numbers of different genes is to perform microarray experiments. Within these, numerous, if not all, known genes of a species can be evaluated in parallel according to their expression / regulation on RNA level (→ **2.2**). The microarray study presented here based on mouse experiments, as a) there are well-established murine lung growth models (→ **1.4**) and b) consecutive studies should be easy to initiate due to a huge available pool of genetically engineered animals as well as good tools for own modifications of gene expression in this species.

To increase the probability of participation in alveolarization, two different models were compared to find the most promising candidates in the intersection: As it represents the regular procedure, it was necessary to firstly study physiological alveolarization in newborn mice - happening unexceptionally postnatally (→ **1.2**). As the intended future treatment mostly aims for mature organs of grown-up humans, a model implying adult mice and omitting extreme influences on the whole body (because of non-excludible interferences) was necessary; due to several reasons, compensatory lung growth was the best choice in this case (→ **1.4.4**).

In both models, two time points each were studied, namely one and three days after birth or surgery, respectively. This was done due to several reasons: a) Genes found in both time points of one model can be expected to have a longer-lasting influence on lung growth with a higher statistical impact. b) Secondary septation as most relevant process in alveolarization is known to begin at P4-5 in mice; this implies that the key genes inducing this process must be active beforehand (at about P3). Results from P1 animals could be used as a comparison representing more general growth processes. c) In compensatory growth, the induction phase can be expected earlier, e.g. one day after surgery (S1); here, S3 served as a control.

As the best way to generate objective data is a direct comparison, dual-colour microarrays with competing hybridization of target and control samples to the same chip were employed (→ **2.2**). In case of newborn mice, adult animals with mature lungs were the best choice for comparison. For the pneumonectomy study, it had to be taken

into account that, even under therapy with antibiotics, influences from an activated immune system could not be excluded. Due to that, sham-operated mice receiving the same overall treatment apart from ligation and resection of the lung tissue served as controls in this case. By pooling samples, a more generalized gene expression profile not depending on falsifying influences of single "outliers" was generated (→ **2.2**).

Performing a genome-wide screening, it could not be excluded to have found some non-regulated candidates just coincidentally - without playing any role in alveolarization; additionally, a difference on RNA level does not automatically cause a change of the associated protein content. Due to these reasons, it was necessary to check the validity of the array data using different approaches: Expression ratios were checked with real-time PCR (→ **2.3**, **3.4.1**), and the amount of expressed proteins was detected using the Western blot technique (→ **2.4**, **3.4.2**).

Subsequently, validated candidates were studied for their localization in growing as well as control lungs to specify the involved parts of the organ; this was done on RNA (in-situ hybridization; → **2.6**, **3.5**) as well as on protein level (immunofluorescence stainings; → **2.9**, **3.6.6**, **3.7.2**). As long as the expression was not only restricted to vessels, but preferentially occurred in bronchi or, even better, the septal area (i.e. tissue involved in the generation of gas-exchanging surfaces), the most promising candidates went on to functional studies.

Within these, effects of overexpression and knockdown of the respective RNA molecules were studied in cell culture experiments to evaluate their influence on cell division, apoptosis induction, migration and adhesion (→ **2.7**+**8**, **3.6**+**7**). Employing different cell types enlarged the result spectrum and helped to judge the importance of the candidate genes regarding their role in alveolarization.

Further studies introducing genetically engineered mice were not part of the work presented here, but consecutively, these animals will be the next step in candidate evaluation.

1.6 Aims of the study

The study presented here intended to identify candidate genes being involved in the regulation of normal and / or compensatory lung growth. This project is a basis for future strategies of regenerative therapeutic approaches in chronic destructive lung diseases.
In detail, following goals were in the centre of interest:

- Establishment of a mouse pneumonectomy model to induce compensatory growth
- Microarray studies of lungs from newborn and pneumonectomized mice at different postnatal and post-surgery time points
- Search for promising candidate genes appearing in one or both approaches
- Validation of array data and quantification of associated proteins
- Localization of target molecules on RNA and protein level
- Functional studies: effects of overexpression or knockdown regarding cell number and behaviour

2 Material and Methods

The origin (manufacturer and city) of important material is given in the text at the position of its first appearance. Everything else, especially consumables, was purchased from varying companies and its origin was not relevant for the experiments.

2.1 Animal surgery

All experiments were performed according to the guidelines of good animal practice of the University of Giessen (Giessen, Germany) and were approved by the local authorities for animal experiments (B2 / K 2237). For expression studies, adult (10 - 12 weeks old) and newborn (P1 or P3) C57BL/6N mice of both genders, purchased from Charles River (Sulzfeld, Germany), were used.

2.1.1 Pneumonectomy

For compensatory lung growth experiments, the left lung lobe of adult mice was removed as described earlier [95]: Animals were anesthetized using 3.5 ml/kg of a 2:1:1 mixture of 0.9 % NaCl (sodium chloride) solution and the anesthetics Ketavet (Ketamin; Pfizer, Karlsruhe, Germany) and Rompun (Xylazine; Bayer, Leverkusen, Germany) as a single intraperitoneal injection. After disinfection and shaving, mice were intubated (21-gauge atraumatic cannula) and ventilated (MiniVent mouse ventilator, Hugo Sachs Elektronik, March-Hugstetten, Germany; 150 x 200 µl/min). Skin, muscle and fat tissue was incised in the left fifth intercostal space. After opening of the pleura, the left lung lobe was lifted out of the thorax. Subsequently, all parts of the left hilus were ligated with 6/0 silk and the lung was resected. After closing of thorax and skin, mechanical ventilation was terminated at the onset of spontaneous breathing. All animals received an intramuscular injection of 1 ml of 0.9 % NaCl as liquid substitution. During the days of recovery, mice were treated with antibiotics (Baytril (Bayer), diluted 1:500 in drinking water) as well as subcutanous analgetics (buprenorphin, twice daily).

For sham-operated mice, the whole treatment was performed identically, but without ligation and resection of the left lobe.

2.1.2 Removal of (residual) lungs

Mice were killed by an overdose of isoflurane gas (Baxter, Unterschleissheim, Germany) and exsanguination via the vena cava inferior. After sacrifice and opening of the skin, the trachea was incised and cannulated. The thoracic cavity was opened by sternotomy, and a second cannula was placed into the pulmonary artery, allowing the removal of residual intrapulmonary blood. Then, the apex of the left ventricle was incised, and the lung was flushed via the pulmonary artery using 20 ml of 0.9 % NaCl solution at a constant pressure of 25 cm H_2O while being inflated with N_2 (nitrogen) gas via the trachea. Afterwards, the organ was removed in total and immediately frozen in liquid nitrogen. In newborn mice, flushing was performed with less NaCl solution using a needle positioned in the right ventricle.

2.2 Generation of array data

A flowchart of how to generate lung gene expression profiles is given in **Figure 1**:

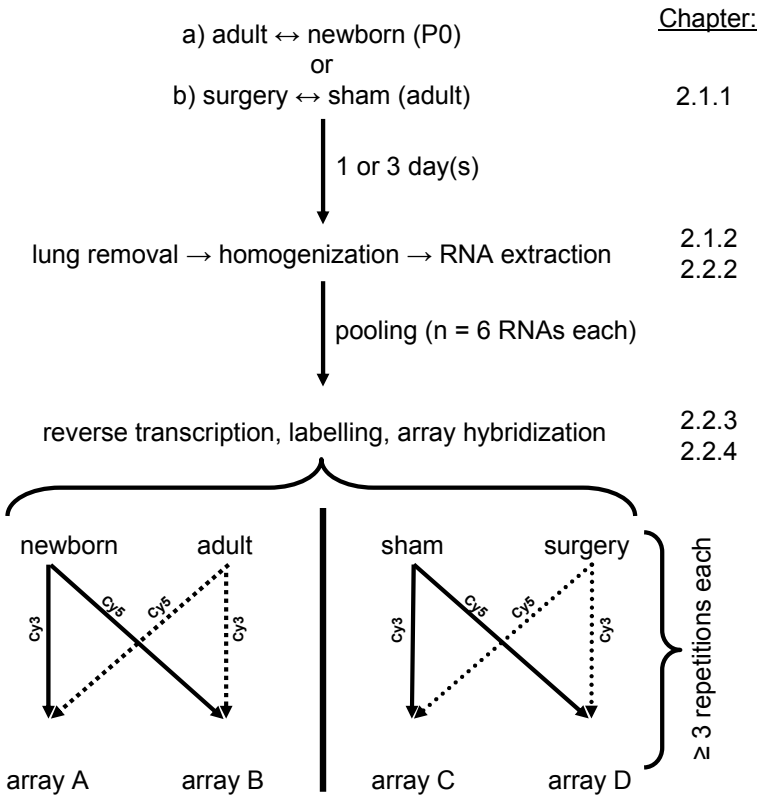

Figure 1: Scheme for mouse lung array experiments.

P0 = day of birth; Cy3 / Cy5 = fluorescent dyes for two-colour labelling; "Chapter" refers to where the mentioned procedures are described in detail.

2.2.1 Experimental design

Profiles of differential gene expression were created by dual colour-hybridizations comparing the data of a) adult versus P1 (**p**ostnatal day 1), b) adult versus P3, c) sham versus S1 (post-pneumonectomy (**s**urgery) day 1), and d) sham versus S3. Each group consisted of 18 individuals. Total RNA from 6 lungs per group was pooled before labelling, resulting in 3 sample pairs per comparison. Each pair was labelled and hybridized in a dye-swap manner (technical replications), resulting in 24 arrays in total.

2.2.2 RNA extraction

To isolate total RNA from whole lungs, 10 µm cryosections of up to 100 mg of tissue were lysed in 1 ml peqGOLD TriFast^{TM} solution (peqLab Biotechnologie GmbH, Erlangen, Germany). After adding 200 µl of chloroform, 15 sec shaking and 5 min incubation at room temperature, samples were centrifuged at 20,000 x g (15 min / 4 °C). The resulting upper phase was transferred into a new tube and mixed 1:1 with ethanol (70 % v/v). For RNA purification, the RNeasy Mini Kit (QIAGEN, Hilden, Germany) was used, following the manufacturer's instructions. Samples were eluted with 34 µl of RNase-free water.

RNA quantity was measured using the NanoDrop ND-1000 system (Fisher Scientific, Schwerte, Germany). Satisfying results were expected to have high nucleic acid concentrations (≥ 2 µg/µl), a good 260/280 ratio (nucleic acids (260 nm) compared to proteins (280 nm) ≥ 1.90) and no phenol contamination at 270 nm. RNA quality was assessed with the Agilent 2100 Bioanalyzer (Agilent, Boeblingen, Germany). Good samples were defined as the appearance of two sharp peaks for 18S and 28S rRNA as well as no (or minimal) RNA degradation and no DNA contaminations (→ **Figure 2A**).

2.2.3 Labelling

Cy-labelled cDNA was generated by reverse transcription of 50 µg of total RNA (pooled from 6 individuals) using the Superscript II reverse transcriptase kit (Invitrogen, Karlsruhe, Germany). Primer annealing was performed with 0.75 µg of oligo-dT primers in a volume of 18.5 µl by heating the samples to 65 °C for 10 min and subsequent chilling on ice. Reverse transcription was performed for 2 h at 39 °C in 40 µl Superscript first strand buffer containing 20 nmol of each dATP, dGTP, dTTP, 8 nmol dCTP and 4 nmol Cy3- or Cy5-labelled dCTP (Perkin Elmer, Waltham,

Massachusetts, USA), respectively, 0.4 µmol DTT (1,4-Dithiothreitol) and 300 U Superscript II enzyme. The reaction was stopped by adding 10 µl 1 M NaOH (sodium hydroxide solution) and heating to 65 °C for 10 min. The mixtures were neutralized with 10 µl 1 M HCl (hydrochlorid acid solution). After addition of 200 µl TE buffer (10 mM Tris, 1 mM EDTA (ethylenediaminetetraacetic acid), pH 8), labelled cDNA was isolated using the PCR purification kit (QIAGEN) according to the manufacturer's instructions, followed by a quality assessment using the NanoDrop instrument (Fisher Scientific; → **Figure 2B**).

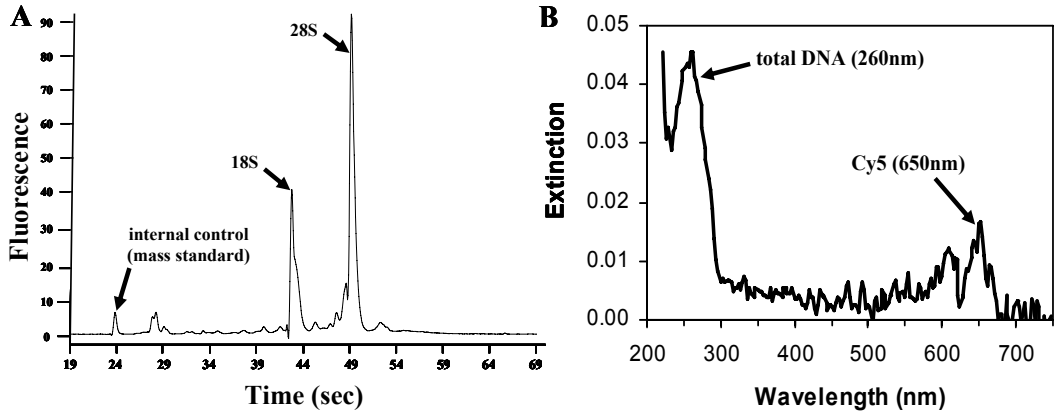

Figure 2: RNA quality assessment (A) and cDNA labelling (B).

(A) RNA sample of good quality: sharp 18 and 28S rRNA peaks (ratio about 1:2), no DNA contamination (broad "peak" right of 28S) or degraded RNA (low rRNA peaks, broad "peak" left of 18S and between 18S and 28S). *Time* = running time of samples through the gel matrix; *fluorescence* parallels RNA concentration. **(B)** Cy5-labelled cDNA sample showing two peaks: total DNA at 260 nm and labelled nucleotides at 650 nm. No peak at 550 nm (Cy3 emission). *Extinction* parallels DNA concentration.

2.2.4 Hybridization, scanning and image analysis

Differently labelled cDNA samples (≥ 20 pmol Cy-dye / sample) were mixed in in-situ hybridization buffer (Agilent Technologies, Waldbronn, Germany) and applied to G4122A microarrays (whole mouse genome 44k arrays spotted with 60mer oligonucleotide probes, Agilent). Hybridization was carried out overnight at 60 °C in rotating hybridization chambers (Agilent). Slides were washed with SSC (standard saline citrate) / Triton-X-102 solutions according to the Agilent protocol. Dried slides were scanned using the GenePix 4100A scanner (Molecular Devices, Ismaning, Germany) at a resolution of 10 µm / pixel. Gains of the photomultipliers were adjusted to utilize the dynamic range and to obtain similar intensity histograms for both wavelengths. Image analysis was perfomed with GenePix Pro 5.0 software.

2.2.5 Statistical analysis

Extracted feature data were analysed in R [106] using the limma package [107] of BioConductor [108]. The spots were weighted for subsequent analyses according to spot intensity, homogeneity and saturation. Spot intensities were corrected for the local background using the method of Edwards [109] with an offset of 64 to stabilize the variance of low-intensity spots. The M/A data were LOESS-normalized [110] before averaging. Genes were ranked for differential expression using a moderated t-statistic [111]. A power of approximately 90 % at a false-discovery rate of 10 % was desired. Microarray data from a similar study (4 arrays with technical dye-swap [= 8 arrays in total], RNA pooled from 6 mice per sample) was available to perform a-priori power tests. The required sample size (i.e. the number of dye-swap array pairs) was estimated based on this data using the method of Ferkinstad et al. [112].

(Image analysis (→ 2.2.4) and statistics were performed by Dr. Jochen Wilhelm.)

2.3 Real-time PCR

In order to validate the on-chip findings, real-time PCR was applied to genes selected from the list of candidates being regulated in at least one time point of both experimental settings (→ **3.3**, **Table 5**) as well as to several Stefins as the most intensively up-regulated genes of the postnatal group. For cDNA synthesis, the GeneAmp RNA PCR kit (Applied Biosystems Applera Deutschland GmbH, Darmstadt, Germany) was used according to the manufacturer's instructions employing random hexamers for the initiation of transcription. Real-time PCR was performed using the 7900HT Fast Real-Time PCR system (Applied Biosystems, Foster City, USA) with porphobilinogen deaminase (PBGD) as reference gene [113]. PCR reactions were set up utilizing the Platinum SYBR Green qPCR SuperMix-UDG (Invitrogen). Differential expression was calculated as $\Delta\Delta C_T$ values [114]. Cycling conditions were: 2 min / 50 °C → 6 min / 95 °C → 45 x [5 sec / 96 °C → 5 sec / 59 °C → 15 sec / 72 °C]. Products were checked by melting curve analysis and agarose gel electrophoresis (primer data → **Table 1**).

Table 1: Real-time PCR primers.

All primer pairs span ≥ 1 long intron. Sequences in 5' → 3' direction, target exons and product lengths (in base pairs) are given.

gene	Accession No.	forward primer	exon	reverse primer	exon	length
c-Fos	NM_010234	gcctttcctactaccattcccc	1	aaagttggcactagagacggacag	2	104
D14Ertd449e	NM_025311	ttccgtgtagccagactctgg	1	gataagggatgctctgaggcc	2	94
Egr1	NM_007913	gagcgaacaaccctatgagca	1	caaccgagtcgtttggctg	2	109
Fstl1	NM_008047	atggcgactctcacctggac	7	caatgagggcgtcaacacag	8	135
Lcn2	NM_008491	tgcggtccagaaaaaaacaga	2	atccagtagcgacagccctg	3	129
PBGD	NM_013551.2	atgtccggtaacggcggc	1	ggtacaaggctttcagcatcgc	3	139
Rras2	NM_025846	gaggcatcggcaaagatcag	4	gttggttctggtgaaggaggg	5	107
StfA1	NM_001001332	gcaaggaagcaactcatcaaga	1	ttgcttcaagctgaggtctgac	2	109
StfA2	M92418	accctgcccagcaatgac	1	ctcttcaagcagtggtctg	2	118
StfA3	NM_025288	cctgcccatcaatgagtcaag	1	tgctcttcaagcagaggtctgac	2	118

2.4 Western blot

Proteins from lung homogenates were denatured in Laemmli buffer (5 min / 95 °C) and separated by SDS-PAGE (sodium dodecylsulfate polyacrylamide gel electrophoresis) using 10 % polyacrylamide gels (stacking gels: 5 %) in a tank blot system (BioRad, Munich, Germany). Blotted membranes were blocked for 2 h with "milk" [PBS (phosphate-buffered saline; 137 mM NaCl / 2.68 mM KCl / 9.23 mM NaH_2PO_4 / 1.76 mM KH_2PO_4) with 5 % skim milk powder and 5 % BSA (bovine serum albumin)]. Primary antibodies (anti (α)-Rras2 / α-c-Fos: Santa Cruz Biotechnology Inc., Santa Cruz, Ca, USA; α-Egr1 / α-Stefin A1: US Biological, Swampscott, Ma, USA) were incubated overnight (in "milk", rotating, 4 °C) and secondary antibodies (with horseradish peroxidase) for 1 h (in "milk", room temperature, shaking). For visualization of bands the Amersham ECL Plus Western Blotting Detection Reagents (GE Healthcare, Munich, Germany) were used. β-actin (antibody: Sigma, Saint Louis, Missouri, USA) served as loading control. Expression ratios were calculated with ImageJ (V1.41a).

For protein extraction from cultured cells, trypsinized cells were centrifuged (100 x g / 10 min), and NP-40 buffer containing 1 % vanadate and 4 % Complete (Roche) was applied to the pellet. After resuspension, followed by 30 min at 4 °C and a second centrifugation (25 min / 20,000 x g), proteins were in the liquid phase which was used for Western blot experiments.

2.5 Cloning

For overexpression of candidate molecules, the whole coding sequences of human (hu) and mouse (m)-specific Egr1 and StfA1 cDNA were amplified in a polymerase chain reaction (PCR; primers and cycling conditions: → **Table 2**), introducing restriction sites for further digestion steps. After gel excision, products were cleaned up with the Min Elute Gel Extraction Kit (QIAGEN) and subcloned into pGEM-Teasy vector (Promega, Mannheim, Germany; overnight ligation at 16 °C). Resulting constructs were introduced into competent bacteria (target cells: E. coli, strain Dh5α) using a 60 sec heat shock at 42 °C for transformation (before and after: cooling on ice). Positive clones were selected by blue-white-screening and amplified in Luria Broth (LB) medium (with ampicillin, 37 °C, overnight). The following day, plasmids were isolated using the Wizard Plus SV Minipreps DNA Purification System (Promega). Sequence validation was achieved with the ABI Prism BigDye Terminator v3.1 Cycle Sequencing Kit (Applied Biosystems).

Table 2: Primers used for cloning.
m = mouse; h = human; FP / RP = forward / reverse primer; capital letters = introduced restriction sites; length = base pairs of total PCR product; polymerase = enzyme used; vector = first target vector.

Gene	Primer	sequence (5´→3`)	length	polymerase / vector
mEgr1	FP	GGATCCatggcagcggccaaggccgagatg	1,614	Taq / pGEMTeasy
	RP	GAATTCttagcaaatttcaattgtcctggg		
hEgr1	FP	actgactgaGAATTCatggccgcggccaaggccgagatgc	1,662	HotStar HiFidelity / pcDNA3.1(+)
	RP	actgactgaCTCGAGttagcaaatttcaattgtcctgggag		
mStfA1	FP	GGATCCatgtacggaggtgtttcagaggccaaacctgccacaccagaaat	303	Taq / pGEMTeasy
	RP	GAATTCttagaagtaggtcagctcatcatccttggttttgtcagtctgg		
hStfA	FP	GGATCCatgatacctggaggcttatctgag	309	Taq / pGEMTeasy
	RP	GAATTCctaaaagcccgtcagctcgtcatc		

Subsequently, vectors were digested using BamHI (target sequence: ggatcc) and EcoRI (gaattc) restriction enzymes (Promega) and ligated with the pcDNA3.1(+) expression vector (Invitrogen), which had been cut in the same way. After another round of transformation, plasmid isolation and sequence validation, plasmids were ready for transfection (→ **2.7.3**). In case of huEgr1, due to problems with the standard procedure, primers were constructed with an overhang of 9 base pairs to enable a direct digestion of PCR products after gel extraction, followed by an immediate ligation with the pcDNA3.1(+) vector, which had been digested identically. Here, instead of a taq polymerase (AmpliTaq Gold, Applied Biosystems) needed for generating “A” (adenine) overhangs in the products essential for ligation with the complementary “T”s (thymines)

in the linearized pGEM-Teasy vector, the HotStar HiFidelity Polymerase Kit (QIAGEN) with proofreading properties was used.
In case of mStfA1, there are numerous differences between the NCBI (NM 001082543.1) and the EMBL reference sequence (M92417). To overcome the inconsistencies in the first 32 nucleotides (containing 8 differences), very long primers were designed to assure a constant, homogenous product according to the PubMed data.
Cycling conditions for all target sequences were: 5 min / 95 °C → 45x [15 sec / 94 °C → 30 sec / 60 °C → 2 min / 72 °C] → 10 min / 72 °C.

2.6 In-situ hybridization

For the localization of mRNAs coding for genes found to be regulated in array experiments (→ **2.2**), in-situ hybridization was performed using paraffin sections. For this issue, specific RNA probes containing sequences complementary to the target molecules were generated and hybridized to the tissue (→ **2.6.1-3**).

2.6.1 Generation of probes

Using mouse lung cDNA, fragments of 350 - 600 base pairs length, spanning at least one long intron (≥ 1,000 bp, if possible) were amplified in a taq polymerase-driven PCR reaction. Products (→ **Table 3**) were excised from agarose gels, cleaned up and ligated to pGEM-Teasy vector (→ **2.5**). After sequence validation, 10 µg of plasmids were cut close to one end of, but outside the insert using restriction enzymes (Fermentas, St. Leon-Rot, Germany; 37 °C / overnight; mostly SalI or SacII, respectively). As for every probe (antisense sequence) a control (sense) was needed, every plasmid was cut on both sides of the insert, but in different reactions. Linearized products were cleaned up using the PCR Purification Kit (QIAGEN). In the following, DNA samples were transcribed into RNA probes using SP6 or T7 RNA polymerase (Promega; 37 °C / 2 h), respectively, beginning with the synthesis close to the 5'-end of the inserts (given binding sequences of the vector) and stopping at the restriction point shortly 3' behind the insert. In this reaction, digoxigenin (DIG)-labelled UTPs (uridine triphosphates), enabling an antibody-driven detection of the probes, were introduced into the products using the DIG RNA Labeling Mix (Roche). Finally, DNA was removed from the samples by DNase digestion (RQ1 RNase-free DNase, Promega), followed by column purification (illustra ProbeQuant G-50 Micro Columns, GE Healthcare, Freiburg, Germany).

Table 3: Data of probes for in-situ hybridization.
For each gene, name and accession number are given. The given probe positions refer to the coding sequence of each gene; length: target PCR products in base pairs.

Gene	Accession No.	Position of probe	length
Egr1	NM_007913	247-827	581
Stefin A1	NM_001082543	29-396	368
c-Fos	NM_010234	257-738	482
Lcn2	NM_008491	276-722	447

2.6.2 Sampling

After opening of the thorax and cannulating the airways, mouse lungs were - in modification from chapter **2.1.2** - flushed with PBS (4 mM $NaH_2PO_4*H_2O$ + 16 mM $Na_2HPO_4*2H_2O$ + 150 mM NaCl, pH = 7.3) via the right ventricle and fixated using 4 % paraformaldehyde (PFA, Carl Roth GmbH, Karlsruhe, Germany; in PBS) via the trachea for 25 min. When removing the organ, PFA was left inside the lungs, and the whole tissue was fixated from in- and outside (4 % PFA / 4 °C / overnight). Afterwards, lungs were dehydrated in a series of ethanol-in-PBS solutions (50 % / 70 % / 80 % / 90 % / 96 % ethanol: 2 h each → 100 % / 2 x 1 h), followed by 100 % butanol overnight. After a night in liquid paraffin (62 °C), the tissue was embedded in paraffin blocks. Finally, samples were cut in 12 µm slices and mounted onto SuperFrost Ultra Plus slides (Thermo Scientific, Schwerte, Germany).

2.6.3 Hybridization

Samples were rehydrated using Roti-Histol (3 x 7 min, Roth) and a series of ethanol-in-PBS dilutions (Roti-Histol / ethanol (1:1) / 2 min → 100 % ethanol / 2 x 2 min → 96 % / 90 % / 70 % / 50 % : 1 min each → PBS / 2 x 1 min). This was followed by a proteinase K digestion (Roth; 15 min, 37 °C, 20 µg/ml in PBS), which was stopped by glycine (Roth; 5 min, 0.2 % in PBS). After washing (PBS, 2 x 5 min), slices were fixated with PFA / 0.1 % glutaraldehyde (Sigma-Aldrich, St. Louis, USA) for 20 min and washed with PBS. Next, samples were preincubated in hybridization mix [70 °C, 2 h; 50 % (v/v) formamide + 25 % SSC (20 x, pH = 4.5) + 20 % H_2O + 1 ‰ Tween 20 (Sigma-Aldrich) with 1 % (w/v) blocking reagent, 5 mM EDTA, 1 mM Chaps, 20 µg / ml Heparin and 1 mg / ml tRNA], followed by an overnight-incubation with preheated probes (1 ng/µl, in hybridization mix; → **2.6.1**) at 70 °C. Then, slides were washed with 2 x SSC (pH = 4.5) and incubated in 2 x SSC / 50 % formamide (2 x 15 min at 65 °C).

For removal of unspecifically bound probes, 3 washing steps (10 min each) using PBT (PBS with 0.1 % (v/v) Tween 20) were performed. This was followed by the usage of blocking solution (1 h / 37 °C; 0.2 % blocking reagent (Roche, Mannheim, Germany) + 10 % goat serum in PBT) and 2 h of blocking solution with anti-DIG antibodies, which were coupled to alkaline phosphatase (37 °C / 1:1,000; Roche). Unbound antibodies were removed by washing with PBT (3 x 5 min), followed by 10 min of NTM (100 mM **N**aCl + 100 mM **T**ris (pH = 9.5) + 50 mM **M**gCl_2). Afterwards, BM Purple substrate solution (Roche) was applied and the samples were incubated overnight. The next day, slices were washed with PBS and mounted with glass cover slides. Target RNA molecules were detectable due to their purple staining.

2.7 Cell culture

2.7.1 Culture conditions

For cell culture experiments, lung epithelial cell lines of human (A549) and mouse origin (MLE-12) as well as primary human fibroblasts and smooth muscle cells (SMSc) and primary mouse alveolar epithelial cells type II (AECs II) were used. Cells were kept at 37 °C in humidified chambers containing 5 % CO_2 (carbon dioxide); media were exchanged according to individual needs (about every 24 to 72 h). In case of A549 cells, RPMI 1640 culture medium (PAA, Pasching, Austria) containing 5 % FCS (fetal calf serum; PAA), 1 % L-glutamine (PAN Biotech GmbH, Aidenbach, Germany) and 1 % penicillin / streptomycin (PAN) was used. Fibroblasts were kept in MCDB 131 medium (PAN) with the same supplements. SMCs received Smooth Muscle Cell Growth Medium II (including the "SupplementMix"; PromoCell, Heidelberg, Germany). MLE-12 cells were cultured in DMEM F-12 medium (PAA) containing 2 % FCS, 10 mM Hepes (4-(2-hydroxyethyl)-1-piperazineethanesulfonic acid, Sigma-Aldrich, St. Louis, MO, USA), 1x insulin (Gibco, Invitrogen GmbH, Karlsruhe, Germany), 2 mM L-glutamine, 1 % penicillin / streptomycin (PAN), 10 nM hydrocortisone (Sigma-Aldrich), and 10 nM estradiol (Sigma-Aldrich). AECs II (isolation procedure → **2.7.2**) were kept in DMEM medium (PAA) containing 10 % FCS and 1 % penicillin / streptomycin (PAN) and L-glutamine (PAN) each. Before transfection, cells were incubated in culture media containing no or very low amounts of FCS (≤ 0.1 %) for up to 48 h. This "starvation" helped to synchronize the cell cycle.

For supernatant experiments, used medium was removed from cultured cells, filtered (MillexGP filters with 0.22 µm pores; Millipore, Schwalbach / Ts., Germany) and re-applied to different cells with no preceding transfection. In opposite to the other experiments, medium was not exchanged here before the readout one to three days after.

2.7.2 Isolation of murine AECs II

The method was adapted from Corti et al. [115]. In brief: After killing of the mice using isoflurane gas (Baxter) and removal of the skin, the diaphragm was opened from intraperitoneally. Then the rip cage was unclosed, the left atrium was incised and the lung was flushed via the right ventricle using sterile HBSS (Hank's Buffered Salt Solution, Gibco) and a 20-gauge needle. In the following, another 20-gauge needle was fixed in the trachea, and the lung was instilled with 1.5 ml dispase (75 U, 37 °C; BD Biosciences, Heidelberg, Germany). To avoid a large-scale contamination due to bronchial cells, 0.5 ml of low-melting agarose (1 % in PBS, Promega) were added on top to cover the bronchi when hardening (2 - 3 min). Then the lung was removed from the thorax, washed with HBSS and incubated in 2 ml (100 U) dispase for 40 min at room temperature. In the following, lungs were put into 60 mm Petri dishes containing 7 ml of DMEM culture medium (→ **2.7.1**) with 10 mM Hepes and 0.01 % DNase solution (Sigma). Tissue was removed from the bronchial tree, minced and incubated for 10 min (room temperature, shaking). The resulting cell suspension was sheared with a pipette, sequentially cleaned up with 100, 40 and 20 µm filters and centrifuged at 100 x g for 8 min (4 °C). The resulting pellet was resuspended in DMEM and incubated with biotinylated anti-CD32 and anti-CD45 antibodies (30 min, 37 °C; 0.65 and 1.5 µg antibodies / 106 cells, respectively). Afterwards, cells were mixed with streptavidin-coated magnetic beads (30 min, shaking), followed by an extraction of cells of the immune system being positive for CD32 or CD45 surface antigens, respectively, using a magnetic separator. Remaining cells were centrifuged (100 x g, 8 min, 4 °C), and the pellet was resuspended in DMEM. Cells were cultured on fibronectin-coated culture dishes (→ **2.7.1**).

2.7.3 Transfection of cultured cells

Plasmids were transfected using Lipofectamine 2000 (Invitrogen) according to the manufacturer's instructions. For transfection of siRNA (Eurogentec, Cologne, Germany), the X-tremeGENE siRNA Transfection Reagent (Roche) was used following

the company's protocol. Lipofectamine and X-tremeGENE were applied in Opti-Mem medium (Invitrogen), and 4 hours after transfection as well as on every following day, supernatant was replaced by fresh medium.

SMCs and fibroblasts were more effectively transfected with the Amaxa Nucleofector II (amaxa biosystems AG, Cologne, Germany) using special nucleofector kits and protocols for primary cells provided by the manufacturer. Culture medium was exchanged beginning 24 h after transfection to assure a good adherence of the cells.

2.8 Functional studies

2.8.1 Proliferation

Cell counts were performed at least in triplicate using either a Neubauer chamber for low or a Casy TT Electronic cell sizer (Innovatis, Bielefeld, Germany) for high cell numbers. For comparison of proliferation data, Student's two-sided t-test was applied. P-values ≤ 0.05 were considered to be significant. In experiments with at least 4 values per group, outliers ≥ 3 standard deviations distant from the mean of the remaining values were excluded to avoid misinterpretations due to handling mistakes etc.

2.8.2 Adhesion assay

Cellstar 96-well tissue culture plates (Greiner Bio-One, Frickenhausen, Germany) were incubated with 50 µl of PBS containing BSA (negative control), collagen (type IV) or fibronectin (2 ng/µl each), respectively, at 4 °C overnight. After 30 min of blocking with 3 % BSA, equal amounts of cells in supplement-free culture medium were applied to the wells. After incubation for 30 - 90 min (37 °C, 5 % CO_2, humidified), the process was stopped when adhesion became visible (unrounding of several cells in ≥ 1 well). Wells were washed three times (with PBS) and fixated with methanol / acetone (1:1, -20 °C, 10 min). After drying, 100 µl of Crystal Violet Solution (Sigma-Aldrich, Munich, Germany) were applied for 30 min. Thorough washing (water) and drying were followed by administration of 100 µl destaining solution (30 % (v/v) methanol, 10 % acetic acid, 60 % aqua dest.) and an immediate quantification using an ELISA reader at 550 nm. Target cells were adhered to the culture plates at least in quadruplicate; as in proliferation studies, extreme outliers were excluded (→ **2.8.1**).

2.8.3 Migration assay

The migratory activity through pores was checked using the BD Falcon™ HTS 24-Multiwell Insert System (5 µm pores, BD Biosciences, Heidelberg, Germany) or ThinCert™ Tissue Culture Inserts for Multiwell Plates (8 µm, Greiner Bio-One), respectively. Cells in supplement-free medium (→ **2.7.1**) were applied to the inserts; medium with supplements (enhancing the migratory stimulus) was given to the wells. Plates were incubated overnight, washed with PBS and fixed / stained with Crystal Violet Solution (15 min). After washing (water) and drying, remaining cells were removed from the inner part of the inserts using a wettish cotton bud; for counting, membranes were excised and fixed on microscope slides.

2.8.4 Detection of apoptosis

To determine the degree of apoptosis, trypsinized cells were labelled with Annexin-V-Fluos (1 : 50, Roche). For exclusion of dead cells, samples were counterstained with 7-AAD (7-Aminoactinomycin D). Data were acquired by flow cytometry.

2.9 Immunofluorescence staining

For immunofluorescence stainings, different kinds of samples were used:

a) To study **paraffin-embedded tissue sections**, the organs were fixated and rehydrated as described for in-situ hybridizations (→ **2.6.2, 2.6.3**; exception: 1 % PFA instead of 4 %). Using 10 µm sections, samples underwent a heat-driven antigen retrieval procedure (8 min / 630 W in preheated EDTA (1 mM, pH 8; applicable for most antibodies) or Tris-HCl solution, respectively (0.1 M, pH 9; for StfA1 stainings)). After 25 min of cooling, samples were encircled using a Dako Pen (Dako, Denmark) to keep the liquids on the sections. Afterward, the common procedure was performed (s.b.).

b) When stainings of PFA-fixated / paraffin-embedded lungs did not provide satisfying results, **cryosections** were studied alternatively, accepting the lower quality of structural preservation. In opposite to a), lungs were instilled with Tissue-Tek O.C.T. Compound (Sakura Finetek, Staufen, Germany) and immediately frozen in base molds (Thermo Scientific) filled with Tissue-Tek as well. For staining, 10 µm cryosections of the organs were air-dried at room temperature and consecutively fixated using methanol /

acetone (1:1 (v/v), -20 °C, 7 min). After drying, the sections were encircled with a Dako Pen and went on to the common procedure (s.b.).

c) For staining of **cultured cells**, BD Falcon CultureSlides (BD Biosciences) were used. After thorough washing with PBS (s.b.), samples were fixated as described in b) and went on to the common procedure after drying.

Common procedure: Sections / cells were washed with PBS (4 mM $NaH_2PO_4*H_2O$ + 16 mM $Na_2HPO_4*2H_2O$ + 150 mM NaCl, pH = 7.3) / 0.1 % (v/v) BSA, followed by blocking (PBS / 3 % BSA, 1 h). Primary (→ **2.4**, **Table 4**) and secondary antibodies (→ **Table 4**; in dark) were applied for 1 h each at room temperature, both followed by 3 washing steps using PBS / 0.1 % BSA. Nuclei were stained with DAPI (AppliChem, Darmstadt, Germany; 1 µmol / ml, 5 min) or To-Pro-3 (1 µM, 20 min; Invitrogen) and fixated with 4 % PFA (10 min, at room temperature). After final washing (PBS / 0.1 % BSA), slides were mounted with Fluorescence Mounting Medium (Dako) and cover glasses (Roth). An incubation at 4 °C (dark / over night) caused the medium to harden before studying the results at a fluorescence or confocal microcope, respectively.

Negative controls were performed with species-fitting IgG samples (isotype controls) instead of the primary antibodies. As many of the required antibodies were only available from rabbits (→ **Table 4**), several double stainings (for cell type characterization plus target antigen detection) were performed comprising the Zenon Rabbit IgG Labelling Kit (Invitrogen). With this tool, one of the rabbit antibodies was preincubated with pre-labelled goat Fab anti-rabbit IgG fragments; the resulting complexes, carrying a fluorescence dye different from that of the secondary antibody, were applied third in line (1 h / room temperature / dark), avoiding pseudo co-localisations.

Table 4: Antibodies used for immunoflurorescence stainings.

Antibodies were diluted in PBS / 0.1 % BSA. Conjugates were applied without secondary antibodies. For double stainings, primary were also used as tertiary and secondary as quarternary antibodies. * final dilution of the labelled primary antibody.

Primary Antibodies: Target Antigens	Host Species	Dilution	Company
Egr1	rabbit	1:100	US Biological
Stefin A1	rabbit	1:100	US Biological
alpha-Smooth Muscle Actin (SMA; Cy3 conjugate)	(mouse)	1:1,000	Sigma
Vimentin (Cy3 conjugate)	(mouse)	1:400	Sigma
proSurfactant Protein C (proSP-C)	rabbit	1:100	Millipore
Cytokeratin	rabbit	1:100	Dako
Ki-67	rat	1:100	Dako
IgG Isotype control	rabbit / rat	1:100	Sigma
Zenon Rabbit IgG Labelling Kit (Alexa 488 or Alexa 555 conjugates)	goat (Fab)	1:100 *	invitrogen / Molecular Probes
Secondary Antibodies			
Alexa Fluor 555 goat anti-rabbit IgG (H+L)	goat	1:1,000	invitrogen
Alexa Fluor 488 goat anti-rabbit IgG (H+L)	goat	1:1,000	invitrogen
Alexa Fluor 555 goat anti-rat IgG (H+L)	goat	1:1,000	invitrogen
Alexa Fluor 488 goat anti-rat IgG (H+L)	goat	1:1,000	invitrogen

3 Results

3.1 Array analysis

Data analysis (→ **2.2.5**) revealed results of satisfying quality for all experimental groups. **Figure 3** summarizes the statistical data and depicts the degree of intersection of the top 50 genes of each time point in both models.

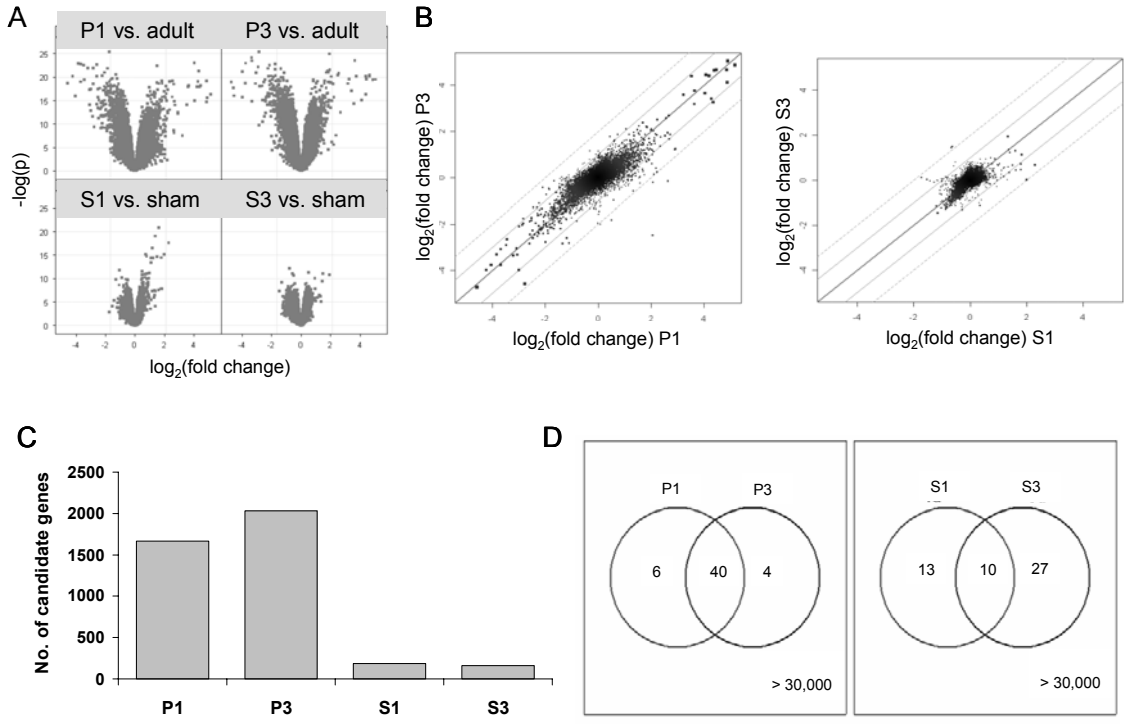

Figure 3: Statistical analysis.

A) Volcano blots depicting regulatory mRNA changes (log_2fold) of all genes tested in all experimental settings [(P1 / P3 and S1 / S3 vs. controls: adult and sham-operated mice] vs. the probability of regulation (-log(p)). 1 spot = mean data of 1 probe on ≥ 6 different arrays. **B)** DE blots (**d**ifferentially **e**xpressed genes) exemplarily comparing the regulation (log_2fold changes) of all genes studied in a) P1 vs. P3 (left panel) and b) S1 vs. S3 mice (right panel). Most obviously changed postnatal candidates (out of the central "cloud") showed very similar regulations at both time points (on or close to the bold line), while post-pneumonectomy genes were regulated more differently. Bold line: perfect correlation; thin and dashed line: ± 1 and 2 log_2fold change units, respectively. **C)** Number of significantly (B ≥ 0) regulated genes in all array series. About tenfold more candidates were found in newborn mice (P1 and P3). **D)** Venn diagrams demonstrating the degree of overlap between the top 50 genes found to be regulated in a) P1and P3 (left panel) and b) S1 and S3 (right panel). Considerably more candidates with multiple appearance were detected in postnatal lung growth, while, in accordance with **B**), post-surgery genes seemed to be regulated for shorter periods, i.e. appeared in only one time point.

By far more significantly regulated genes (with B values ≥0) were found in newborn compared to adult mice (1,669 P1 and 2,032 P3 candidates, respectively) than in the surgery model (S1 = 183, S3 = 161), probably due to the extreme difference in maturity in the former collective. Additionally, 40 of the top 50 most significantly differentially expressed genes were changed in both postnatal time points, while there were only 10 intersection candidates in post-surgery lung growth (→ **Figure 3**).
All candidates found to be changed 1 and 3 days after birth or surgery, respectively, were uniformly up- or down-regulated, none showed a model-intern switch.

Due to the huge amount of data, it was not possible to include the complete array results into this thesis, but a combined list of all study groups is available as an online supplement of the publication in the European Respiratory Journal [116].

3.2 Top-regulated genes of each model

Screening both lung growth models separately first, the most intensively up- and down-regulated genes of postnatal and post-surgery experiments were selected. **Figure 4** gives an overview of the functions of these candidates as defined in PubMed / Entrez Gene (http://www.ncbi.nlm.nih.gov/gene/) and / or GeneOntology (http://www.geneontology.org/). Categorization was performed irrespective of promoting or inhibitory effects of the molecules.
The most striking finding was a unique dominating function or combination of functions in each condition: In newborn mice, predominantly growth / differentiation and translation genes as well as enzymes and their inhibitors were found to be up-regulated (**Figure 4A**), while a large group of genes ascribed to the immune system and defence mechanisms was most intensively down-regulated (**Figure 4B**). Similar to newborn mice, post-pneumonectomy lung growth was characterized by an involvement (i.e. up-regulation) of growth processes and enzymes. Interestingly, there also was a non-negligible amount of more intensively expressed immune response genes in this category, although the sham-operated animals in the control group were presumed to "neutralize" this effect (**Figure 4C**). The genes being down-regulated following surgical intervention were dominated by molecules found in mitochondria, mostly members of the respiratory chain (**Figure 4D**). Several collagen molecules unexceptionally being up-regulated were detected in both models, namely 13 genes in the postnatal and six in the post-surgery group (overlap: 5 candidates; → **3.3**).

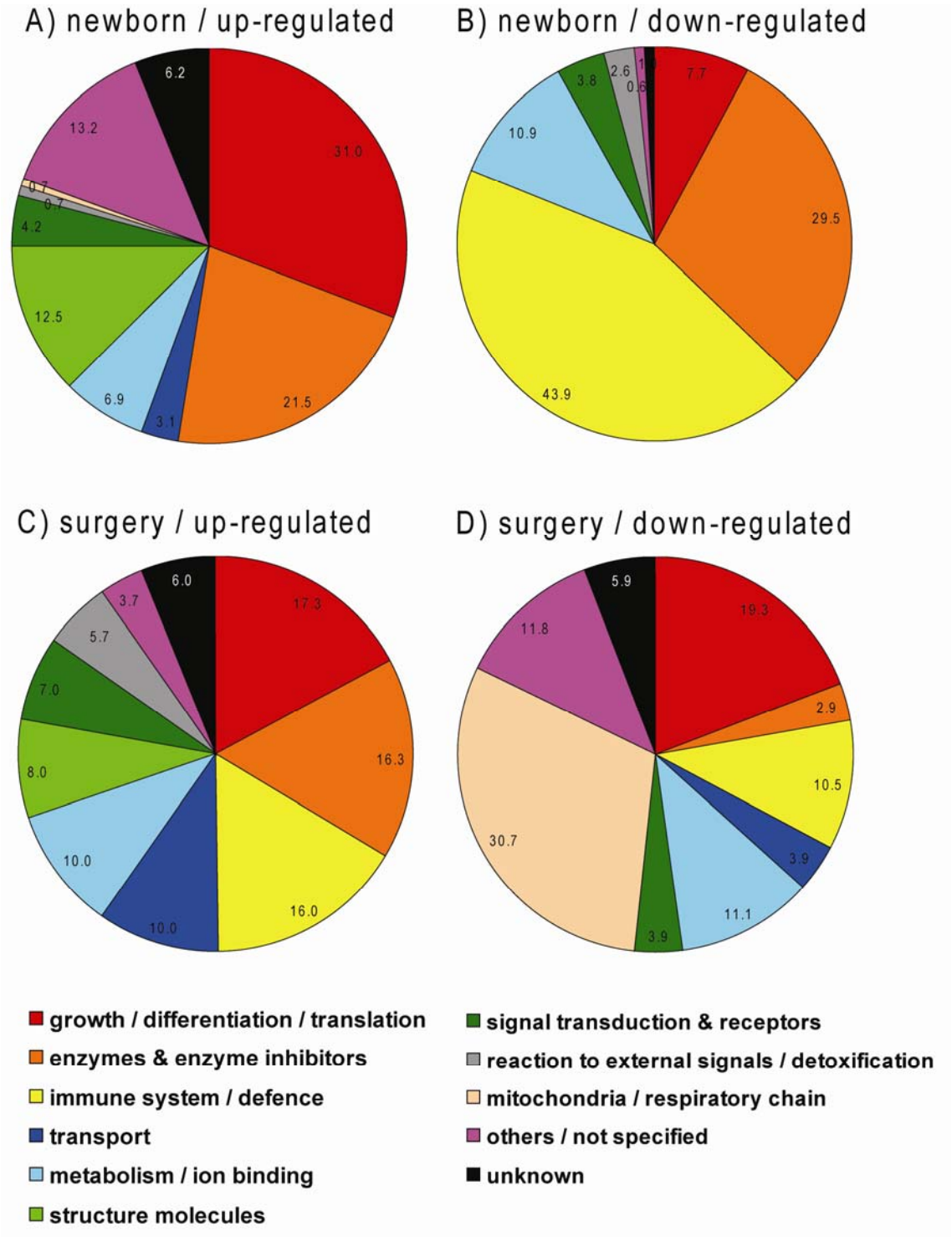

Figure 4: Functions of genes significantly regulated postnatally or after pneumonectomy.

Each pie chart (**A-D**) represents the distribution (inserts: percentage) of global molecular functions found to play a role 1 and / or 3 day(s) after birth (newborn, **A+B**) or surgery (**C+D**) according to PubMed / GeneOntology assignments. The top 50 most intensively up- (**A+C**) and down-regulated genes (**B+D**), independent of whether changed after 1 or 3 days or both, were studied in each case. When more than one function was found, values were proportionally assigned. In every chart, up to 3 functions are emphasized, e.g. growth molecules and enzymes being up-regulated in newborn mice and members of the respiratory chain being less intensively expressed after surgery.

3.3 Intersection: newborn and pneumonectomy mice

In total, 58 genes with significantly altered expression in both experimental settings (in at least one time point each) were found (→ **Table 5:** Genes being regulated in newborn and pneumonectomized mice.**Table 5**). Nineteen of these were mutually up- and 21 down-regulated; the remaining 18 candidates either showed higher levels in newborn and lower amounts in pneumonectomized animals (6) or vice versa (12).

Table 5: Genes being regulated in newborn and pneumonectomized mice.
up / down: direction of regulation; **Acc.-No.:** accession number of the gene; **P1** / **3** = **p**ostnatal day(s) **1** / **3**; **S1** / **3** = post-**s**urgery day(s) **1** / **3**; --- = no significant regulation detectable; **log_2-fold changes**: $2^{(given\ value)}$ = regulation factor; sorting: alphabetical order of gene abbreviations (**Name**) in each group.

newborn / surgery	Acc.-No.	Name	P1 log2-fold change	P3 log2-fold change	S1 log2-fold change	S3 log2-fold change
up / up	BC068175	BC068175	0.72	0.89	---	0.39
	NM_007742	Col1a1	1.52	1.18	0.99	---
	NM_007743	Col1a2	0.91	1.31	0.66	0.82
	NM_031163	Col2a1	1.41	1.53	0.89	---
	NM_009930	Col3a1	---	1.03	0.74	---
	NM_007737	Col5a2	0.98	1.37	---	0.69
	NM_025311	D14Ertd449e	1.00	0.87	0.61	0.66
	NM_007925	Eln	2.77	1.97	0.84	---
	NM_007993	Fbn1	1.75	1.51	0.61	---
	NM_021891	Fignl1	---	0.99	0.66	---
	NM_008047	Fstl1	1.61	2.03	0.53	---
	NM_013602	Mt1	0.57	---	2.04	---
	NM_008630	Mt2	1.08	0.68	2.34	0.93
	NP064182	NP064182	---	1.86	2.19	---
	NM_008987	Ptx3	0.76	0.72	1.03	---
	AK007354	Rbm3	1.85	1.66	0.94	---
	NM_025846	Rras2	0.80	0.91	0.63	---
	BC024606	Saa2	---	0.86	1.39	2.44
	NM_010931	Uhrf1	---	0.92	0.56	---
up / down	NM_009653	Alas2	1.17	0.91	-0.92	-1.22
	NM_009749	Bex2	1.65	1.43	-0.56	---
	NM_009789	Calb3	2.13	---	-1.22	-1.32
	AB015136	Ccl20	---	1.44	-1.69	---
	NM_010174	Fabp3	1.40	---	-0.49	---
	NM_011353	Serf1	1.83	1.52	-0.76	-0.64
down / up	NM_029000	9130002C22Rik	-0.56	-0.69	---	0.58
	NM_009915	Ccr2	-0.84	-0.79	---	0.63
	NM_007913	Egr1	-0.58	---	1.21	---
	NM_028784	F13a	---	-0.45	---	0.68
	NM_010234	c-Fos	---	-0.81	1.07	1.07
	NM_008491	Lcn2	-1.18	---	0.81	0.73
	NM_010809	Mmp3	-2.12	-2.12	0.89	---
	NAP056316-1	NAP056316-1	---	-0.54	---	0.45
	NM_009252	Serpina3n	---	-1.12	1.26	---
	NM_008871	Serpine1	---	-0.74	0.78	---
	NM_011595	Timp3	---	-1.12	0.66	---
	NM_011756	Zfp36	---	-0.60	0.62	---
down / down	BC048560	1700094D03Rik	---	-0.81	-0.74	---
	NM_029803	2310061N23Rik	-1.69	---	---	-1.15
	AK013920	3100002J23Rik	-0.81	-0.94	-0.81	---
	AK020314	9230104L09Rik	-2.18	-2.56	-0.69	---
	NM_177624	A430083B19Rik	---	-1.03	-0.62	---
	AA726875	AA726875	---	-2.18	-0.92	---
	NM_009605	Acdc	-1.32	-1.69	---	-0.84
	NM_007447	Ang1	-1.03	-1.03	-0.54	---
	NM_023617	Aox3	-1.89	-1.84	-0.51	---
	NM_009943	Cox6a2	---	-0.86	---	-0.86
	NM_007812	Cyp2a5	-2.56	-2.94	-0.71	---
	NM_016974	Dbp	-1.15	-1.12	-0.56	---
	NM_023612	Esm1	---	-0.51	-0.51	---
	NM_022023	Gmfb	-0.60	---	---	-0.60
	NM_139269	Hrasls3	-0.81	-0.81	-0.51	---
	NM_010654	Klrd1	-1.22	-1.09	-0.94	---
	NM_010742	Ly6d	-0.74	---	---	-1.12
	NM_013593	Mb	---	-3.06	-1.22	-1.89
	NM_011584	Nr1d2	-1.89	-1.47	-0.45	---
	NM_012050	Omd	-0.79	-1.36	-0.64	---
	NM_011255	Rbp4	---	-0.89	-0.74	---

Checking the functions of the intersection genes (→ **Table 5**) revealed many candidates being involved in growth and differentiation, followed by variable / unknown roles and immunomodulatory tasks (→ **Figure 5**):

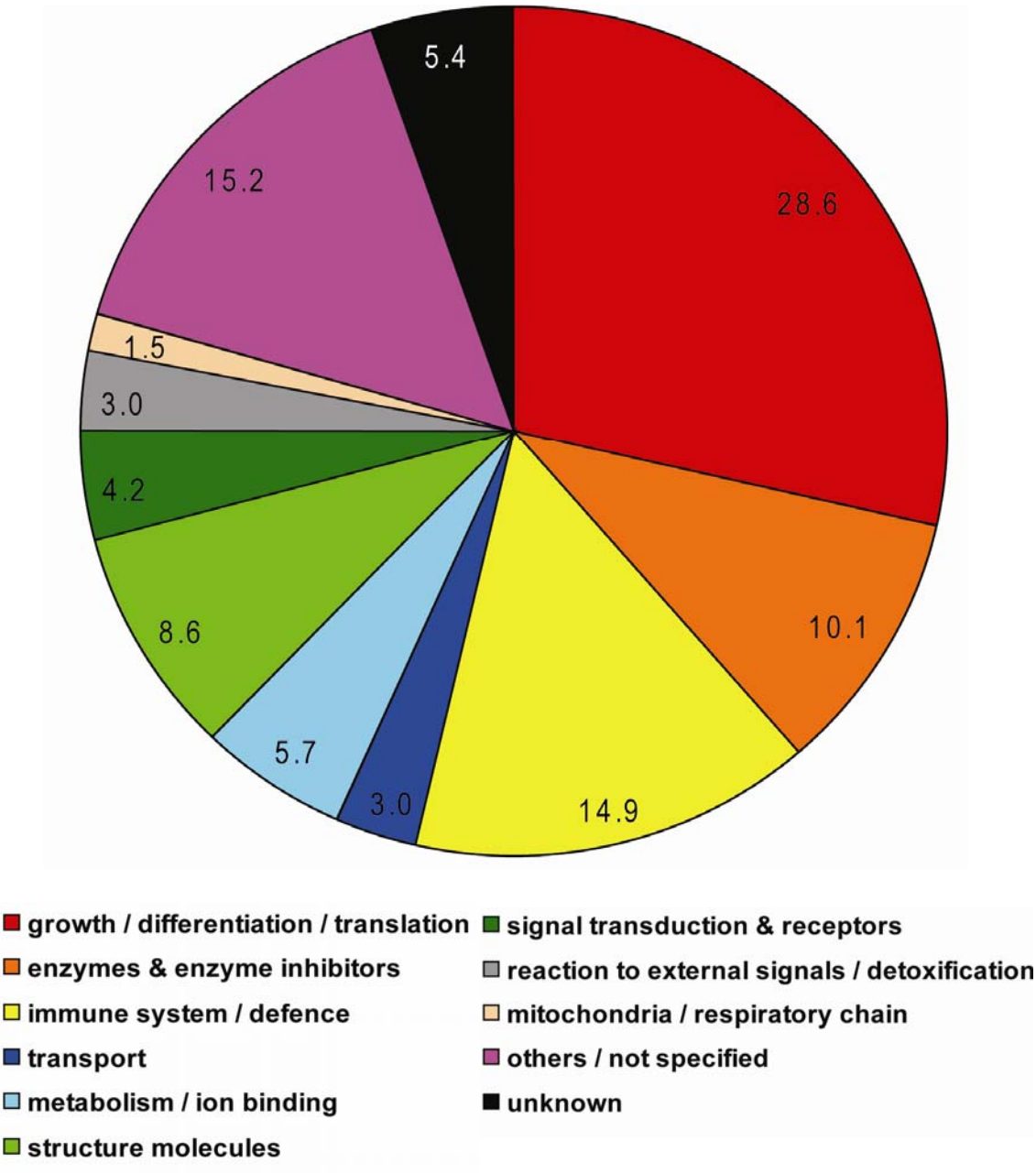

Figure 5: Functions of genes regulated postnatally and post-pneumonectomy.
Distribution (inserts: percentage) of global molecular functions found to play a role in all 58 candidate genes (→ **Table 5**). Functions were assigned according to PubMed / GeneOntology, independent of the direction and the time point of detected changes in array experiments. In case of more than one known function, values were proportionally assigned.

3.4 Validation of array data

3.4.1 Real-time PCR

To check the accuracy of the array data, real-time PCR controls of six candidates from the intersection list of both growth models (→ **Table 5, Figure 5**) were performed. For this, three randomly chosen candidates with consistent post-pneumonectomy and postnatal regulation and three with differing directions were studied (→ **Figure 6**).
In total, all regulatory tendencies found in the array experiments could be reproduced, mostly with good accordance in the regulation factor.

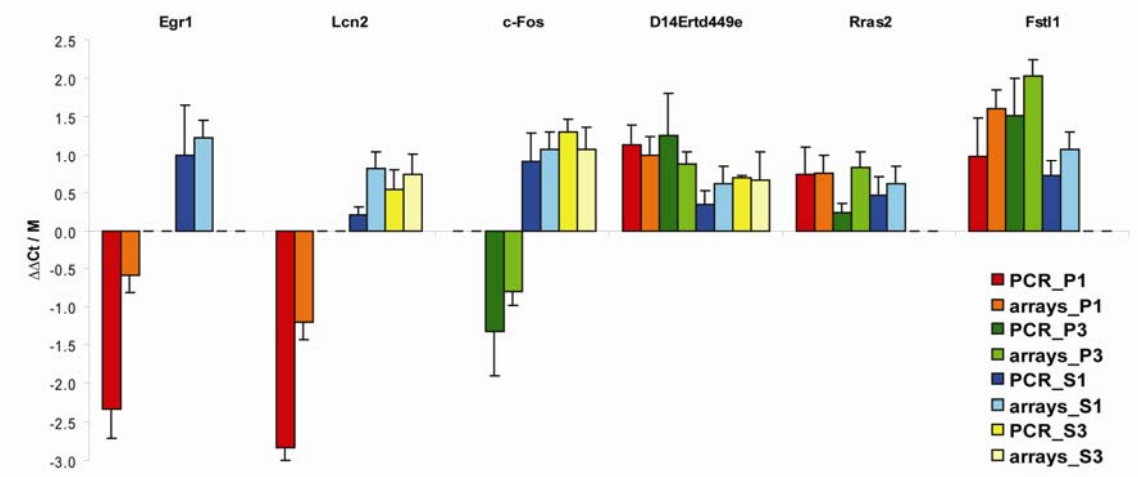

Figure 6: Real-time PCR controls of selected genes.
Bar pairs with similar colours represent the regulation of the same gene in PCR and array studies. PBGD was used as reference gene; missing bar pairs = time point with no significant regulation in array experiments; PCR: ΔΔCt values, array data: M values; $2^{\Delta\Delta Ct} = 2^{M}$ = regulation factor; **P1 / 3** = postnatal days 1 / 3; **S1 / 3** = 1 / 3 days after pneumonectomy; n = 3-4; values ± SEM. All regulatory tendencies of genes with different direction of change (Egr1, Lcn2 and c-Fos) as well as with unique up-regulation (D14Ertd449e, Rras2 and Fstl1) could be validated.

3.4.2 Western blot

As differential regulations on RNA level (→ **Table 5, Figure 6**) not necessarily mean a change of the appropriate protein content, the expression levels of three of the PCR validation molecules, namely Rras2, c-Fos and Egr1, were checked using Western blot (→ **Figure 7**). For all of the target molecules, the same tendency of regulation as found on microarrays (same model, same time points) could be validated.

A

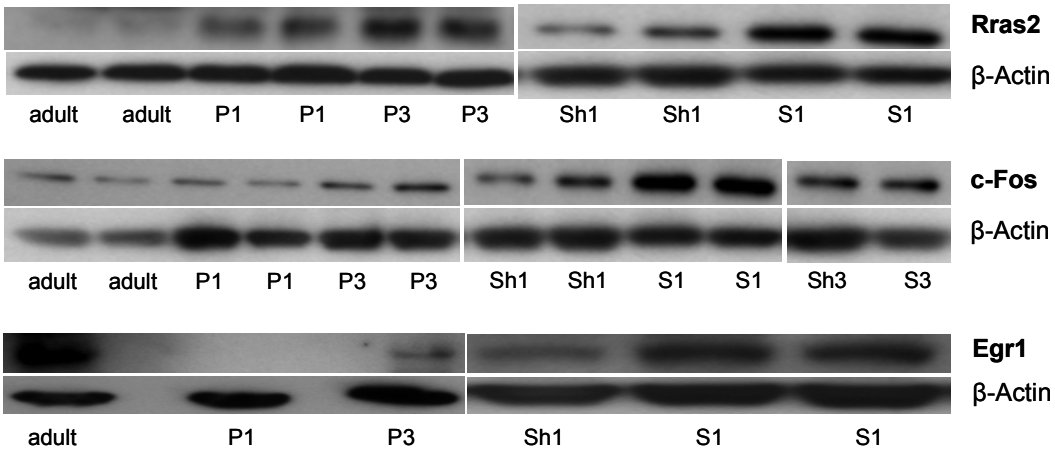

B

	average regulation factors									
regulatory level	**Rras2**			**c-Fos**				**Egr1**		
	P1	**P3**	**S1**	**P1**	**P3**	**S1**	**S3**	**P1**	**P3**	**S1**
mRNA	**1.74**	**1.88**	**1.55**	**---**	**0.57**	**2.10**	**2.10**	**0.67**	**---**	**2.32**
proteins	**13.34**	**17.94**	**2.64**	**[0.52]**	**0.74**	**1.47**	**1.44**	**0.03**	**[0.52]**	**3.74**

Figure 7: Protein expression.

Using Western blot, three selected candidate genes (from PCR validations, → **Figure 6**) were checked for their protein expression: **A)** Rras2, c-Fos and Egr1 blots, each with individual β-Actin expression for normalization. **B)** For a comparison of array and Western blot data, average mRNA and protein regulation factors of Rras2, c-Fos and Egr1 are given. (For calculation of protein values, more bands than shown in A) were utilised.) All regulatory tendencies found on mRNA level could be validated; where significant array data are missing, blot data are given in parentheses. **P1 / 3** = postnatal day(s) 1 / 3; **S1 / 3** = 1 / 3 day(s) after surgery; **Sh1 / 3** = 1 / 3 day(s) after sham.

3.5 Localization of mRNA: in-situ hybridizations

For a proper decision whether candidate genes might be interesting for further investigations (i.e. expression in septal cells during alveolarization), in-situ hybridizations were performed to check the localization of mRNA formation. Two genes with interesting, changing profiles are exemplarily given in **Figure 8**, namely c-Fos and Lcn2, known from PCR validations (→ **3.4.1, Figure 6**). Both mRNAs were expressed in single septal cells in newborn mice and switched to a bronchial expression in adult animals. In the pneumonectomy model, there was an intensive up-regulation of both candidates in single cells of the peripheral lung where the largest changes due to expansion could be expected.

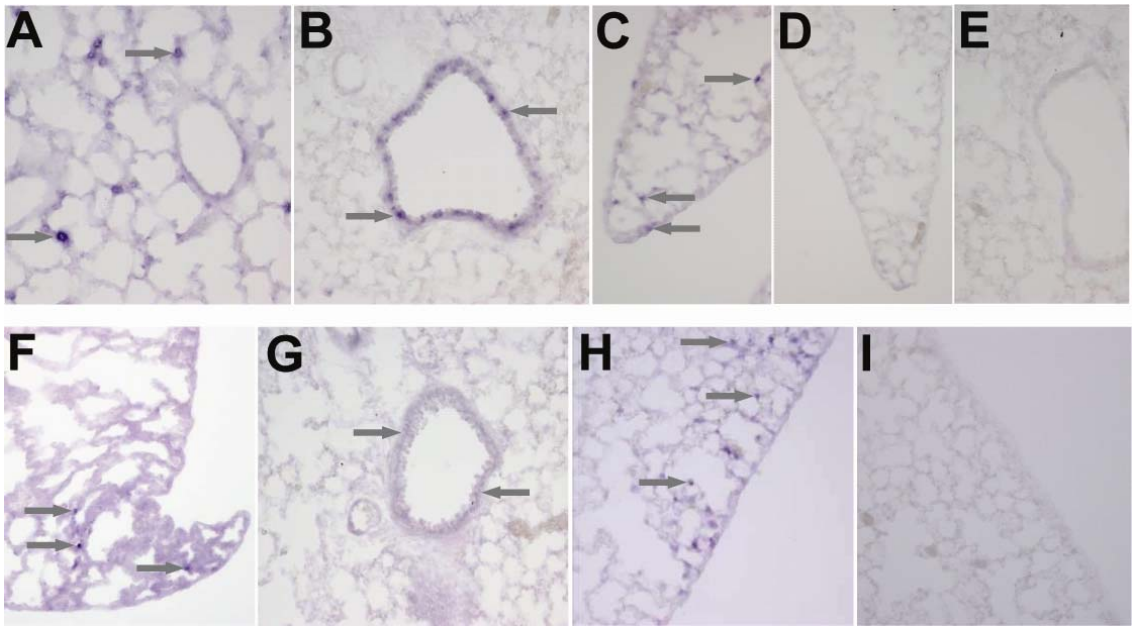

Figure 8: Localization of mRNA.

Using in-situ hybridization, mRNA coding for **c-Fos** was found to be intensively expressed in single septal cells of newborn mice (**A;** here: P3, similar in P1) and mainly in bronchial cells of adult animals (**B**). Post-pneumonectomy mice showed an up-regulation of c-Fos in single cells at the tip of a lobe (**C**; here: S1), which was missing in sham-operated animals (**D**; here: after 1 day). **E**) Control using c-Fos sense instead of antisense probes (S1 lung). In case of **Lcn2**, single, mainly peripheral septal cells expressed the target mRNA in newborn mice (**F**; here: P1), while adult animals produced only small amounts of the molecule in their bronchi (**G**). In compensatory growth, Lcn2 was extremely up-regulated in the peripheral lung (**H**; here: S1), but lacking in the same area of sham mice (**I**; here: after 1 day). Arrows exemplarily indicate peak expressions; magnification: 200 x.

3.6 First candidate gene: Egr1

Having found Egr1 as a growth factor with promoting as well as inhibitory effects to be up-regulated in post-surgery, but down-regulated in newborn mice (→ **Table 5, Figure 6 + Figure 7**) made this molecule an interesting candidate for further investigations.

3.6.1 Proliferation

In cell culture experiments, equal amounts of A549 cells were transfected with either plasmids causing an overexpression of Egr1 (→ **2.5**; control: empty vector) or siRNA knocking down Egr1-specific mRNA (→ **2.7.3**; control: si**R**, different ("**r**andom") order of nucleotides). After 48 or 72 h, respectively, cell numbers were compared (→ **2.8.1**). **Figure 9** depicts the determined anti-proliferative effect of Egr1 overexpression; the opposite result was obtained by the application of siRNA. Similar findings were achieved using MTS (3-(4,5-dimethylthiazol-2-yl)-5-(3-carboxymethoxyphenyl)-2-(4-sulfophenyl)-2H-tetrazolium) assays mirroring the mitochondrial activity of the cells and ^{3}H-Thymidine incorporation representing newly formed DNA (both not shown).

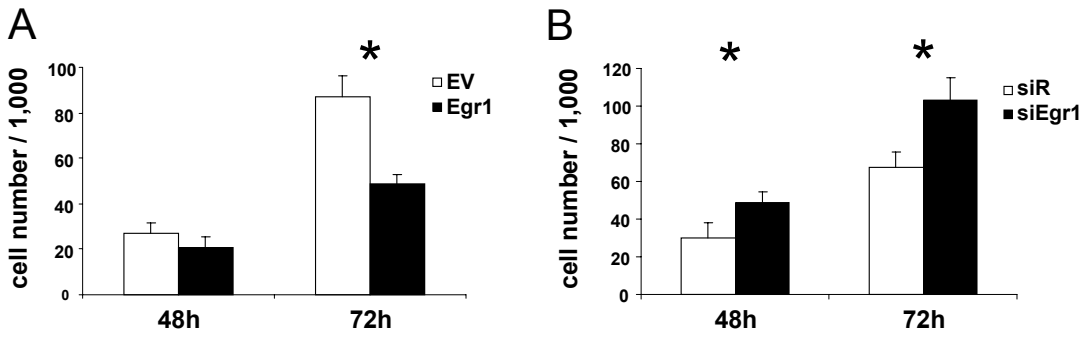

Figure 9: Egr1-dependent proliferation of A549 cells.

Example of a transfection with n = 4 samples / group using 20,000 cells / well at 0 h. Samples were counted twice per well using a Neubauer chamber. An overexpression of Egr1 (**A**; control: empty vector = EV) showed a significant anti-proliferative effect after 72 h. Reducing the amount of Egr1-specific mRNA copies using siRNA (**B**; control: siR, nucleotides in random sequence) had the opposite effect of increasing the speed of cell division; * $p < 0.01$.

To check the specificity of these findings and to evaluate their relevance / potential influence on lung growth, further lung cell types were transfected: In human fibroblasts and mouse AECs II and MLE-12 cells, Egr1 had the same anti-proliferative effect as above, and in fibroblasts, division ratios were increased by siRNA. Only human smooth muscle cells (SMCs) showed an inconsistent behaviour (→ **Figure 10**).

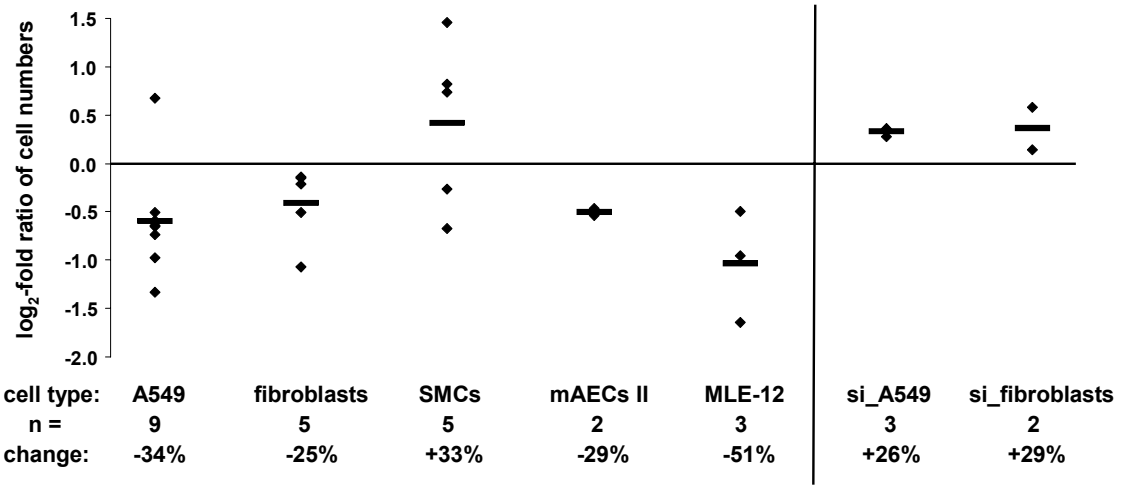

Figure 10: Proliferation of different cell types after Egr1 overexpression or knockdown.
Given cell types were transfected with plasmids or siRNA according to the scheme in **Figure 9**. Egr1 overexpression had an anti-proliferative effect (negative ratios) onto human **A549** cells and **fibroblasts** as well as mouse alveolar type II (**mAECs II**) and **MLE-12** cells. The opposite effect was observed after Egr1 knockdown (**si_A549**, **si_fibroblasts**). Only human smooth muscle cells (**SMCs**) showed an inconsistent reaction. each spot = $\log_2$[mean cell number (treated) / mean cell number (control)] of 1 experiment with 4 treated and 4 untreated samples / group; n = number of experiments in the respective cell type; ─ = mean value; change = mean percental difference of treated cells compared to controls.

3.6.2 Secreted mediators

Technical procedures could not assure to transfect every target cell - and especially not to apply identical amounts of plasmids / siRNA molecules (→ **2.7.3**). But as cell quantifications revealed comparatively constant results (→ **3.6.1**), it was speculated that inconstancies may have been overcome by secreted mediators equilibrating the proliferative programs of neighbouring cells. To test this hypothesis, filtered (i.e. cell-free) supernatants of transfected A549 cells were applied to non-transfected A549 cells and fibroblasts (→ **2.7.1**). After 72 h, cell numbers were compared to those of cells proliferating in control cell supernatants (→ **Figure 11**).

Interestingly, the result matched that one of the original transfection experiment: Supernatant of Egr1-transfected cells had an anti-proliferative effect onto identical (A549) as well as - with limitations - different cells (fibroblasts). The influence of 2nd day-supernatant was more pronounced than that of day 1. This can be regarded as a strong hint for secreted mediators being involved in the anti-proliferative Egr1 effect.

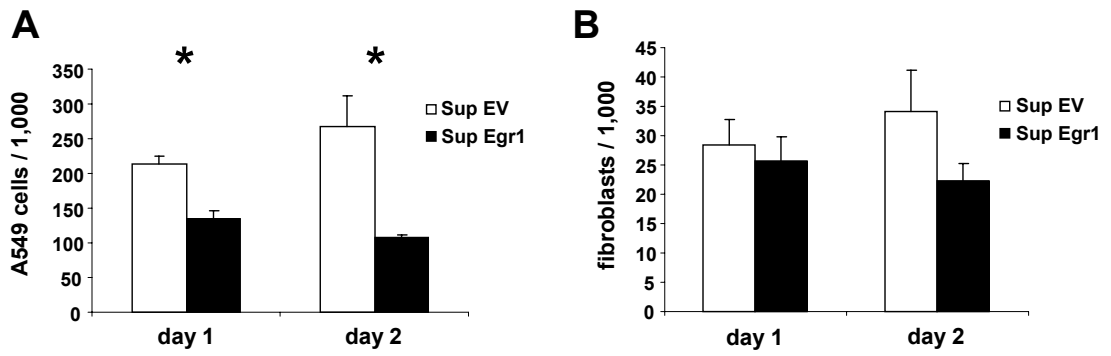

Figure 11: Effect of cell culture supernatants onto proliferation.

Untransfected cells were incubated with supernatant of Egr1-overexpressing (**Sup Egr1**) or control A549 cells (**Sup EV**) for 72 h before quantification. The supernatant was taken from the first (**day 1**) or second 24 h period after transfection (**day 2**). As in the original experiment (→ **Figure 9**), the supernatant of Egr1-transfected cells had an anti-proliferative effect onto identical (A549, **A**) as well as - in tendency - different cells (fibroblasts, **B**; $p_{(day\ 2)} = 0.056$). In consequence, secreted molecules seem to mediate the Egr1-specific effect. * $p < 0.01$; $n = 3 - 4$ samples / group.

3.6.3 Apoptosis

Searching a reason for the lower cell numbers due to Egr1 overexpression (→ **Figure 10**), one possible explanation was an increased apoptosis ratio as Egr1 is also known to promote this type of programmed cell death. In flow cytometry, annexin-V-stained A549 cells showed a higher degree of apoptosis due to Egr1 overexpression than empty vector-transfected control cells (→ **2.8.4**, **Figure 12**).

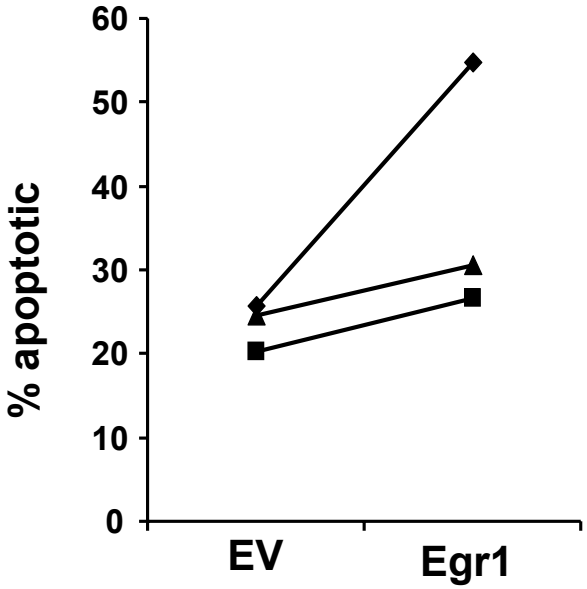

Figure 12: Fraction of apoptotic A549 cells.

Using flow cytometry, A549 cells were checked for the fraction of apoptotic cells 48 h after transfection. In comparison to control cells (transfected with empty vector, "**EV**"), all Egr1-overexpressing samples ("**Egr1**") showed a higher degree of apoptosis in the respective in-parallel experiment (connected symbols).

3.6.4 Migration

Checking the migratory activity, different Egr1-overexpressing cell types migrated through the pores of multiwell plate inserts overnight, attracted by supplement gradients (→ **2.7.1**, **2.8.3**). While there was no obvious difference in the number of migrating cells, i.e. the migratory activity, in SMCs and fibroblasts, A549 cells seemed to show a tendency of increased migration due to Egr1 overexpression (→ **Figure 13A**).

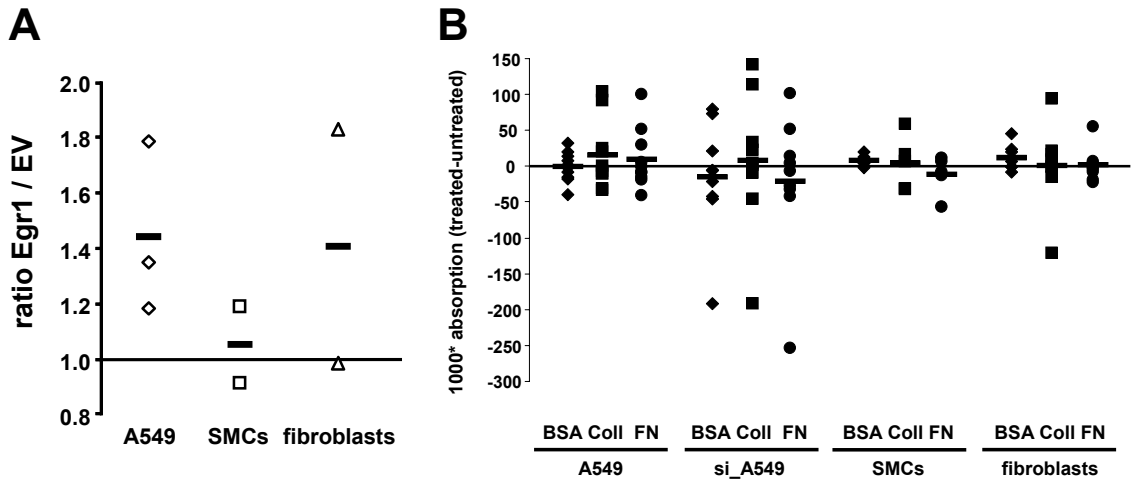

Figure 13: Migratory activity and adhesion.

A) Ratios of cells migrating through 5 µm (**A549**) or 8 µm pores (**SMCs** and **fibroblasts**), respectively, overnight. After 48 h of post-transfection culture, equal numbers of **Egr1**-overexpressing and control cells ("**EV**") were applied to the migration experiment. Only for A549 cells, a tendency of increased migratory activity was detected. Each value was calculated from ≥ 2 overexpression and ≥ 2 control samples processed in parallel; ─ mean values. **B**) Egr1-overexpressing (**A549**, n = 10; **SMCs**, n = 5; **fibroblasts**, n = 8) or -lacking (siRNA-transfected, "**si_A549**", n = 9) cells adhered to culture plates pre-coated with either **BSA** or collagen IV ("**Coll**") or fibronectin ("**FN**"). Every value was calculated from the absorption difference between ≥ 3 treated and ≥ 3 control samples (EV or siR) processed in parallel. ─ mean values.

3.6.5 Adhesion

Studying potential changes in adhesion behaviour, different Egr1-overexpressing or -lacking human cell types were adhered to culture plates which had been coated with BSA (as control), human collagen (type IV) or human fibronectin, respectively (→ **2.8.2**). There were no significant changes according to cell type or coating substance detectable (→ **Figure 13B**).

3.6.6 Localization

Using immunofluorescence stainings (→ **2.9**), Egr1 protein expression was localized to different areas / cell types of the lung (→ **Figure 14**). The molecule was mainly detected in septal and bronchial cells, often co-localizing with SP-C. As far as possible, the lower degree of expression in newborn mice and the up-regulation due to pneumonectomy (→ **Table 5, Figure 6 + Figure 7**), could be reproduced in the staining series. Egr1 did not co-localize with smooth muscle-actin and the fibroblast and mesoderm marker vimentin (→ **Figure 14B, C+E**). There also was no obvious correlation between Egr1 localization and mitotic activity (detected by Ki-67 antigen expression; → **Figure 14D**).

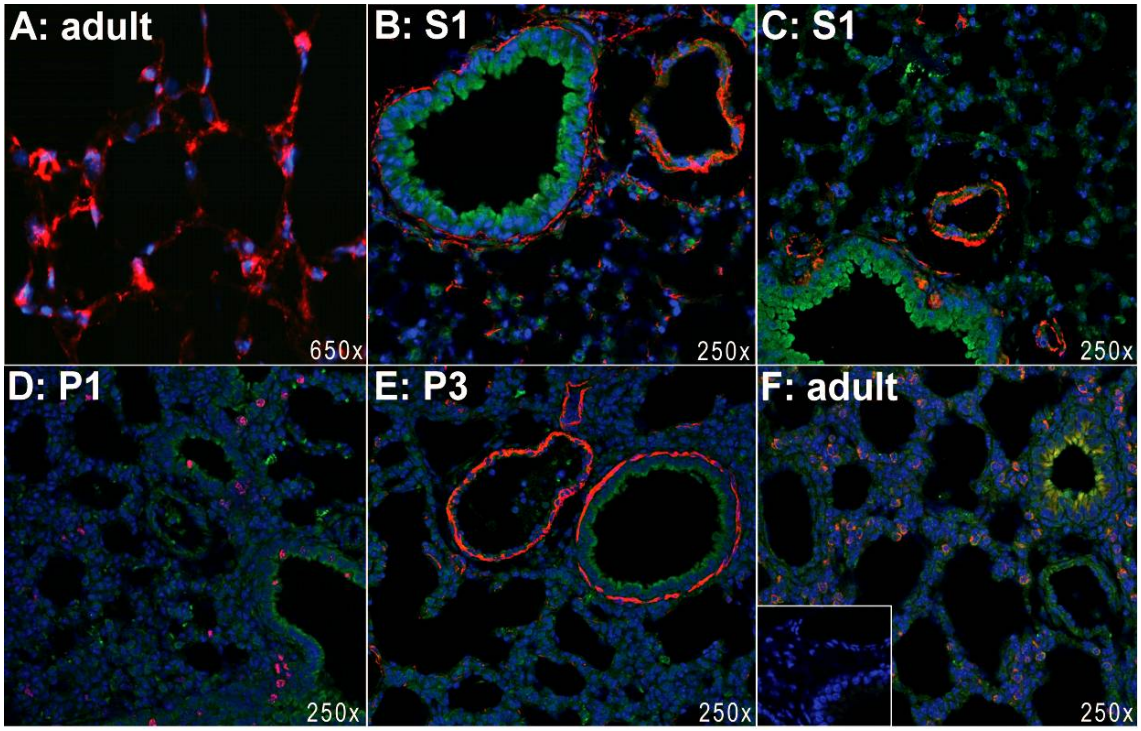

Figure 14: Egr1 localization using immunofluorescence.

In adult mice, Egr1 was heterogeneously expressed in septal cells and in bronchial epithelium (**A + F**). An increased bronchial Egr1 expression was seen after pneumonectomy (**B + C**), while there was a tendency of postnatal bronchial down-regulation (**D + E**), especially at P1. In all time points, there was no obvious co-localization with vimentin (**B**), smooth muscle actin (**C + E**) and the proliferation marker Ki-67 (**D**). Egr1 co-localized with SP-C-positive cells in bronchi and, with a less prominent expression, with peripheral AECs II (**F,** yellow staining). Colours: Egr1: red (**A**) or green (**B - F**); vimentin: red (**B**); smooth muscle-actin: red (**C + E**); Ki-67: red (**D**); SP-C: red (**F**); nuclei: blue (**A - F**); insert (**F**): negative control; magnifications given in each picture; **S1** = one day after surgery; **P1 / 3** = 1 / 3 day(s) after birth.

Localizing Egr1-specific mRNA, various expressions were found in different time points and models (→ **Figure 15**): Instead of the basal bronchial expression in adult mice, newborn animals showed an up-regulation in single septal cells and post-surgery mice in the area of the most intensive extension in the periphery of the lung.

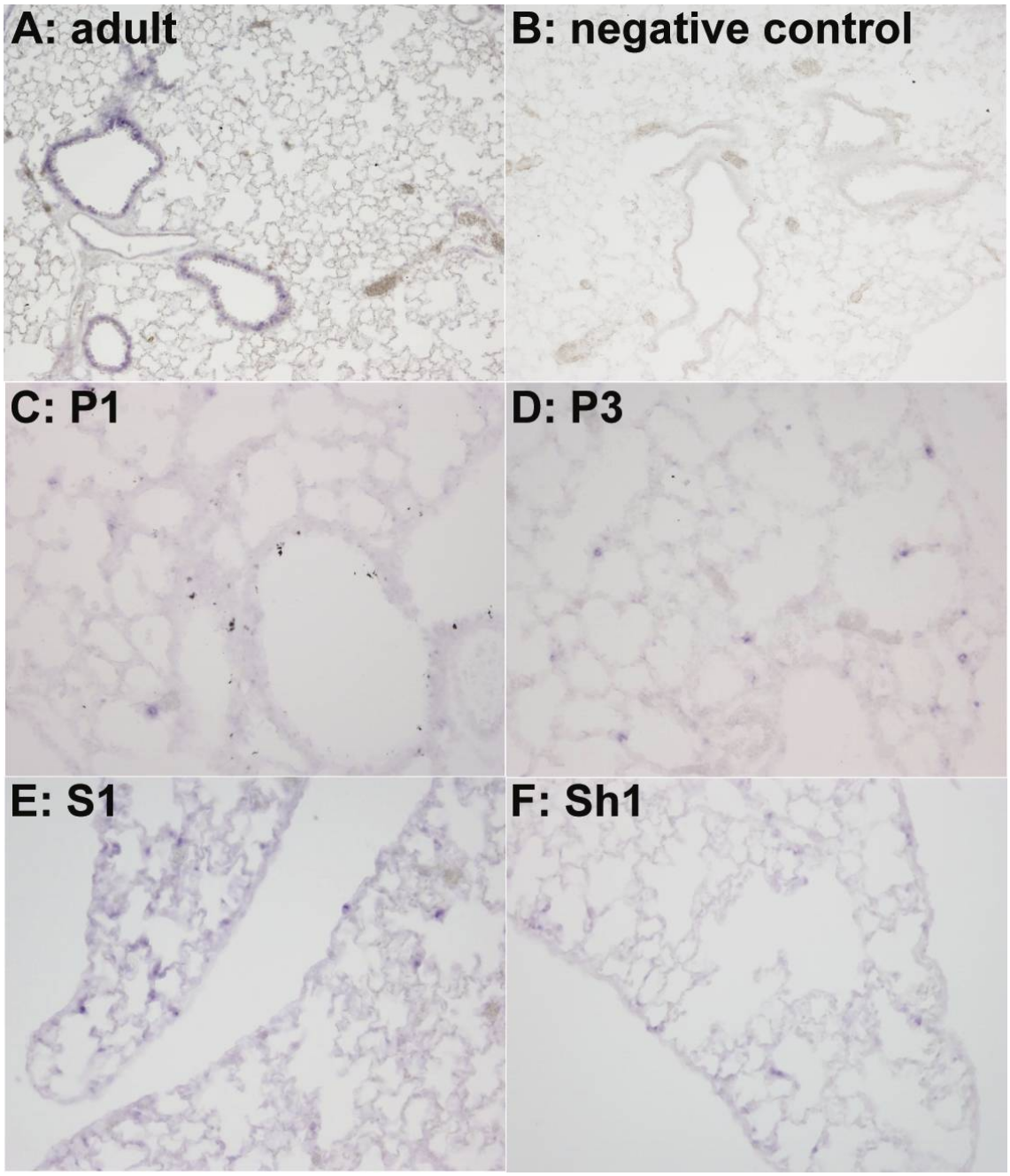

Figure 15: Detection of Egr1-specific mRNA using in-situ hybridization.

A) In adult mice, Egr1 was mainly expressed in bronchi (**B**: negative control (hybridization of sense probes)). Newborn animals (**C + D**) focussed mRNA formation onto single septal cells, and post-surgery mice (**E**) overexpressed the molecule in the area of greatest extension in the lung periphery (**F**: sham control). **P** = postnatal day / **S** = post-surgery day / **Sh** = post-sham day; magnifications: **A + B**: 100 x; **C - F**: 200 x.

3.7 Second candidate gene: Stefin A1

Stefin A1 was one of the most intensively up-regulated mRNA molecules in newborn mice (P1: 29.7fold / P3: 32.9fold; → **online supplement**). As such an extreme regulation could be expected to indicate a functionally important role in the usual alveolarization procedure it was regarded as reasonable to study this gene in detail.

3.7.1 Quantification

Measuring the regulatory changes of Stefin A1 expression, real-time PCRs validated the on-chip findings of a strong postnatal up-regulation (→ **Figure 16A**). Additionally, quantification of the protein expression revealed even extremer results: Stefin A1 seemed not to be of a greater necessity for normal adult lungs or compensatory growth as - at best - minimal protein formation was detected (→ **Figure 16B**).

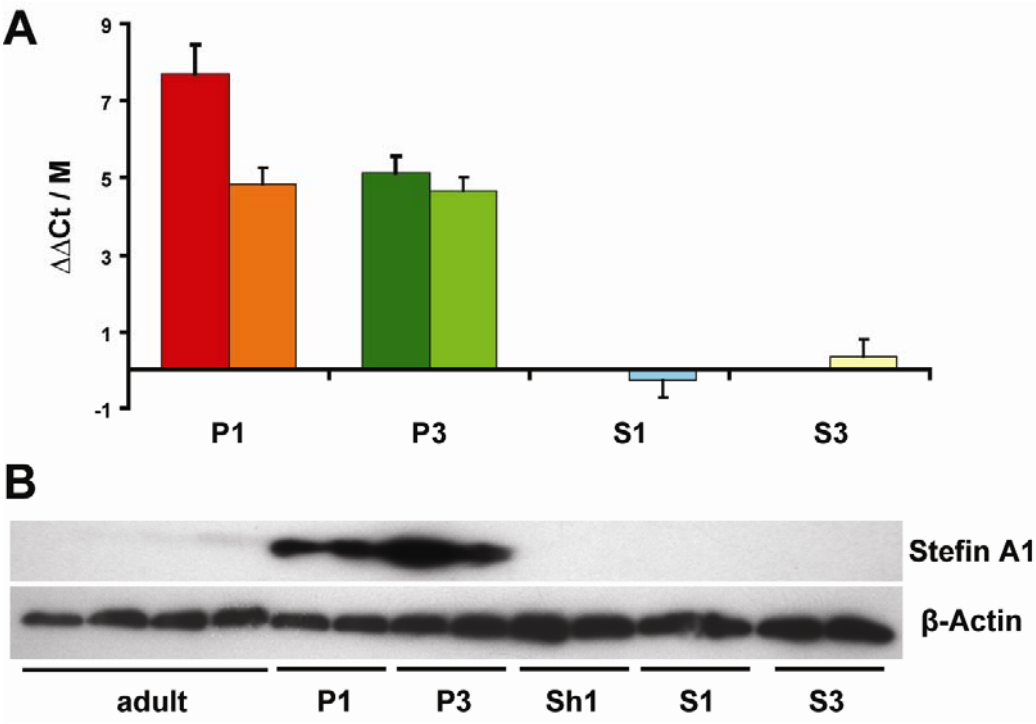

Figure 16: Postnatal and post-surgery Stefin A1 expression.

A) Using real-time PCR (left bar of each pair) and microarrays (right bars), Stefin A1-specific mRNA was shown to be extremely up-regulated postnatally (**P1 / P3**), but not after pneumonectomy (**S1 / S3**). Reference gene: PBGD; missing PCR bars: not done, because post-surgery array data showed no significant regulation. PCR: **ΔΔCt** values; array data: **M** values; $2^{\Delta\Delta Ct} = 2^{M}$ = regulation factor; n = 3 - 4; values ± SEM. **B**) Western blot proving Stefin A1 expression in **P1** and **P3** mice, but not in normal **adult** or pneumonectomy (**S1 / S3**) animals; reference: β-Actin; every band = 1 individual animal. **P1 / 3** = postnatal days 1 / 3; **S1 / 3** = 1 / 3 days after pneumonectomy; **Sh1** = 1 day after sham surgery.

3.7.2 Localization

Using immunofluorescence stainings (→ **2.9**), Stefin A1 protein was localized to cells with epithelial characteristics in bronchi and septae. Single septal cells, postnatally expressing Stefin A1 on a very high level, were missing in all adult and surgery mice (→ **Figure 17**). This explains the extreme regulatory difference found in array data.

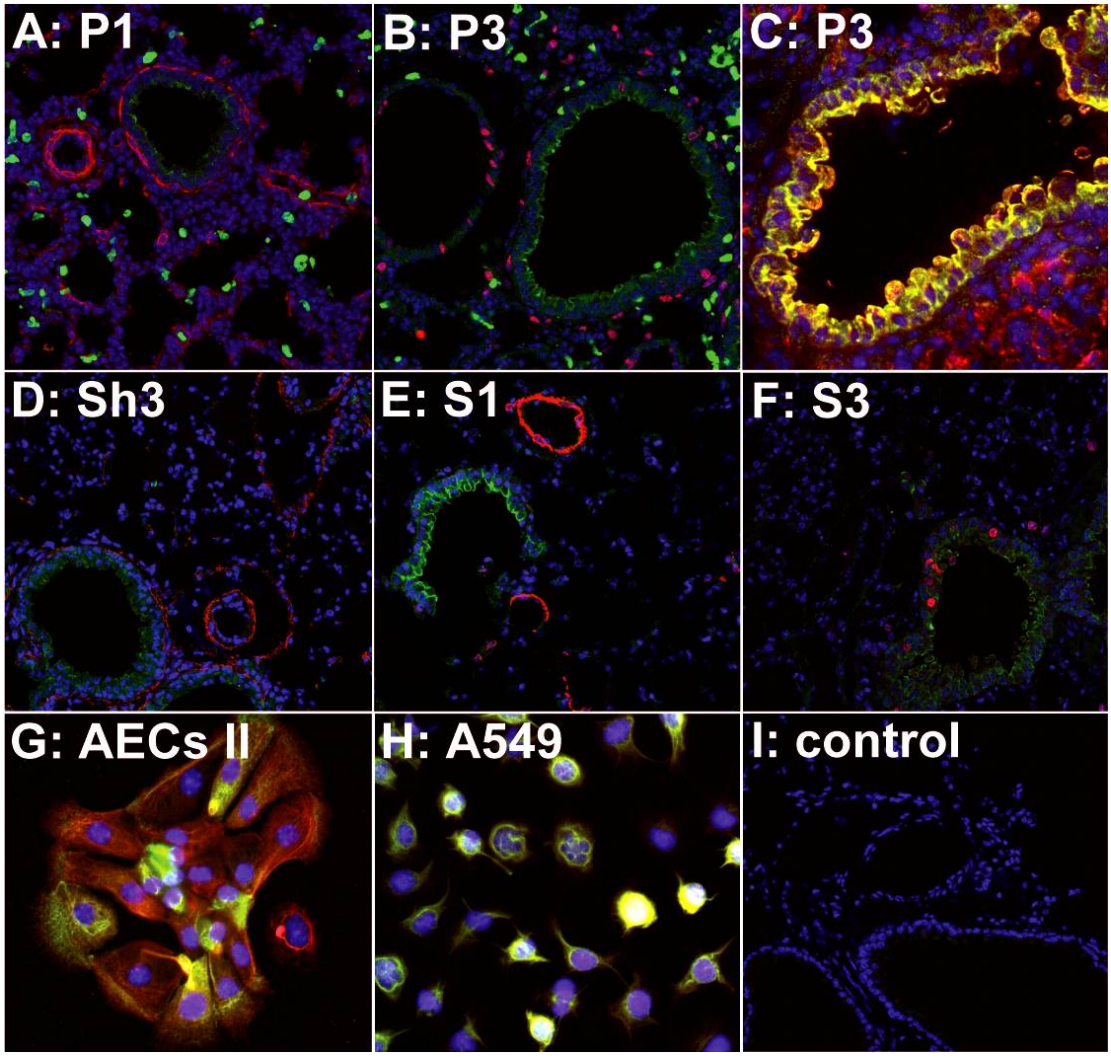

Figure 17: Stefin A1 localization using immunofluorescence.

Stefin A1 was strongly expressed in single septal cells of newborn mice (**A + B**). Independent of age and model, it was constantly found in bronchial epithelial cells of newborn (**A - C**) as well as adult / post-pneumonectomy animals (**D - F**) and - to a lower degree - in septal cells. In culture, AECs II (**G**) as well as A549 cells (**H**) stained positive for the molecule. Stefin A1 showed a co-localization with cytokeratin (**C, G + H**), but not with smooth muscle-actin (**A + E**) or vimentin (**D**, also representative for normal adult). There also was no obvious association with the proliferation marker Ki-67 (**B + F**). Colours: Stefin A1: green; all co-staining molecules: red; co-expression: yellow; nuclei: blue; **I:** negative control (adult lung); **P** = postnatal day / **S** = post-surgery day / **Sh** = post-sham-surgery day; magnifications: **A + B / D - F / I:** 250 x; **C / G + H:** 400 x.

To localize Stefin A1-specific mRNA, in-situ hybridization screenings of all models and time points were performed. As on protein level (→ **Figure 17**), single septal cells showed a unique, intensive expression in newborn mice, while all experimental groups contained a basal bronchial mRNA level (→ **Figure 18**).

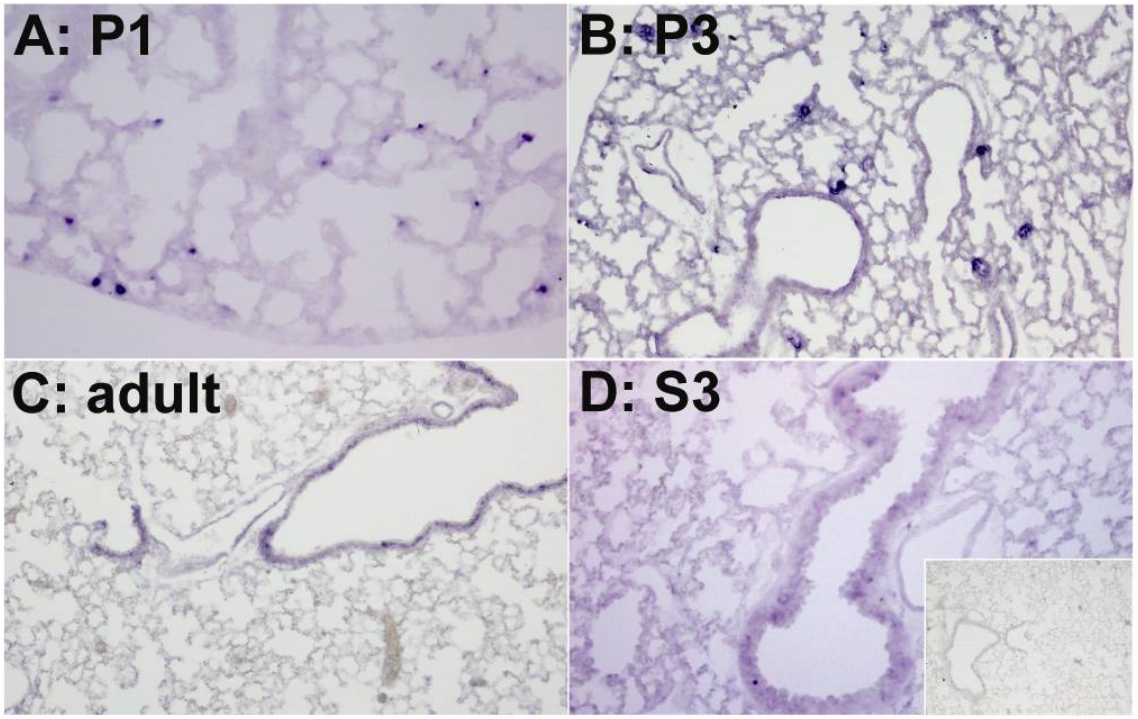

Figure 18: Detection of Stefin A1-specific mRNA using in-situ hybridization.
In newborn mice, Stefin A1-specific mRNA was intensively expressed in single septal cells of the peripheral (**A**) and central lung (**B**). In all models and time points, the molecule additionally appeared in bronchi (**B - D**). Comparing with untreated adult animals (**C**), there was no detectable change due to pneumonectomy (**D**). **P** = postnatal day / **S** = post-surgery day; magnifications: **A + D**: 200 x / **B + C**: 100 x; insert in **D:** negative control (hybridization of sense probe).

3.7.3 Functional studies

As for Egr1 (→ **Figure 9, Figure 10 and Figure 13**), the Stefin A1-driven influence on proliferation, migration and adhesion was tested for different cell types (→ **Figure 19**). In proliferation, Stefin A1 accelerated the division speed of MLE-12 cells, while it inhibited that of A549 cells. Studying adhesion, two significant changes were detected, namely an increased activity of A549 cells to adhere to fibronectin and a small decrease in the ability of fibrocytes to adhere to collagen. Checking for migratory activities, no influence of Stefin A1 became obvious (→ **Figure 19**).

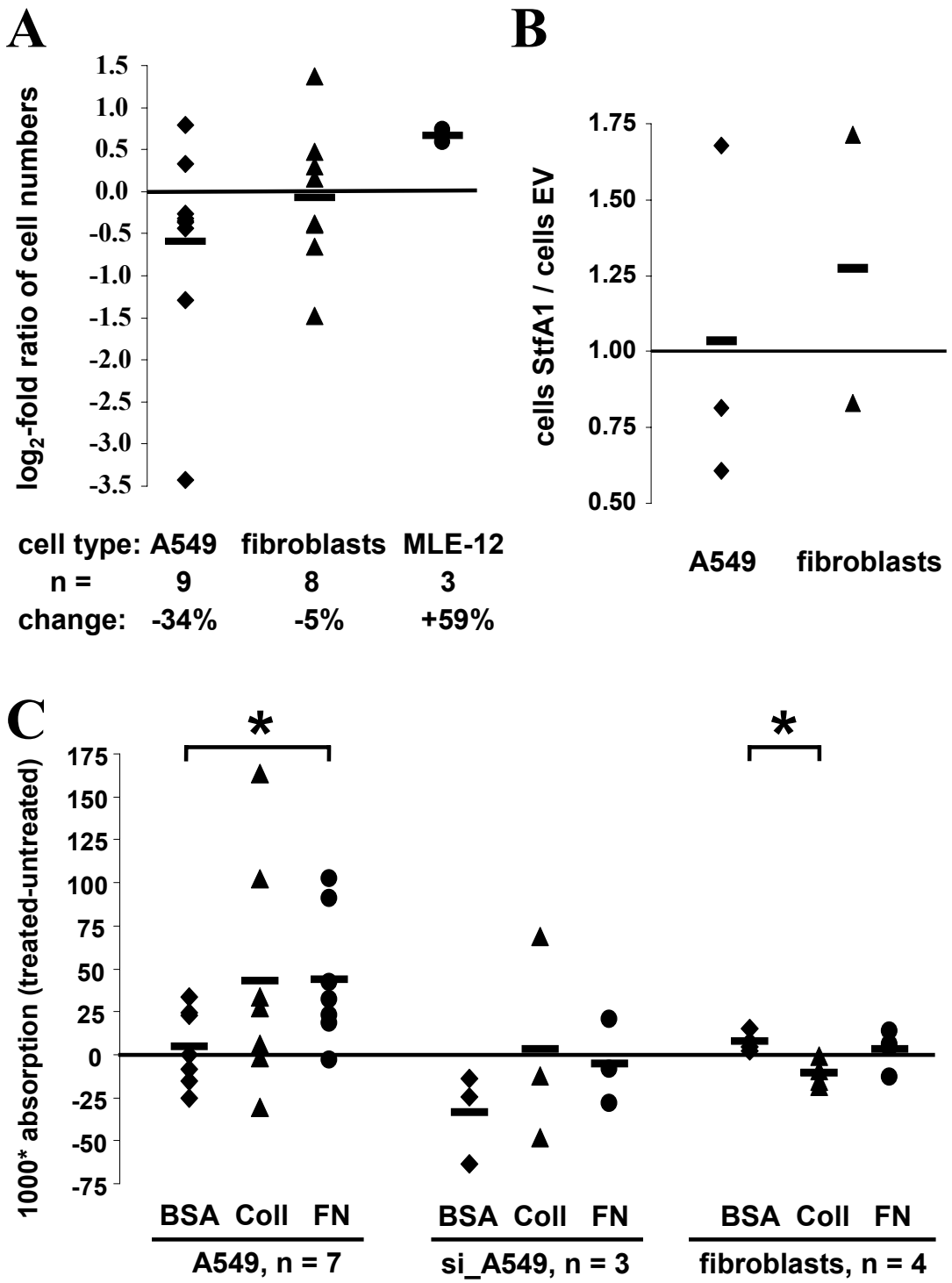

Figure 19: Functional aspects of Stefin A1 overexpression and -knockdown.

Cultured cells were transfected with Stefin A1-overexpressing plasmids (**A - C**) or Stefin A1-specific siRNA (**C,** "**si_A549**"). Checking proliferation (**A**), **A549** cells showed a tendency of down-regulating their growth activity (in 7 of 9 experiments), while **fibroblasts** did not react uniformly and **MLE-12** cells proliferated faster. The migratory activity (**B**) of **A549** cells and **fibroblasts** was not obviously influenced at all. Studying adhesion (**C**), a statistically significant increase in the affinity to fibronectin (**FN**, in comparison to **BSA**) was observed in **A549** cells, while **fibroblasts** showed a low, but significant decrease in adhesion to **collagen (Coll)**. Each spot represents the difference between ≥ 3 treated and ≥ 3 control samples (EV or siR) processed in parallel. ─ mean values; * $p < 0.05$.

4 Discussion

4.1 Experimental design and technical approaches

Performing screens in mouse models offered the chance to employ genetically engineered animals for in-vivo studies, as for mice large numbers of constitutive and conditional knockout and knockin animals are available. Additionally, the potential generation of own lines could be expected to be easier than in other species.

The study presented here based on whole mouse genome screens employing microarray technology. As this procedure always bears the risk of just-by-chance findings due to simple statistical reasons without any connection to an altered gene expression, several tasks have been included in the whole process of data generation to avoid large numbers of false positives:

- By using pooled RNA samples, the disturbing effect of single animals with unusual expression levels could be largely excluded. This was supported by the fact that at least three experiments (i.e. dye-swap array pairs) were performed per group of interest (→ **2.2.3+4**). On the other hand, sample sizes were designed as small as possible to gain significant results without unnecessarily killing too many animals.
- Hybridizing each target sample in competition with an appropriate control helped to overcome potential local inhomogeneities on the chip as a direct comparison was still possible (→ **2.2.4+5**). Additionally, for several genes more than one sequence was spotted on the microarrays.
- To exclude an influence of the labelling dyes, which was imaginable because of their different chemical structures, all samples were studied in a dye-swap manner, i.e. the same pair of samples was hybridized onto two microarrays, carrying opposite labellings each time (→ **2.2.4+5**).
- Applying analysis software, well-established procedures in combination with strict inclusion criteria for spot quality and statistical significance were used (→ **2.2.5**).
- Having chosen two different lung growth models (→ **1.2, 1.4.4**), the most promising candidate genes could be expected in the intersection list; comparing different time points of the same approach (→ **2.1, 2.2**) was regarded as a possibility to distinguish between longer-lasting influences (e.g. general lung development) and short-term activities, e.g. pathway activation (see below; → **1.5**).

In general, the quality of array data was very convincing, as a) there was a high inter-chip concordance (i.e. constant biological replications) and b) dye-swap experiments showed no obvious variations (i.e. constant technical replications). Analysis revealed more than 160 significantly regulated genes per time point after pneumonectomy and more than 1,600 postnatally (→ **3.1**) with an intersection of 58 genes (→ **3.3**). Of the latter ones, 40 were regulated synergistically; this made them promising candidates for further studies.

One might doubt that the time points 1 and 3 days after birth or surgery, respectively, were chosen ideally. Indeed, secondary septation is known to begin at about P4 - 5 in mice (→ **1.2**), but as the main intention of this study was to find key regulators of this process, looking right before its onset, i.e. at P3, was expected to reveal numerous important pathway inducer molecules. On the other hand, in the pneumonectomy model the most intensive growth stimulation is present in the beginning of the process (→ **1.4.4**). Consequently, genes found to be selectively regulated at P3 and S1 had a higher probability of being important alveolarization inducers with therapeutic potential than P1 and S3 candidates. The latter ones may be regarded as a measure of longer-lasting, more general lung growth or, in case of some P1 candidates in newborn mice, may be located very early in extensive regulatory pathways. Regarding the 58 intersection genes (→ **3.3**), there were only 8 postnatal candidates being solely regulated at P1, but even 20 at P3; in the pneumonectomy group, an opposite distribution showing 37 genes being selectively changed at S1, but only 11 at S3, became apparent. In total, 14 intersection candidates were exclusively expressed at P3 and S1, with 9 of them being uniformly up- or down-regulated. The importance of these genes as well as the validity of the theory regarding the role of the different time points, should be verified in further studies.

To avoid working with one of the few false-positive genes potentially remaining in the list and as a regulation on mRNA level does not necessarily mean a change in the appropriate protein content, it was very important to prove the array data with different methods. Due to that, real-time PCR and Western blot controls (→ **2.3, 2.4**) were applied to promising candidates before considering any functional experiments with them. In all cases evaluated with these approaches, array data could be confirmed according to the direction of change; in PCR controls, most regulation factors matched quite well (→ **3.4.1**), while some protein quantifications tended to be extremer than mRNA values (→ **3.4.2**).

4.2 Interpretation of array data

4.2.1 Comparison with previous investigations in the field

Several groups also studied lung growth and regeneration in whole-genome approaches before, concentrating on specific aspects, medication effects or cell types, respectively:

Mariani et al. analysed a time-course from embryonic day 12 to adulthood focusing on extracellular matrix molecules and generating functional gene clusters [117]. Here, one of the most interesting up-regulated candidates in the postnatal phase was (Tropo)elastin, which also was intensively induced in postnatal as well as post-surgery animals (→ **Table 5**). The group further analysed several collagens found to be overexpressed in either interstitial tissue or basement membranes. In both models presented within this thesis, the up-regulation of interstitial type I and III collagens could be confirmed (→ **Table 5**), while basement membrane collagen (IV) was found to be elevated only after surgery (→ **online supplement** of Wolff et al., [116]: Col4a2, NM_009932; $M_{S1} = 0.86$).

Foster et al. generated mRNA expression data from the tips of growing P6 septae isolated by laser-capture microscopy [118]. Interestingly, only 3 of the 25 genes being most intensively up-regulated in Foster's study were also significantly changed in own homogenate data, namely Tenascin-XB and C as well as Drebrin 1, whereas Tenascin-XB was down-regulated (→ **online supplement**). Also Galectin-1, being the main focus of interest in the laser-capture study, could not be confirmed. These differences in expression profiles may be due to the varying time points of investigation (P1 and P3 versus P6), but it also has to be taken into account that the use of lung homogenate instead of selected parts of the organ may have hidden certain findings, e.g. in case of different cell types regulating genes in distinct directions at the same time or due to a mass effect with mostly unregulated tissue components.

Studying rat fibroblasts, Boucherat et al. searched for genes being up- or down-regulated on P7 (phase of secondary septum formation) compared to P2 and P21 [119]. Among the 141 candidates with significant changes, there was a quite substantial overlap of 38 genes (27%; → **online supplement**) with own data. Of these, 35 were exclusively regulated in the newborn model and 16 were found to be changed in a different direction. Consequently, although the number of common genes appeared to be relatively high at a first glance, one has to be careful in directly comparing these data

as a) a different species was used, b) only a single cell type was studied and c) another (relative) time point within septation has been chosen. This is also reflected by the 10 genes in the focus of interest of the study: Only Wnt5a, Fzd1 and Tnx were changed in concordance with own data (→ **online supplement**), while the remaining candidates, e.g. Ndp and Hox 1, 2 and 5, were not changed at all in homogenate.

The group of D. Massaro performed several array-based lung growth studies, either on corticosteroid-triggered inhibition of alveolarization in young mice [72] or after calorie restriction and refeeding [76, 77]. In the former experiments, dexamethasone-treated animals (→ **1.4.1**) were administered retinoic acid (→ **1.3.1**) causing 46 drug-influenced genes to be "rectified" in their regulatory tendency [72]. Only 4 of these candidates, namely Ly6a, Chi3l3, Clca1 and Rnf2, were found to be significantly changed in normal postnatal (and none in post-surgery) mouse lungs, and only the latter two showed the same regulatory tendency (→ **online supplement**). Especially Flk-1, the main focus of the manuscript, was not changed at all in usual growth. These findings support the assumption that corticosteroids seem to prevent lung growth by an inhibition of genes and pathways different from the candidates inducing regular secondary septation.

In another series of experiments the group focused on time-related regulatory changes due to calorie restriction (→ **1.4.2**) [76]. Screening for apoptosis-related genes, 63 candidates with significant expressional changes were found; 10 of these (16 %) also appeared postnatally and / or post-pneumonectomy, and, matching the opposite intention of tissue growth instead of degradation, most of them (e.g. Casp1 and 3, Birc2) were regulated in a different direction. Regarding proteolysis-related genes, there was an overlap of 31 % (24 of 78 genes), again with most of the candidates (e.g. Psmb8, Gzma and Gzmb) exhibiting contrary alterations (→ **online supplement**). Having found so many common, lung growth-related genes being changed in opposite directions due to opposite stimuli upgrades the validity of own as well as that of Massaro's data.

In a recent approach, the group intensively studied mice being refed after two weeks of calorie restriction with focus on angiogenesis-, extracellular matrix- and cell replication-related genes as well as steering elements of guided cell motion [77]. Altogether, data again showed a high degree of overlap (between 30 and 50 %) with newborn and / or pneumonectomized mice throughout the groups, with special focus on angiogenesis and cell replication.

4.2.2 Genes and functional groups found in at least one model

Newborn mice:

The largest group of genes found to be up-regulated was coding for molecules involved in growth and differentiation (31%; → **3.2, Figure 4**). These mediators, e.g. Igf2 (insulin-like growth factor 2), Cdc2a (cell division cycle 2 homolog A) and Tcf21 (transcription factor 21), are known to have stimulating effects, fitting the necessity of growth promotion in this period of life. Additionally, for Igf2 deficiency, a delayed lung development has already been described [120], and Tcf21 (= Pod1) knock-outs were found to have a severely impaired lung and kidney development [121].

In the group of enzymes and their regulators, many molecules with inhibitory effects were up-regulated, e.g. several Stefins, which prevent proteases from the degradation of essential, just-built extracellular matrix material. Stefin A1 as one of the most intensively up-regulated candidates of all array series was studied more differentiatedly (→ **3.7**) and will be discussed in detail later (→ **4.4**).

There were several down-regulated molecules with enzymatic activities as well, e.g. a procollagen endopeptidase enhancer (Pcolce2, [122]) and the proapoptotic allyldehydrogenase Aldh1a1 (→ **3.2**); both of these findings also match the need of growth and stabilisation. For Aldh1a1, an enhanced retinoic acid (→ **1.3.1**) metabolism and an overexpression in lung tumour cells have been described [123]. Accordingly, for normal lung growth, low Aldh1a1 levels can be regarded as helpful.

Another interesting point was to find ten different cytochrome P450 oxidase (CYP) molecules to be down-regulated (→ **online supplement**). As these enzymes play a role in preventing damage through xenobiotics [124], one could speculate that in this early stage of life metabolites of these molecules would significantly harm the immature organ structure and that lower CYP levels prevent such damage. Regarding this point, the lack of Cyp2f2, which was down-regulated 3.4-fold in P3 lungs, has been shown to have a protective role in Naphthalene-induced Clara cell damage [125]. The down-regulation of the microsomal epoxide hydrolase 1 (Ephx1), which also plays a role in detoxification, further supports this thesis. On the other hand, it was recently shown that Clara cell-specific stabilisation of β-Catenin leads to immature "progenitor"-like epithelial cells of the respiratory epithelium with significantly reduced expression of P450 cytochromes [126]. Therefore, a low CYP expression could also reflect the immature state of the epithelial cells during rapid cell expansion.

Having found Xdh (xanthine dehydrogenase) and Ly6a (lymphocyte antigen 6 complex, locus A), which both have a pro-differentiative influence, to be down-regulated, additionally confirms the immature state needed in postnatal alveolarization. This is underlined by the finding that large amounts of Ly6a have been detected in mature pulmonary vasculature [127].

The most striking finding in the down-regulated group was to see numerous candidates involved in immune response mechanisms (→ **3.2, Figure 4, online supplement**). Taken together, the detected genes covered many areas of defence, e.g. antigen presentation via MHC (Major Histocompatibility Complex) molecules (H2-Eb1 / -D1 / -Ab1 / -Aa etc.), leukocyte surface receptors (Klra15, Ly6a / i / f / c etc.) and the complement system (Cfh). For explanation of the missing activity, one may assume that the immune system is still in an immature state in this developmental period and comparably few inflammatory cells reside in the lung. This may be tolerable as long as the babies receive antibodies via milk and it may also be happening "on purpose", meaning to develop a certain degree of tolerance against own tissue components.

Surgery model:

In compensatory lung growth, there was a relatively homogenous distribution of most global molecular functions among the up-regulated genes (→ **3.2, Figure 4**). Again, the largest group of candidates consisted of growth and differentiation molecules, especially transcription factors or mediators of pro-proliferative pathways (e.g. Creb3l3, Egr1, c-Fos; as the latter two were studied in detail (→ **3.4 - 3.6**), they will be discussed separately: → **4.2.4, 4.3**).

As in newborn mice, numerous collagens were more intensively expressed (→ **online supplement**), underlining the need of connective tissue generation in compensatory lung growth. Due to the high overlap with the newborn model, the genes are discussed elsewhere (→ **4.2.1, 4.2.3**).

Interestingly, some immunomodulatory genes were detected to be up-regulated within the pneumonectomy model as well, although sham-operations were performed on control animals (→ **Figure 4**). Indeed, some of these candidates may have been induced by potentially more severe wounding than in the control animals, but among the genes there were also some with inhibitory and / or secondary (side-) effects, which may have been emphasized here, e.g. Lcn2 (= lipocalin 2; a) acute phase reaction, b) regulates epithelial morphogenesis; [128, 129]). On the other hand, some stimulators of the

immune system were found to be down-regulated as well, e.g. Ccl20, a pro-inflammatory cytokine mediating B cell adhesion and leukocyte recruitment [130, 131].

A very interesting finding was to detect several members of respiratory chain and mitochondrial metabolism to be down-regulated after pneumonectomy (→ **Figure 4**). At a first glance, this was surprising, as a high degree of energy demand could be assumed during lung growth, needing to rebuild about one third of the total respiratory surface. One might think about a relative effect as the mitochondria may not have divided as quickly as their "mother" cells, but all of the genes detected to be less intensively expressed were encoded by the cellular genome and none by the mitochondria themselves. The down-regulation may be explained by the autophagy phenomenon and the resulting lower needs of mitochondria-stimulating mRNA: For the heart it is known that in periods of extreme demand cells are able to "burn up" their mitochondria to quickly gain large amounts of energy and amino acids [132, 133]. Something similar may also be assumed in the onset of compensatory lung growth.
On the other hand, a physiological switch to a pronounced anaerobic metabolism to cope with (initially) reduced amounts of oxygen, implying an increased production of appropriate mRNAs and a parallel reduction of mitochondrial "stimulators" may also be possible. As such "anaerobic genes" were not frequently changed in array data and as the lacking lobe should be compensatable by an increased breathing frequency etc., these processes probably only play an inferior role.

In summary, both lung growth models revealed numerous significantly regulated genes with interesting aspects according to growth regulation, connective tissue generation, immunological competence, energy balance etc. Assuming a more precise selection of the most promising candidates, the intersection of postnatal and post-pneumonectomy alveolarization needed to be evaluated as well to see whether both types are of the same origin or if they are differentially regulated (→ **3.3, 4.2.3**).

4.2.3 Intersection genes of newborn and pneumonectomy mice

In total, 40 genes were concordantly up- or down-regulated in both experimental groups, while 18 candidates with opposite directions of change could be detected (→ **Table 5**). Among the former genes one can assume to have found some important regulators or operators of alveolarization as the "accidental" finding of uniform expressional changes without any functional mutuality in the intersection of two

independent models is unlikely. The discordant genes have to be judged more differentiatedly: Some, if not most of them, may simply not play an important role in lung growth, but the findings of few candidates could mirror different stages in a long regulatory pathway where opposing or completely distinct influences are needed, e.g. transcription factors like Egr1: This molecule promotes proliferation, differentiation, angiogenesis, induction and inhibition of apoptosis etc. [134-136] (→ **3.6, 4.3**). All of these features are necessary for lung growth, but have to appear in correct order and location, what may cause the differing results seen for the two models studied.

Among the candidates in the intersection list, the by far largest functional group was "growth and differentiation" (→ **3.3, Table 5, Figure 5**): 10 of 19 (53 %) corporately up- and 9 of 21 (43 %) down-regulated genes were, at least in part, involved in these processes. Rbm3 (= RNA binding motif protein 3), being corporately up-regulated in both models, is necessary for mitosis progression [137]. Another example from this category is Fstl1 (Follistatin-like 1, TSC36): The protein has an anti-apoptotic, heart-protecting effect and is thought to play a role in organogenesis. An expression in embryonic mouse lung and kidney development has already been described [138]. Uhrf1 (= ubiquitin-like, containing PHD and RING finger domains, 1; Np95), a molecule responsible for S-phase entry and genome stability, was found to be elevated in both models [139]. Rras2 (= related RAS viral (r-ras) oncogene homolog 2; TC21) is known to stimulate migration; in some cases it can even induce tumours [140]. The detected concordant up-regulation of its mRNA points to the need of cell migration for proper lung growth.

In addition to these growth-promoting factors, there were several structural molecules concertedly up-regulated as well, providing a stabilizing and guiding scaffold for emerging tissue components (→ **Table 5**): Five different collagens were up-regulated in both models, complemented by eight solely induced in newborn and one in post-pneumonectomy mice, respectively (→ **online supplement**). Additionally, Elastin and Fibrillin1 presented a uniformly elevated expression level. Lacking or not correctly cross-linked Elastin results in failing formation of regular alveoli or, e.g. in case of α1-Antitrypsin deficiency, causes a severe emphysema, while Fibrillin1 mutations result in the Marfan syndrome [141-143]. Taken together, the induction of these genes strongly underlines the need of connective tissue generation in the growing lung, being a major aspect in both models.

Among the down-regulated genes (→ **Table 5**), several candidates responsible for maintenance procedures and metabolism of differentiated cells were found, but also growth inhibiting molecules, e.g. Pla2g16 (= phospholipase A2, group XVI = Hrasls3 = H-rev107), which is a well-known cell cycle inhibitor [144].

Omd (= OSAD, osteoadherin / osteomodulin) is known to support osteoblast differentiation, while a lack of this molecule increases proliferation and migration [145]. Although bone cells are not directly involved in lung growth, similar effects onto pulmonary cells are imaginable. Therefore, the detected down-regulation could increase division ratios and migratory activities, both fitting the needs of alveolarization.

Klrd1 (= CD94) is a surface receptor for MHC class I molecules on mature and differentiating natural killer cells [146]. As in newborn mice the immune system is still very immature and many relevant genes are expressed on low levels, e.g. for induction of self tolerance, a down-regulation in this group is not surprising. Due to the fact that the overall function of Klrd1 is inhibitory [147], the intention to lower its expression in post-pneumonectomy mice may be the necessity of an increased killer cell activity after surgical intervention, although sham controls should have "eliminated" most of the infection parameters (→ **4.2.2**).

Nr1d2 (nuclear receptor subfamily 1, group D, member 2) is a steroid (thyroid) hormone receptor; it indirectly induces lipogenesis and plays a role in the circadian rhythmic of gene expression [148, 149]. As these processes are not of high relevance during growth, a down-regulation in both models is comprehensible.

Interestingly, the intersection of both models (58 candidates) was relatively small, although > 160 (pneumonectomy) and > 1,600 (postnatal) genes were significantly regulated in each setting and at each time point, respectively (→ **3.1**). There are two different explanations for this outcome: On the one hand, the whole alveolarization procedure may be depending on few initiating and / or executing molecules. In this case, many of the key genes should have been found. On the other hand, both models could be relatively independent, showing similar features regulated by different pathways. Then the idea of future lung tissue regrowth in humans would have to be realized with genes from one or the other model, but preferably with pneumonectomy candidates, as this issue is closer to what can be expected to happen in adults.

In the following chapters, findings regarding location and functional aspects of some interesting candidates from array experiments will be discussed in detail (→ **4.2.4, 4.3, 4.4**).

4.2.4 Known and new alveolarization candidates

Array data narrowed down the number of genes which can be regarded as potential candidates for septation regulation, but functional and location studies have to reveal their actual role and answer the question whether there indeed is a common background of both models. In this chapter, candidates from own array data as well as genes already known to participate in lung growth are reflected, mainly addressing the question why they have (not) been detected, i.e. whether there may be a functional connection to alveolarization. Afterwards, two of the most interesting genes, namely Egr1 and StfA1, will be discussed, based on the results of evaluating functional studies (→ **4.3, 4.4**)

In a first step, intending to validate a growth participation of septal cells as probably most important region within alveolarization, c-Fos and Lcn2, showing a divergent regulation in array experiments (→ **Table 5**), could exemplarily be localized in in-situ hybridizations (→ **3.5, Figure 8**). Both molecules revealed a switch of expression being present in, what was hoped for, single septal cells after birth, but in the bronchi of adult mice. The down-regulation detected in array data may be explained with the widely missing expression of mRNA in bronchi during the postnatal period. Regarding the surgery model, specific stainings were seen, in addition to bronchi, in the periphery of pneumonectomized, but not of sham-operated lungs. With respect to cell division ratios, this location feature has been described before [95], and it may be explained with the need of the outer part of the lung to more intensively grow than internal regions, e.g. due to different degrees of tissue tension. The findings do not only explain the detected up-regulation in post-pneumonectomy data (→ **3.3**), but they can be regarded as a hint for a functional link between c-Fos / Lcn2 and compensatory lung growth (s.b.).

Lcn2 (= Lipocalin 2, 24p3, Sip24, NGAL):

The Lcn2 molecule is a 25 kD glycoprotein, which can form homodimers and which is part of a complex with neutrohil gelatinase, known as matrix metalloproteinase 9 (MMP9) [150].

Being down-regulated in newborn mice, but overexpressed in the compensatory lung growth model, Lcn2 seems to be rather uninteresting at a first glance, but the divergent directions could simply mirror two different functional aspects of the appropriate protein, with one of them being of relevance for alveolarization: In its role as an acute phase molecule, Lcn2 is induced by reactive oxygen species [150]. Being secreted e.g. by epithelial cells and macrophages, it provides an innate immunity to protect numerous

organs from bacterial infections. The ability to interfere with various types of bacteria is based on its binding behaviour: In addition to being a member of a physiological iron delivery pathway [151], Lcn2 can tightly bind to bacterial iron-laden siderophores; this causes a sequestration of iron supplies resulting in a bacteriostatic effect [152].

Having found an up-regulation of Lcn2 in pneumonectomized mice may have two major reasons fitting the functions explained above: Although comparing to sham-treated animals and administering antibiotics, removal of the left lung lobe could have induced more inflammatory reactions than expected, e.g. by introducing small numbers of bacteria. Alternatively, as the intervention causes significant physiological changes to immediately cope with and although compensation mechanisms are quick and restore the lost surface area within days to weeks, a non-negligible early disturbance of normal metabolic processes can be assumed. Within this, cellular stress reactions resulting in the generation of reactive oxygen species, which in turn induce Lcn2, are expectable. Moreover, in vitro, pro-migratory and pro-branching effects of Lcn2 were found [129]; both of these would characterize the molecule as potential key player in lung (re-) growth.

In addition to the facts mentioned above, Lcn2 is expressed in blood cells (erythrocyte precursors and hematopoietic cells in the bone marrow) and has an anti-differentiative, pro-apoptotic effect [153]. This was interpreted as one potential reason for anaemia in chronic inflammations, where the molecule is up-regulated (s.a.). Furthermore, several studies proved tumour-inducing or -promoting effects and an easier metastasis formation within high Lcn2 levels [154, 155]. Taking these findings into account, a down-regulation of the molecule as found in postnatal lung growth can be justified: Needing cell divisions as well as differentiations, while urgently having to avoid a tumour formation in the quickly growing immature tissue, effects of “missing” Lcn2 should be more helpful than the regular influence. As newborn mice are immunologically protected by antibodies from their mother, there is also no need to induce Lcn2 expression due to defence reasons.

In summary, Lcn2 is an interesting candidate gene potentially involved in several aspects of lung growth, but due to its numerous effects, being adverse in some cases, a general on / off-regulation of alveolarization cannot be expected. Establishing a cell type- and situation-dependent expression / inhibition may provide a useful therapeutic approach anyhow.

c-Fos (= Fos, FBJ osteosarcoma oncogene, D12Rfj1):

c-Fos is the cellular homologue of a viral oncogene (v-Fos) initially identified in transformed cells of a murine osteosarcoma [156]. It belongs to the group of immediate early genes, meaning a) a low basal expression level rapidly going up due to external stimuli, plus b) a transient induction of transcription, independent of the protein synthesis, plus c) a high turnover of its RNA and the appropriate protein[157].

To become an active transcription factor, phosphorylated members of the c-Fos family (c-Fos, FosB, Fra-1, Fra-2) form heterodimers with members of the Jun family (c-Jun, JunB, JunD), which have to be phosphorylated as well [158]; the resulting complex, called AP-1 (activator protein-1), binds to DNA motifs with the frequent consensus sequence TGACTCA [159]. According to its composition, AP-1 has different effects, e.g. a stimulation of target gene transcription (c-Fos + c-Jun) or its inhibition (c-Fos + JunB). Apart from the usual feature, c-Fos can also interact with other transcription factors and cellular molecules, each time causing different effects according to activity, localization or turnover, respectively (e.g. ubiquitinylation, sumoylation) [160].

When c-Fos is involved in proliferation or differentiation, respectively, the MAPK (mitogen-activated protein kinase) signalling pathway can be regarded as the main route of activation, but numerous effects compassing apoptosis, migration, cell death, organogenesis, immune response and tumour growth / progression etc. have also been ascribed to this mediator:

One important physiological function of c-Fos is bone development and remodelling, implemented by osteoclast maturation; in company with this, a side effect of disturbed signalling is a reduced number of B cells, probably due to the impaired bone marrow environment (osteopetrosis) [161]. Additionally, c-Fos plays a role in T cell development and mast cell degranulation, and even a contribution to rheumatoid arthritis via induction of inflammatory cytokines and matrix metalloproteases could be shown [162].

In the neuronal system, the molecule is an important regulator of cellular survival and excitability and participates in the molecular effects of learning and memory [163]; due to its expression in this cell type, c-Fos has become a widely-used biomarker for monitoring activated neurons.

According to pathological conditions, c-Fos can have numerous adverse effects as well: Being an oncogenic transcription factor, bone tumours like osteosarcomas may be initiated, possibly due to an intensive up-regulation of cell cycle regulators, e.g. cyclins

[164]. For skin tumours, a promotion of severity because of c-Fos activity could be shown [165]; there also was a maintenance effect of tumours losing their degree of severity after c-Fos withdrawel. Even the generation of metastasis by inducing an epithelial-mesenchymal transition (featured by loss of cell-cell adhesions and cellular polarity, increased motility, loss of epithelial cell markers etc.) facilitating an invasion of tissue, was ascribed to c-Fos [166].

In the lung growth studies presented here, c-Fos was found to be down-regulated postnatally, but overexpressed after pneumonectomy (→ **3.3-5**). Different functional needs may be a justification for this antagonism: While surgery causes a sudden, intensive stimulation of growth, which might be induced or steered by an immediate early gene like c-Fos, the alveolarization of newborn mice, although involving extreme alterations, is a more permanent process without the necessity of quick changes. c-Fos plays an important role in the development of the immune system, which was found to be down-regulated in newborn mice as well (→ **3.2**); this may be another reason for the postnatal findings. In addition to that, the induction of tumours by significant levels of c-Fos has to be excluded as far as possible; this may be more difficult in the labile phase of regular secondary alveolarization than in compensatory growth, affecting widely mature tissue. In consequence, expression levels may have to be adjusted to the degree of maturity.

As the main interaction partners of c-Fos, namely the Jun family members, were all not significantly changed in their expression (→ **online supplement**), relatively uncommon pathways may be involved in lung growth. Having found its mRNA to be expressed in single septal cells in both models (→ **3.5**) made c-Fos an interesting candidate for further experiments, despite still not knowing which of its multiple roles is relevant for alveolarization.

Sonic hedgehog (Shh):

Sonic hedgehog is a well-known mediator of branching morphogenesis in the frame of early lung development (→ **1.2**) [167, 168]. It was found to be up-regulated 2.2- (P1) and 2.6fold (P3), respectively, in the postnatal phase, while there were no significant changes in the surgery model (→ **online supplement**). Array data may be interpreted in two different ways here: Either Shh still plays an important role in the postnatal phase, or the observed regulatory difference is a residuum from extreme embryonic expression levels and not of greater functional relevance any more. Favouring the former assumption, one might argue that there still is a clear difference from adult gene

expression, which is even slightly increasing when approaching the beginning of secondary septation at P4-5. In this case, a different function of Shh, possibly influencing dividing / migrating septal cells, could be assumed. According to the latter idea, one has to admit that the detected regulatory effect is relatively small (compared to the top postnatal genes; → **3.2, 4.4**) and that the expressional decay may just take longer than expected, possibly due to a long half-life of the mRNA molecules or because of inhomogeneities in lung growth, i.e. an overlap of developmental phases (→ **1.2**).
As, due to a lacking change after pneumonectomy, Shh seems to be irrelevant for the compensatory growth model, further studies regarding its usefulness for adult organ regrowth may not be very promising.

Fibrillin 1 / collagens:

These molecules are of highest importance regarding the generation of a guiding and stabilizing scaffold for the expanding lung tissue during alveolarization. As stated before (→ **3.3, 4.2.3**), there was a uniform up-regulation of Fibrillin 1 and five different collagens detected in both models studied here. This finding can be regarded as a proof of principle, showing that the generation of array data has worked correctly and that the time points chosen indeed involve active lung growth. Due to their widely structural demands, neither Fibrillin 1 nor collagens can be regarded as major steering elements of alveolarization, what makes them candidates of minor interest for functional experiments.

Homeobox (Hox) genes:

Being master regulators of developmental processes by steering the positioning of organs (→ **1.3.1**) [29], the Hox transcription factors are very important also for lung growth. Interestingly, by far the most of these genes were found to be unregulated in the alveolarization models studied here (→ **online supplement**); only Hox b2 and Hox b3 (2.0- and 1.3fold up-regulated at P3, respectively) showed significant expressional changes, but on a low level. As even the latter candidates may have been detected just coincidentally (false-positive rate of up to 10 % (→ **2.2.5**) within 49 Hox spots in four screens; second Hox b2 spot unregulated), one can assume that the fundamental prenatal role of the Hox genes is mostly irrelevant after birth and in compensatory growth. This result is not surprising, as most of the organ positioning should have been finished in the models / time points tested. On the other hand, it cannot be excluded that there still may be some active members of the Hox family in the lung periphery, what may be hidden due to the screening of lung homogenate samples.

Hypoxia-induced mitogenic factor (= HIMF, FIZZ1, RELMα, Resistin-like alpha):

HIMF is a potent pulmonary vasoconstrictor; it is induced by hypoxia and plays a role in different types of lung inflammation. In addition to these functions, an up-regulation in the developing lung, having an anti-apoptotic effect, was shown [169]. Interestingly, in the models studied here, HIMF was exclusively up-regulated three days after pneumonectomy (S3, 2.8fold; → **online supplement**). This finding may be explained in two different ways: Either the molecule is not relevant for both types of alveolarization and the up-regulation may be based on a reaction to inflammatory stimuli (as seen before with other mediators of the immune system; → **3.2**), or there is a specific induction in compensatory lung growth, possibly mediating anti-apoptotic effects in a phase of increasing cell numbers. If the latter influence could be proven, HIMF would be an interesting candidate for further functional studies, being a mitogenic factor specifically regulating adult post-surgery lung growth.

Further candidates:

Although playing an important role in early lung development, **TTF-1** (→ **1.3.1**) did not show any significant regulation after birth or surgery, respectively (→ **online supplement**). While TGF-beta 1 and 3 were not found to be changed, **TGF-beta 2** was induced up to 1.6fold postnatally. Which of its numerous - mostly inhibitory - effects (→ **1.3.1**) is relevant in this phase still needs to be evaluated.

Regarding surfactant molecules, only postnatal **SP-A** showed a significant expressional difference from adult conditions (up to 2.9fold down-regulation (P1); → **online supplement**), while the remaining mRNAs already tended to normal levels. In consequence, the surface tension (represented by SP-B and SP-C; → **1.3.1**) should have reached satisfying conditions even one day after birth, while there was still a lacking defence against microbial attacks; this is in line with other observations of an immature immune system (→ **3.2, 4.2.2**). Although surfactant molecules are essential for a regular lung function, array data imply that they are probably not directly involved in guiding alveolarization. Due to that, further surfactant molecule studies in the frame of the search for molecular mediators of alveolarization would not be promising.

Due to space limitations, only a few interesting candidates could be mentioned within this chapter. Having omitted numerous genes does not mean that they are of no relevance or are necessarily unregulated. For further search, the **online supplement** contains all statistical data of all four experimental groups.

4.3 First candidate gene: Egr1

Egr1 (Early growth response 1) is a transcription factor also known as Krox24, NGFI-A, Zif268, Zfp-6 etc. Being an immediate early gene (for definition see c-Fos description; → **4.2.4**), it is quickly induced by multiple stimuli, e.g. other growth factors, mechanical stretch, hypoxia or radiation (→ **Figure 20**), and it has many, highly context-dependent and often even antagonizing effects (see below) [134].

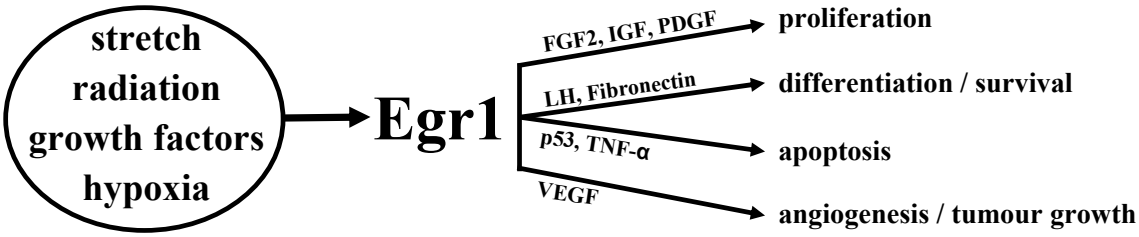

Figure 20: Inducers and downstream effects of Egr1.
The transcription factor Egr1 can be induced by many different stimuli and has numerous influences itself. Here, examples of regulatory chains, their mediators and the resulting cellular responses are given to indicate the broad field of Egr1's interactions (modified from Adamson and Mercola, [134]).

Array data:

In array experiments, Egr1-specific mRNA was found to be down-regulated in newborn mice (factor 0.7 / P1), but more intensively expressed after pneumonectomy (2.3fold / S1; → **3.3**). Although a common regulatory influence on alveolarization in both models was improbable due to these findings, the growth factor with its multiple effects was still regarded as an interesting candidate for functional experiments: Egr1 was among the most intensively induced post-surgery genes (→ **Table 5**), what was more promising for potential future therapies in adult human patients than an isolated postnatal regulation. Additionally, arrays might have depicted a stimulatory as well as an inhibitory level of this molecule due to slightly different relative time points within lung growth, with both regulatory changes fulfilling the needs of a corporate program.
To more obviously monitor the effects of Egr1 and to check their compatibility with the expected growth regulation, overexpression and knockdown studies were performed with different lung cell types (→ **3.6**, see below).

Background:

The Egr1 protein is an 80 kD molecule derived from a posttranscriptionally modified 59 kD polypeptide. It has three zinc finger domains for DNA binding and numerous phosphorylation sites; being generally very short-lived, phosphorylation stabilizes the

protein. Egr1 belongs to a family of growth factors (Egr1 - 4), all binding to the same GC-rich DNA consensus sequence (GCG[G/T]GGGCG) as monomers [134]. The activity of Egr1 can be blocked by binding of one of two specific inhibitors / co-repressors, namely NAB (NGFI-A binding protein) 1 and 2, to the repressive domain [170, 171]. While NAB1 is constitutively expressed, NAB2 seems to be induced by similar stimuli as Egr1 and possibly abrogates excessive stimulations within a negative feedback loop. Apart from these specific interactions, there are numerous interplays with molecules from very different fields of activity, e.g. a competition with the growth factors SP-1 (trans-acting transcription factor 1) and SP-3, which provide basal transcription levels, at overlapping DNA sites [172] or the binding of p53, which induces apoptosis [173]; some of these features will be discussed in detail (see below).
Although being a growth factor with multiple interactions, a knockout of Egr1 is not lethal, probably due to an (at least partial) adoption of its functions by other family members: Affected mice are significantly smaller than wild type animals (lack of growth hormone) and, due to a lack of LH (luteinizing hormone) and the resulting severe affection of their reproductive system, homozygous mutants are infertile [174]. Interestingly, another group not even saw any significant changes in growth and differentiation due to an Egr1 deficiency some years before [175]. This inconsistency may be caused by the different mouse strains used for the studies with imaginable variable degrees of functional overlap with other members of the gene family.

Egr1 functions:

As an overview, basic functions with Egr1 involvement are given here; due to the extremely broad range of interactions, only a selection of target molecules and their effects could be shown.

Being a growth factor, Egr1 plays an important role in promotion of **proliferation**. Examples of well-known target genes are Cyclin D1 (Ccnd1; [176]), platelet-derived growth factors (PDGF) A and B and insulin-like growth factor (Igf) 2 [177]. As the latter candidate was one of the top up-regulated postnatal genes (→ **online supplement**), while Egr1 was found to be less intensively expressed at the same time, there seems to be no link between these genes within the alveolarization models. Interestingly, Ccnd1 paralleled the down-regulation of Egr1 (-50 % at P1; → **online supplement**), even if without the opposite reaction in the post-surgery model. While inducing FGF (fibroblast growth factor) 2 [178], a molecule with multiple functions in proliferation, differentiation and development etc., Egr1 is up-regulated by FGF1 [179],

another member of the same family. The latter candidate was found to be down-regulated by 45 to 50 % in the postnatal model, giving a hint for a possible interaction of both growth factors here. Unfortunately, the stimulation of proliferation can induce growth and invasiveness of **tumours** as well, as shown for prostate cancers [180].

Egr1 can also induce the **differentiation** of cells / organs, as described above: By inducing LH in the pituitary gland, a correct development of the reproductive organs is assured; otherwise, affected individuals may be infertile [174]. In own experiments, LH was not changed postnatally or after surgery, respectively (→ **online supplement**).

Regarding **apoptosis**, Egr1 induces TNFα (tumour necrosis factor alpha) as well as p53, both leading to programmed cell death [181, 182]. These genes were not found to be regulated in own array data (→ **online supplement**). Apart from TNFα regulation, different functions within the **immune system** have also been ascribed to Egr1 [183].

In **angiogenesis**, Egr1 plays a role as well: VEGF (vascular endothelial growth factor), a well-known target gene, is induced in concert with HIF (hypoxia-inducible factor) 1α, [184, 185]. Being a growth factor itself, this molecule has multiple different functional targets including angiogenesis, differentiation, migration, proliferation, apoptosis inhibition etc. However, none of the VEGFs A, B and C was found to be regulated in any experimental group, making an Egr1-driven influence within alveolarization improbable (→ **online supplement**).

Despite all of these promoting activities, Egr1 has **inhibitory effects** as well. One familiar example is TGF-beta, which is directly induced by the growth factor [186] and which was, amongst others, shown to inhibit branching, proliferation of epithelial cells and SP-C expression (→ **1.3.1**, [27]). As no uniform regulation was detectable in both models (→ **online supplement**), a direct interplay could not be assumed here.

Apart from promoting prostate cancer (s.a.), Egr1 is also known to regulate **tumour inhibition**: By induction of PAI-1 (plasminogen activator inhibitor-1; mediated by TGF-beta; [187]), Pten (phosphatase and tensin homolog; [188]), p53 and fibronectin, a protective network is thought to be generated [189]. While PAI-1 and fibronectin increase the attachment of cells to the extracellular matrix to aggravate metastasis formation [190], the other two candidates have proapoptotic effects. According to array data, a postnatal up-regulation of TGF-beta 2 and fibronectin was detected, but a lower expression of Pten; as only the latter one ran conform with Egr1 expression and as none of the genes was changed after surgery (→ **online supplement**), the relevance of the mentioned inhibitory network seemed not to be high during alveolarization.

Another aspect of inhibition could be shown by overexpressing or knocking down the Egr1 protein in tumour cell lines: Growth rates and degree of transformation were inversely related to the amount of Egr1 being present; this was also true when only the DNA-binding zinc-finger domain was overexpressed. The effect was cell type-specific, as it was detected only in lines which had lost the ability of autonomous Egr1 expression; it also did not appear in healthy or immortalized cells [191].

Recently, Egr1 was also shown to participate in **autophagy**: This process of "burning up" cellular mitochondria / organelles (→ **4.2.2**) was mediated by an Egr1-induced up-regulation of the LC3B gene (= MAP1LC3B, microtubule-associated protein 1 light chain 3 beta) in lung tissue of COPD patients [192].

Egr1 and the lung:

Egr1 was found to be up-regulated in array studies of **COPD** lungs [193], what made the growth factor a potential target for treatment of the disease [194] - similar to what was intended with the growth studies presented within this thesis. Another group showed that cigarette smoke induces Egr1 expression in cultured lung epithelial cells, leading to an up-regulation of proinflammatory cytokines, e.g. IL (interleukin)-1β and TNFα [195], which are thought to significantly contribute to COPD development.

Being induced by **hypoxia** in an ischemia / reperfusion model, Egr1 was shown to trigger processes of an **acute lung injury** including inflammatory reactions, blood coagulation and vascular hyperpermeability by up-regulating appropriate genes [136, 196]; as proof of principle, knock-out animals presented with strongly diminished symptoms [136].

Cyclic stretch, e.g. administered by artificial ventilation with high tidal volumes, was shown to transiently up-regulate Egr1 expression [197]. In its function as an immediate early response gene, Egr1 was ascribed to the **MAPK** (mitogen-activated protein kinase) **pathway** here: An increased Ca^{2+} influx due to the cyclic stretch activated the GTPase Ras, which itself mediated an activation of the p44/42 MAPK, leading to Egr1 expression. As Ras (here: Rras2), Egr1 and c-Fos, a further target of this regulatory chain, were concertedly induced after pneumonectomy (→ **Table 5, 4.2.4**), a functional relevance of the MAPK pathway for compensatory lung growth seems to be likely.

Own functional experiments:

Having found divergent regulatory directions for Egr1, i.e. an induction after pneumonectomy, but a lower postnatal expression (→ **3.3, 3.4**), made it difficult to find a common functional background for both lung growth models - unless both detected

values might have mirrored an early and a late stage of the same pathway (s.a.). Functional studies involving different pulmonary cell types (→ **3.6**) were performed to evaluate at least the basic effects probably involved in one or both alveolarization procedures.

Checking the influence on **proliferation**, Egr1 overexpression had a growth-inhibitory effect as significantly fewer cells were found in comparison to empty vector-transfected controls (→ **3.6.1**). This was true for all cell types / lines tested (except for smooth muscle cells, which reacted inconstantly) and made up a loss of about one third of the control cell number. To exclude a toxic effect due to an extreme overexpression of the molecule, the opposite experiment using siRNA to reduce the amount of Egr1-specific mRNA was performed, expecting increased growth ratios this time. Indeed, data showed an up-regulation of final cell numbers in a similar magnitude as seen before (→ **3.6.1**). Another proof of growth inhibition, going even one step further, was the anti-proliferative effect seen when applying the supernatant of transfected cells to untreated cultures (→ **3.6.2**): The cells growing in media from Egr1-overexpressing dishes, which should contain more nutrients due to fewer "consumers", showed a decreased proliferative activity; this was a clear hint for the secretion of inhibitory mediators following the transfection.

Having found a down-regulation of a molecule which has an anti-proliferative effect in consequence means an intended increase in the division ratio of cells; this absolutely matches the situation in the growing postnatal lung. As Egr1 is a potent inducer of cellular differentiation, the main reason for its lower expression at P1 may also be the need of numerous immature, actively dividing cells in this early stage of lung growth. On the other hand, having found an up-regulation of Egr1 after pneumonectomy may be a sign for an exclusive pro-proliferative growth factor activity without the need of inhibition of differentiation, as most of the adult lung cells should be mature; in this case, an interplay with factors different from those in newborn mice would have to be expected. Additionally, other reasons for the up-regulation after surgery may be an increased degree of inflammation (even in comparison to sham animals; → **3.2, 4.2.2**) or a hypoxic situation within the first time after removal of the left lobe. The latter points would match the known wide spectrum of Egr1 (s.a.), but, if being true, also lower its value as a potential growth initiator in adult individuals.

Coming to the **apoptosis** studies (→ **3.6.3**), Egr1 overexpression was shown to increase the fraction of apoptotic cells in comparison to empty vector-transfected controls, what

is a good justification for the slower proliferation described above. As typical apoptosis inducers like TNFα and p53 were not found to be regulated in array experiments (→ **online supplement**), also less well-known candidates may have been involved.
Due to practical reasons (e.g. cell numbers, reproducibility), only one cell type, namely the A549 cell line, could be evaluated in flow cytometry. This may explain the high basal apoptosis rate of about 20 %; apart from this, one has to take into account that in malignant cells physiological mechanisms may be altered and non-transformed cells may have shown a different behaviour.

Studying **migration and adhesion** (→ **3.6.4, 3.6.5**), Egr1 was found not to change these parameters. The only exception was the migratory behaviour of A549 cells, which tended to increase due to higher Egr1 levels. As this line was the only epithelial cell type evaluated here, one might assume that the growth factor specifically supports the locomotoric activity of future AECs within alveolarization. This would be in line with the detected regulation in the surgery model, but not with that of the postnatal stage, where even more cellular movements have to be made.
One effect of Egr1 is to provide a scaffold, protecting from malignant invasions (s.a.), mirrored e.g. by an increased adhesion. This would match a postnatal down-regulation as here proliferative and locomotoric activities could be disturbed by high Egr1 levels. Having found no effect at all in the adhesion study may either be due to technical reasons or because the "protecting network" (s.a.) is the result of an interplay of numerous factors, and essential Egr1 interaction partners were missing.

According to **localization**, in immunofluorescence stainings (→ **3.6.6, Figure 14**), Egr1 was found to be intensively expressed in SP-C-positive bronchial epithelial cells and, to a smaller degree, in alveolar septal cells, where it was emphasized in AECs II. There was no co-localization with other cell type-specific markers, qualifying epithelial cells as potential key players of Egr1 function within alveolarization. The detection of a postnatal down-regulation of the growth factor seems to have been caused by a less intensive bronchial expression, while septal levels remained approximately constant.
Having found Egr1 mainly in the cytoplasm of positive cells and only sometimes within the nuclei may be a hint for a global "expecting" status, waiting for external coordinating stimuli before nuclear translocation of the growth factor. As Egr1 is, if not phosphorylated, very short-lived (s.a.), a high turn-over with most of the molecules not becoming active at all is probable, which was underlined by numerous degradation products in Western blot experiments (not shown).

Coming to in-situ hybridizations depicting Egr1-specific mRNA (→ **3.6.6, Figure 15**), a similar localization as in immunofluorescence could be shown: In adult mice, the expression / de-novo generation accumulated in bronchi, while these structures were only weakly stained in newborn animals. Postnatal lungs presented numerous single positive septal cells, which may be regarded as (mostly) AECs II. Interestingly, in-situ hybridizations revealed a new area of overexpression in pneumonectomized animals: In the tips of the remaining lobes, where the most intensive stimulation due to distension forces could be expected, many cells expressed Egr1-specific mRNA. This is conform with the behaviour known from cyclic stretch involving the MAPK pathway, of which several candidates were found to be up-regulated after surgery (s.a.).
Taken together, both staining techniques detected AECs II / septal epithelial cells as the probably most relevant Egr1-expressing cells within the growing lung.

Summary:

Egr1 is a growth factor with multiple different interaction partners and numerous effects covering most of the known cellular processes. Having found a postnatal down-regulation of this anti-proliferative, pro-apoptotic molecule fits the needs of high division ratios within alveolarization, but may also depict a diminished necessity of differentiation. Stainings revealed single alveolar septal cells of both models to (over-) express Egr1, potentially emphasizing a local pro-proliferative influence of the growth factor within this lung region.
The pneumonectomy model, showing an up-regulation of Egr1, probably involves the MAPK signalling pathway, as some additional members of this regulatory chain were found to be overexpressed as well. In consequence, not only Egr1, but also these candidates should be further studied in order to find targets for potential tissue regrowth. In a first step, lungs of Egr1-knockout or -overexpressing mice may be stereologically quantified to curtail the degree of influence the growth factor has on both models presented here.

4.4 Second candidate gene: Stefin A1

With a regulation factor of > 32, Stefin A1 was one of the most intensively up-regulated genes in all experimental settings (→ **3.2, 3.3**); including this molecule, six of the top 10 most intensively up-regulated genes in the postnatal period had a cysteine protease inhibitor function (→ **Table 6**). These findings clearly indicated an important role within alveolarization of newborn mice, justifying further functional studies, although no regulation was detectable in the pneumonectomy model (→ **online supplement**).

Table 6: Cysteine protease inhibitors among the top 10 postnatally up-regulated genes.
The genes are given with their individual **rank**, accession number (**Acc.-No.**), **name(s)** and regulation factor (**Fold change**).

Top 10 rank	Acc.-No.	Name	Alternative / full name	Fold change
1	NM_029733	**2010005H15Rik**		35.75
2	NM_001001332	**Stfa1**	**Stefin A1**	32.90
3	M92418	**Stfa2**	**Stefin A2**	25.11
5	NM_173869	**LOC268885**	**Stfa2l1 = Stefin A2 like 1**	21.86
7	NM_025088	**Stfa3**	**Stefin A3**	20.97
10	XM_148650	**LOC209294**	**Cystatin A = Stefin A**	13.45

Background:

Stefin A1 belongs to the **Cystatin super-family**. The appropriate molecules contain up to three cystatin domains, each implementing a cysteine protease inhibitor function. One domain consists of about 100 amino acids and has the structure of a five-stranded β-sheet, partially wrapped around a central α-helix [198].

In their best-known function, the family members competitively block papain-type proteolytic enzymes, defined by a combination of a cysteine (making up the name "cysteine proteases") and a basic (mostly histidine) residue in their active site. According to localization and structure, the super-family can be divided into at least five different groups, namely Stefins, Cystatins, Latexins, Fetuins and Kininogens [199].

Both having only a single cystatin domain, the main difference between the first two of these sub-families is the localization: Stefins (Stf) are mostly found intracellularly, while Cystatins (Cst) are secreted molecules. For discrimination, the former ones, which are also called Cystatins nowadays, were given alphabetic character codes (StfA - D = CstA - D), and the latter molecules received arabic numbers (Cst1 - 14) [199]. While Stefins consist of about 100 amino acids, Cystatins are a little larger and more complex, i.e. they contain about 140 amino acids (with about 20 serving as extracellular signalling peptide) as well as two disulphide bridges [200].

In the following, the focus is directed to Stefin A, as numerous subtypes of this cysteine protease inhibitor were found to be regulated (→ **Table 6**). The primary **function** of Stefin A is the inhibition of intracellular cysteine proteases, mainly lysosomal Cathepsins (e.g. type B, H, L and S), but also of other enzymes like Calpains, Legumains or ubiquitin processing and recycling endopeptidases [199].

High concentrations of Stefin A were found in epithelial cell types (e.g. in the epidermis of postnatal mice; [201]) and different members of the immune system (s.b.) [202]; additionally, the molecule was detected in serum samples and **extracellular matrix (ECM)** regions. In the epidermal ECM, Stefin A was found to contribute to the bacteriostatic properties of the skin [203], probably by inhibiting the proteolytic activities of bacteria being necessary for invasion [204].

According to the **immune system**, Stefin A was for example found in polymorphonuclear granulocytes; additionally, follicular dendritic cells in the germinal centres of tonsils were shown to express the molecule [205]. Here, Stefin A was thought to prevent B lymphocytes from apoptosis [206]: This process can be induced by Cathepsins [207], which are in turn main targets of the cysteine protease inhibitor discussed here. Coming to another aspect, Cathepsins S and L, which play an important role in endosomal and lysosomal antigen processing and presentation [208], were shown to be effectively inhibited by Stefin A [209].

Apart from their typical protease inhibitor function, several other immunological functions were ascribed to Cystatins in general, mediated via putative cystatin-binding cell surface molecules: They can stimulate a nitric oxide release from macrophages [210], modulate respiratory burst and phagocytosis in neutrophils [211] and alter the interleukin / cytokine production [212].

Cystatins are often mentioned in connection with **tumour** growth and severity. According to Stefin A, it was shown that the expression of this molecule is often lost with tumour progression, e.g. in breast, prostate and lung cancer [213-215], and that it is able to reduce the motility of malignant cells when exogenously administered [216]. The inverse correlation between Stefin A expression and degree of malignancy is supported by the fact that in many tumours Cathepsin B is overexpressed. Due to the missing inhibitor, this protease can subsequently cause an increased invasiveness of the malignant cells by degrading protective matrix tissue. Following this line, Li et al. showed that an overexpression of Stefin A in an oesophageal squamous cell carcinoma was able to significantly inhibit / reduce several aspects of tumour severity, namely

growth speed, associated angiogenesis, invasiveness and metastasis formation; these effects were primarily mediated by inhibiting Cathepsin B [217].
On the other hand, if Stefin A is exceptionally expressed in cancer, the average outcome of patients seems to be worse [213], probably due to the extreme malignancy overwhelming the inhibitory function.

When talking about Stefins and their effects, one should not ignore the **target molecules**. Especially **Cathepsins** are known to be involved in many extra- and intracellular processes like ECM degradation (e.g. digestion of Elastin, Laminin, Fibronectin, different Collagens etc.), cell motility and adhesion (e.g. tumour invasiveness, ECM organization, migration of immune cells), angiogenesis and cell signalling (e.g. by cleaving surface molecules on immune cells) [218, 219]. Some further examples for Cathepsin-specific effects are: Type S mediates antigen presentation via MHC-II molecules [220] and type L regulates kerationcyte differentiation [221]; Cathepsin K steers bone remodelling [222], while type D has mitogenic properties [223].
As all of these enzymes can be inhibited by Stefins (or other Cystatins), an indirect participation of the inhibitory molecules in numerous intra- and extracellular processes is given. This makes the protease inhibitors interesting candidates for numerous experimental questions as well.

Own experiments:

Having validated the extreme up-regulation found in array experiments also for protein levels, subsequently the localization and cell type-specificity of Stefin A1 was checked (→ **3.2, 3.7.1, 3.7.2**). Using **immunofluorescence**, a largely constant expression was detected in bronchial epithelial cells of all models and time points, complemented by low levels in septal cells. Interestingly, in postnatal lungs large amounts of single septal cells with intensive positive staining were found additionally (→ **Figure 17A + B**), obviously being the reason for the detected up-regulation.
Due to the fact that no co-staining for immune cells or cell type markers different from cytokeratin revealed an obvious and constant co-localization with Stefin A1, these single overexpressing cells can be regarded as (mostly) AECs. From their position, many of them may be classified as AECs II, but some are also type I cells involved in secondary septum formation, e.g. being situated on the top of outgrowing tips.
Performing cell culture, both lung cell lines tested (human: A549; mouse: MLE-12) validated the finding of an epithelial expression. Especially in A549 cells it could be

nicely shown that Stefin expression is locally enhanced in regions with intercellular contacts (→ **Figure 17G**) where the degrading influence of Cathepsins would be deleterious.
The findings from immunofluorescence stainings could be validated using **in-situ hybridizations** (→ **Figure 18**), where also numerous single septal cells were positive. Here, the ratio of cells expressing Stefin A1-specific mRNA within the tips of secondary septae appeared to be slightly higher than that of the protein level.

Taken together, in addition to the common bronchial expression, Stefin A1 was found to be intensively expressed in single septal / epithelial cells of postnatal lungs, what can be explained with the need of massive tissue generation within this phase: Any inappropriate affection of the septal cells or, more important, the ECM, by Cathepsins or other degrading enzymes would severely damage the growing tissue and either cause structural abnormalities or reveal the necessity of rebuilding structures by the expense of energy and supplies. Due to that, the extensive generation of inhibitory molecules like Stefin A1, which can stop the action of cysteine proteases within cells as well as within the ECM (s.a.) can be regarded as a suitable way of self protection.
Another reason for the extreme expression levels may be an immunological: As the immune system is still very immature in this early stage of development (→ **4.2.2**), Stefins may be intended to be disposed in the ECM of the postnatal lung to fulfil a similar bacteriostatic function as shown for the epidermis (s.a.; [203]). As the lung comes into contact with microorganisms from the outer environment immediately after birth, an additional basal, rather unspecific protection would help the young animals to survive.
The extensive postnatal growth always bears the risk of cancer development. Due to that, Stefin A's role in tumour inhibition (s.a.) may also be of some importance. As the cells with extreme expression showed no co-localization with the proliferation marker Ki-67 (→ **Figure 17B**), this idea looks rather improbable. What may be more reasonable is the known influence of Cathepsin L on the regulation of keratinocyte differentiation (s.a.): If this molecule is also intensively involved in AEC maturation, there needs to be a certain stop point not to allow the protease to immediately destroy the "ready" cells again. This may be implemented by a strong Stefin A expression.
Having found no single septal cells with extreme Stefin A1 overexpression in the pneumonectomy model (→ **Figure 17E + F, Figure 18D**) is a little surprising as there's also the need of tissue and ECM generation as well as mitosis and maturation within

proven growth processes (→ **1.4.4**). To explain this finding implicating the ideas discussed above, there may be less need of ECM restructuring and of immunological influence in the operated lung due to the higher degree of maturity. Additionally, the relative time points within alveolarization are probably not completely identical in both models, meaning that the moment of cellular maturation, ECM alterations etc. may not be clearly visible in the one and three day post-surgery lungs.

Coming to the **functional experiments** (→ **3.7.3, Figure 19**), it has to be stated that human cells only express one type of Stefin A, while mice have more (A1 - 3, A2 like 1 etc.). According to the examined species, the appropriate nomenclature will be used.

Overexpressing Stefin A(1), changes in the **proliferative behaviour** were studied first (→ **Figure 19A**): While fibroblasts reacted indifferently, the epithelial cell types revealed contrary results as mouse cells (MLE-12) increased their ratio of mitosis, while human cells (A549) tended to grow slower. This finding may be explained either with (rather improbable) inter-species reaction differences or with the cell culture environment: As the usage of a single cell type can never completely resemble a real in-vivo situation, important interaction partners may simply be missing, leading to atypical reactions in one case, while the other cell type may receive necessary "stimulators" with the culture medium. One also should not forget that both epithelial cell types tested here are cell lines, i.e. cancer cells. Although reacting like untransformed tissue in most of the cases, special features / behaviours may be altered by the mutations leading to malignancy. This is supported by the fact that normally cancer cells do not express Stefin A(1) any more (s.a.), while the molecule was detectable within A549 and MLE-12 cells (→ **Figure 17G + H**).

Checking **migration** (→ **Figure 19B**), there was no clear tendency of in- or decrease detectable. Although this may have been caused by the low number of experiments, the most probable explanation is the need of interplay with other cell types. As Stefin A is basically an enzyme inhibitor (s.a.), its amount does not necessarily need to change the behaviour of single (cultured) cells. The environment, i.e. other cell types and ECM, can be expected to play a more important role than in case of e.g. growth factor application (→ **4.3**).

Coming to **adhesion** (→ **Figure 19C**), there was a small, but significant increase in the adherence to Fibronectin and (in tendency) to Collagen. This fits to the function of Stefin as an inhibitor of ECM-degrading proteases: The less Cathepsins etc. are active,

the better the respective cells can adhere to "sticky" surfaces, while there was no difference in the control group (BSA-coated wells). This finding was supported by the fact that, although not significant, the majority of siRNA experiments showed an opposite reaction in case of Stefin A knockdown, resulting in fewer cysteine protease inhibitors as usual. Surprisingly, the adhesion to Collagen decreased in Stefin-overexpressing fibroblasts. Although being significant, the practical relevance of this finding is questionable, as the detected difference is minimal. If there was any real effect, it may be explained with the overexpression of the inhibitory molecule in an untypical, normally non-Stefin A-expressing cell type, leading to rather untypical behaviour.

Summary:

Being strongly up-regulated in postnatal lung tissue, several subtypes of Stefin A can be assumed to play an important role in regular alveolarization. Inhibiting cysteine proteases, their main function is probably based on preventing ECM degradation, but also other aspects like bacteriostatic effects or influencing cellular maturation have to be considered. In functional studies, no clear association with proliferation and migration could be detected, while there was an increase in adhesion due to Stefin A overexpression.

Unfortunately, there was no detectable Stefin A1 regulation after pneumonectomy, making the molecule a less promising candidate for future lung regrowth approaches in adult humans.

From the functional point of view, experiments simultaneously changing the concentrations of Stefin A1 and different Cathepsins, which were mostly unregulated in array studies (→ **online supplement**), in identical as well as opposite directions might be interesting, as Stefin effects could become more obvious.

To elucidate the complete band with of influences Stefin A1 has on alveolarization, studies should be performed in an appropriate environment, i.e. in vivo. For this approach, knockout and / or overexpressing animals should be generated, enabling structural analyses and stereological quantifications.

4.5 Conclusions and outlook

Comparing postnatal and post-pneumonectomy lung growth, the intention of the study presented here was to see whether there are genes involved in both processes and, if yes, what may be their actual function. Doing so, the imaginable future goal was to find a way of potentially inducing lung tissue regrowth in severely handicapped patients by reactivating or inhibiting the most promising intersection genes (→ **1.5**).

Having found more than 1,600 candidates in both postnatal time points, there were less than 200 significantly regulated genes on each post-pneumonectomy day (→ **3.1**); this difference probably resulted from the extreme discrepancy in maturity in the former studies. A model intersection of 58 genes sounded promising at a first glance, and indeed, there were several candidates with known participation in lung growth being uniformly up-regulated, e.g. some collagens and Elastin (→ **3.3, 4.2.3**). On the other hand, 18 genes with opposing regulatory directions were found, which may have been detected just "by accident", i.e. as false positives due to statistical reasons, or which may represent various regulatory stages at different relative time points within alveolarization. A closer look onto candidates like c-Fos and Egr1 revealed multiple, sometimes even contrary functions, which may explain the findings (→ **4.2.4, 4.3**).

Although there were several intersection genes, it can still not be clearly stated whether postnatal and compensatory lung growth are guided by the same genes. If so, these candidates should have been detected by the array screens, and in the following, interaction partners and involved pathways would have to be clearly elucidated; if not, also genes with a detection in only one model would come into play, e.g. Stefin A1 with its extreme up-regulation (→ **3.7, 4.4**). In this case, candidates found in the surgery model might be preferable as they should better resemble the adult (patient) situation.

One disadvantage of the microarray studies presented here is the usage of lung homogenate as this means a general pooling of RNA from all lung cell types; this bears the risk of overlooking interesting candidates due to the mixture of contrary regulatory directions. On the other hand, one had to find a reasonable starting point for experiments, and a preselection of cell types also has disadvantages as either the manipulation procedure may affect the target mRNA composition or the real molecular interplay necessary for a proper alveolarization may not be mirrored correctly. In further steps, selection techniques like microdissection should be used to verify the regulatory change of candidate genes in the expected cell types and to examine dependent pathways.

To reduce the risk of false selection, it may be worth to further curtail the number of candidate genes, e.g. by introducing an additional model like the glucocorticoid treatment or the refeeding procedure (→ **1.4.1, 1.4.2**) or by studying human samples. The latter ones could be taken in different stages of chronic diseases in order to elucidate the degree of influence of certain candidates and to see whether the worsening can be reversed.

Having finally found candidate genes like Egr1 and Stefin A1 (→ **4.3, 4.4**), which may indeed influence / (re)induce lung growth, has to be followed by in-vivo studies validating the expected effects. For this issue, constitutive and / or inducible knockout or knockin mice should be evaluated.

One major risk of selecting genes just from an array list is to ignore or underestimate the overall interplay of molecules within living organisms, meaning that although the expected effect of a candidate gene might be seen, its overexpression or knockdown could have side-effects severely harming the individual. Even if this could be excluded in extensive animal studies, it would not mean that a transfer to another species, e.g. humans, could be easily performed. There might always be interactions with up-to-date unknown gene products or metabolites disturbing or endangering the success of a gene therapy. Due to that, every trial to genetically manipulate "natural" conditions especially in sick individuals has to be weighed thoroughly.

Although only being a first step on a long way to potential lung regrowth, the study presented within this thesis revealed interesting candidate genes potentially involved in one or both evaluated types of lung growth. Further experiments will try to prove their value using in-vivo models.

4.6 Summary: Results of the study

Within the study presented here, following goals of a microarray approach searching for genes involved in the regulation of postnatal and / or compensatory lung growth were achieved:

- A mouse model for compensatory lung growth after left-sided pneumonectomy was established.
- Microarray data depicting mRNA expression levels in postnatal as well as post-pneumonectomy lungs were generated for two different time points each.
- Studying the significantly regulated genes, more than 1,600 candidates were found in both postnatal time points, while less than 200 were regulated on each post-surgery day. The intersection constituted 58 genes.
- For validation of array data, selected intersection genes were re-quantified using real-time PCR. Some promising candidates were also measured on protein level.
- The expression of the most interesting genes was localized on mRNA and protein level, followed by functional analyses:
    - With Egr1, a growth factor, being down-regulated postnatally, but induced after pneumonectomy, was found. An anti-proliferative, pro-apoptotic effect of Egr1, mediated by secreted molecules, was demonstrated, and a bronchial and AEC II-specific expression was complemented by single peripheral overexpressing cells in both models. For compensatory growth, a participation of the MAPK signalling pathway was regarded as probable.
    - The cysteine protease inhibitor Stefin A1 was among the most intensively up-regulated postnatal genes. Mainly interacting with Cathepsins, its goal in lung growth was probably the inhibition of ECM degradation. The molecule was found to increase the adhesion tendency of epithelial cells.
- Having found some, but not many intersection candidates between the models, a common regulatory mechanism cannot be excluded, but is also not highly probable. At least molecules definitively known to be essential for lung growth like collagens and Elastin were likewise up-regulated.

Important aspects of the data presented within this thesis were published in the European Respiratory Journal [116].

4.7 Zusammenfassung

Hintergrund und Ziel: Obwohl zunehmend mehr Patienten an chronisch-destruktiven Lungenerkrankungen leiden, ist die bislang einzige „Heilung“ eine Transplantation. Falls man am Lungenwachstum beteiligte Gene ausfindig machen und reaktivieren könnte, wäre es ggf. möglich, eigenes Gewebe nachwachsen zu lassen. In einem ersten Schritt wurde nun in zwei Maus-Modellen nach solchen Regulatoren gesucht.

Material und Methoden: Mittels Microarry-Screening wurde bei postnatalen und sich im kompensatorischen Wachstum befindenden Mäuse-Lungen zu jeweils zwei Zeitpunkten nach differentiell regulierten Genen gesucht. Aus der statistischen Analyse hervorgehende interessante Kandidaten wurden mittels Real-time-PCR und Western blot validiert, auf ihre Lokalisation in der Lunge hin untersucht und schließlich funktionellen Tests unterzogen.

Ergebnisse: Es konnten pro Zeitpunkt über 1.600 postnatal regulierte Gene gefunden werden, jedoch jeweils nur knapp 200 im Pneumonektomie-Modell; die Schnittmenge betrug 58 Gene. Zwei interessante Kandidaten waren der Wachstumsfaktor Egr1 und der Cystein-Protease-Inhibitor Stefin A1. Für ersteres Molekül konnte gezeigt werden, daß es einen anti-proliferativen, pro-apoptotischen Effekt auf die meisten Lungen-Zelltypen ausübt, welcher über sezernierte Moleküle vermittelt wird. Ein Typ II- und Bronchialepithel-spezifisches Expressionsmuster wurde in beiden Modellen noch um einzelne, in der Lungenperipherie liegende, überexprimierende Zellen ergänzt. Für das kompensatorische Wachstum wurde Egr1 eine Mediator-Rolle im Rahmen des MAPK-Pathways zugeschrieben. Stefin A1 war eines der postnatal am intensivsten hochregulierten Gene; seine Aufgabe im Rahmen des Lungenwachstums besteht wahrscheinlich in einer Hemmung Matrix-abbauender Cathepsine. Für Stefin A1 konnte ein Adhäsions-steigernder Effekt bei Epithelzellen nachgewiesen werden.

Diskussion und Ausblick: In beiden Modellen wurden zahlreiche regulierte Gene gefunden, wobei die Schnittmenge sich in Grenzen hielt. Falls es sich bei den gefundenen Kandidaten, neben den bekanntermaßen am Lungenwachstum beteiligten (z.B. Kollagene und Elastin), nicht um zentrale Steuerelemente handelt, wäre es möglich, daß beide Prozesse über unabhängige Wege gesteuert werden. Weitere funktionelle und In-vivo-Experimente sollen unter anderem diese Fragestellung klären.

Wichtige Teile der hier vorgestellten Daten wurden im European Respiratory Journal veröffentlicht [116].

References

1. McDonald JA. Lung Growth and Development. In: Lenfant C, ed. Lung Biology in Health and Disease. Dekker, 1997; pp. 1-33.
2. Bucher U, Reid L. Development of the intrasegmental bronchial tree: the pattern of branching and development of cartilage at various stages of intra-uterine life. Thorax 1961: 16: 207-218.
3. Boyden E. Development and growth of the airways. Dekker, New York, 1977.
4. Davies G, Reid L. Growth of the alveoli and pulmonary arteries in childhood. Thorax 1970: 25(6): 669-681.
5. Schittny JC, Djonov V, Fine A, Burri PH. Programmed cell death contributes to postnatal lung development. Am J Respir Cell Mol Biol 1998: 18(6): 786-793.
6. Massaro D, Teich N, Maxwell S, Massaro GD, Whitney P. Postnatal development of alveoli. Regulation and evidence for a critical period in rats. J Clin Invest 1985: 76(4): 1297-1305.
7. Morishige WK, Joun NS. Influence of glucocorticoids on postnatal lung development in the rat: possible modulation by thyroid hormone. Endocrinology 1982: 111(5): 1587-1594.
8. Henning SJ. Plasma concentrations of total and free corticosterone during development in the rat. Am J Physiol 1978: 235(5): E451-456.
9. Burri PH. The postnatal growth of the rat lung. 3. Morphology. Anat Rec 1974: 180(1): 77-98.
10. le Cras TD, Markham NE, Morris KG, Ahrens CR, McMurtry IF, Abman SH. Neonatal dexamethasone treatment increases the risk for pulmonary hypertension in adult rats. Am J Physiol Lung Cell Mol Physiol 2000: 278(4): L822-829.
11. Sahebjami H, Domino M. Effects of postnatal dexamethasone treatment on development of alveoli in adult rats. Exp Lung Res 1989: 15(6): 961-973.
12. Maden M, Hind M. Retinoic acid, a regeneration-inducing molecule. Dev Dyn 2003: 226(2): 237-244.
13. Hind M, Maden M. Retinoic acid induces alveolar regeneration in the adult mouse lung. Eur Respir J 2004: 23(1): 20-27.
14. Maden M, Hind M. Retinoic acid in alveolar development, maintenance and regeneration. Philos Trans R Soc Lond B Biol Sci 2004: 359(1445): 799-808.

15. Belloni PN, Garvin L, Mao CP, Bailey-Healy I, Leaffer D. Effects of all-trans-retinoic acid in promoting alveolar repair. Chest 2000: 117(5 Suppl 1): 235S-241S.

16. Chinoy MR. Lung growth and development. Front Biosci 2003: 8: d392-415.

17. Blanco LN, Massaro D, Massaro GD. Alveolar size, number, and surface area: developmentally dependent response to 13% O2. Am J Physiol 1991: 261(6 Pt 1): L370-377.

18. Tenney SM, Remmers JE. Comparative quantitative morphology of the mammalian lung: diffusing area. Nature 1963: 197: 54-56.

19. Massaro GD, Massaro D, Chan WY, Clerch LB, Ghyselinck N, Chambon P, Chandraratna RA. Retinoic acid receptor-beta: an endogenous inhibitor of the perinatal formation of pulmonary alveoli. Physiol Genomics 2000: 4(1): 51-57.

20. Bellabarba D, Fortier S, Belisle S, Lehoux JG. Triiodothyronine nuclear receptors in liver, brain and lung of neonatal rats. Effect of hypothyroidism and thyroid replacement therapy. Biol Neonate 1984: 45(1): 41-48.

21. Morishige WK, Joun NS, Guernsey DL. Thyroidal influence on postnatal lung development in the rat. Endocrinology 1982: 110(2): 444-451.

22. Massaro D, Teich N, Massaro GD. Postnatal development of pulmonary alveoli: modulation in rats by thyroid hormones. Am J Physiol 1986: 250(1 Pt 2): R51-55.

23. Lazzaro D, Price M, de Felice M, Di Lauro R. The transcription factor TTF-1 is expressed at the onset of thyroid and lung morphogenesis and in restricted regions of the foetal brain. Development 1991: 113(4): 1093-1104.

24. Kimura S, Hara Y, Pineau T, Fernandez-Salguero P, Fox CH, Ward JM, Gonzalez FJ. The T/ebp null mouse: thyroid-specific enhancer-binding protein is essential for the organogenesis of the thyroid, lung, ventral forebrain, and pituitary. Genes Dev 1996: 10(1): 60-69.

25. Massague J. TGFbeta signaling: receptors, transducers, and Mad proteins. Cell 1996: 85(7): 947-950.

26. Roberts AB, Thompson NL, Heine U, Flanders C, Sporn MB. Transforming growth factor-beta: possible roles in carcinogenesis. Br J Cancer 1988: 57(6): 594-600.

27. Bragg AD, Moses HL, Serra R. Signaling to the epithelium is not sufficient to mediate all of the effects of transforming growth factor beta and bone

morphogenetic protein 4 on murine embryonic lung development. Mech Dev 2001: 109(1): 13-26.

28. Kaartinen V, Voncken JW, Shuler C, Warburton D, Bu D, Heisterkamp N, Groffen J. Abnormal lung development and cleft palate in mice lacking TGF-beta 3 indicates defects of epithelial-mesenchymal interaction. Nat Genet 1995: 11(4): 415-421.

29. Laughon A, Scott MP. Sequence of a Drosophila segmentation gene: protein structure homology with DNA-binding proteins. Nature 1984: 310(5972): 25-31.

30. Kappen C. Hox genes in the lung. Am J Respir Cell Mol Biol 1996: 15(2): 156-162.

31. Aubin J, Lemieux M, Tremblay M, Berard J, Jeannotte L. Early postnatal lethality in Hoxa-5 mutant mice is attributable to respiratory tract defects. Dev Biol 1997: 192(2): 432-445.

32. Korfhagen TR, Sheftelyevich V, Burhans MS, Bruno MD, Ross GF, Wert SE, Stahlman MT, Jobe AH, Ikegami M, Whitsett JA, Fisher JH. Surfactant protein-D regulates surfactant phospholipid homeostasis in vivo. J Biol Chem 1998: 273(43): 28438-28443.

33. Korfhagen TR, Bruno MD, Ross GF, Huelsman KM, Ikegami M, Jobe AH, Wert SE, Stripp BR, Morris RE, Glasser SW, Bachurski CJ, Iwamoto HS, Whitsett JA. Altered surfactant function and structure in SP-A gene targeted mice. Proc Natl Acad Sci U S A 1996: 93(18): 9594-9599.

34. Botas C, Poulain F, Akiyama J, Brown C, Allen L, Goerke J, Clements J, Carlson E, Gillespie AM, Epstein C, Hawgood S. Altered surfactant homeostasis and alveolar type II cell morphology in mice lacking surfactant protein D. Proc Natl Acad Sci U S A 1998: 95(20): 11869-11874.

35. Ikegami M, Whitsett JA, Jobe A, Ross G, Fisher J, Korfhagen T. Surfactant metabolism in SP-D gene-targeted mice. Am J Physiol Lung Cell Mol Physiol 2000: 279(3): L468-476.

36. Clark JC, Wert SE, Bachurski CJ, Stahlman MT, Stripp BR, Weaver TE, Whitsett JA. Targeted disruption of the surfactant protein B gene disrupts surfactant homeostasis, causing respiratory failure in newborn mice. Proc Natl Acad Sci U S A 1995: 92(17): 7794-7798.

37. Glasser SW, Burhans MS, Korfhagen TR, Na CL, Sly PD, Ross GF, Ikegami M, Whitsett JA. Altered stability of pulmonary surfactant in SP-C-deficient mice. Proc Natl Acad Sci U S A 2001: 98(11): 6366-6371.

38. Rottier R, Tibboel D. Fetal lung and diaphragm development in congenital diaphragmatic hernia. Semin Perinatol 2005: 29(2): 86-93.

39. van den Hout L, Sluiter I, Gischler S, De Klein A, Rottier R, Ijsselstijn H, Reiss I, Tibboel D. Can we improve outcome of congenital diaphragmatic hernia? Pediatr Surg Int 2009: 25(9): 733-743.

40. Lally KP. Congenital diaphragmatic hernia. Curr Opin Pediatr 2002: 14(4): 486-490.

41. Boloker J, Bateman DA, Wung JT, Stolar CJ. Congenital diaphragmatic hernia in 120 infants treated consecutively with permissive hypercapnea/spontaneous respiration/elective repair. J Pediatr Surg 2002: 37(3): 357-366.

42. Chinoy MR. Pulmonary hypoplasia and congenital diaphragmatic hernia: advances in the pathogenetics and regulation of lung development. J Surg Res 2002: 106(1): 209-223.

43. Clugston RD, Klattig J, Englert C, Clagett-Dame M, Martinovic J, Benachi A, Greer JJ. Teratogen-induced, dietary and genetic models of congenital diaphragmatic hernia share a common mechanism of pathogenesis. Am J Pathol 2006: 169(5): 1541-1549.

44. Montedonico S, Sugimoto K, Felle P, Bannigan J, Puri P. Prenatal treatment with retinoic acid promotes pulmonary alveologenesis in the nitrofen model of congenital diaphragmatic hernia. J Pediatr Surg 2008: 43(3): 500-507.

45. Tibboel D, Gaag AV. Etiologic and genetic factors in congenital diaphragmatic hernia. Clin Perinatol 1996: 23(4): 689-699.

46. Klaassens M, Galjaard RJ, Scott DA, Bruggenwirth HT, van Opstal D, Fox MV, Higgins RR, Cohen-Overbeek TE, Schoonderwaldt EM, Lee B, Tibboel D, de Klein A. Prenatal detection and outcome of congenital diaphragmatic hernia (CDH) associated with deletion of chromosome 15q26: two patients and review of the literature. Am J Med Genet A 2007: 143A(18): 2204-2212.

47. Deprest J, Jani J, Van Schoubroeck D, Cannie M, Gallot D, Dymarkowski S, Fryns JP, Naulaers G, Gratacos E, Nicolaides K. Current consequences of prenatal diagnosis of congenital diaphragmatic hernia. J Pediatr Surg 2006: 41(2): 423-430.

48. Migliazza L, Bellan C, Alberti D, Auriemma A, Burgio G, Locatelli G, Colombo A. Retrospective study of 111 cases of congenital diaphragmatic hernia treated with early high-frequency oscillatory ventilation and presurgical stabilization. J Pediatr Surg 2007: 42(9): 1526-1532.

49. Kinsella JP, Abman SH. Inhaled nitric oxide in the premature newborn. J Pediatr 2007: 151(1): 10-15.

50. Michelakis E, Tymchak W, Lien D, Webster L, Hashimoto K, Archer S. Oral sildenafil is an effective and specific pulmonary vasodilator in patients with pulmonary arterial hypertension: comparison with inhaled nitric oxide. Circulation 2002: 105(20): 2398-2403.

51. Cilley RE, Zgleszewski SE, Krummel TM, Chinoy MR. Nitrofen dose-dependent gestational day-specific murine lung hypoplasia and left-sided diaphragmatic hernia. Am J Physiol 1997: 272(2 Pt 1): L362-371.

52. Bartlett D, Jr. Postnatal growth of the mammalian lung: influence of low and high oxygen tensions. Respir Physiol 1970: 9(1): 58-64.

53. Bucher JR, Roberts RJ. The development of the newborn rat lung in hyperoxia: a dose-response study of lung growth, maturation, and changes in antioxidant enzyme activities. Pediatr Res 1981: 15(7): 999-1008.

54. Warner BB, Stuart LA, Papes RA, Wispe JR. Functional and pathological effects of prolonged hyperoxia in neonatal mice. Am J Physiol 1998: 275(1 Pt 1): L110-117.

55. Frank L, Bucher JR, Roberts RJ. Oxygen toxicity in neonatal and adult animals of various species. J Appl Physiol 1978: 45(5): 699-704.

56. Burri PH, Weibel ER. Morphometric estimation of pulmonary diffusion capacity. II. Effect of Po2 on the growing lung, adaption of the growing rat lung to hypoxia and hyperoxia. Respir Physiol 1971: 11(2): 247-264.

57. Asikainen TM, White CW. Pulmonary antioxidant defenses in the preterm newborn with respiratory distress and bronchopulmonary dysplasia in evolution: implications for antioxidant therapy. Antioxid Redox Signal 2004: 6(1): 155-167.

58. Crapo JD, Barry BE, Foscue HA, Shelburne J. Structural and biochemical changes in rat lungs occurring during exposures to lethal and adaptive doses of oxygen. Am Rev Respir Dis 1980: 122(1): 123-143.

59. Kapanci Y, Weibel ER, Kaplan HP, Robinson FR. Pathogenesis and reversibility of the pulmonary lesions of oxygen toxicity in monkeys. II. Ultrastructural and morphometric studies. Lab Invest 1969: 20(1): 101-118.

60. Crapo JD. Morphologic changes in pulmonary oxygen toxicity. Annu Rev Physiol 1986: 48: 721-731.

61. Jobe AH. Pulmonary surfactant therapy. N Engl J Med 1993: 328(12): 861-868.

62. Kinsella JP, Abman SH. Inhaled nitric oxide: current and future uses in neonates. Semin Perinatol 2000: 24(6): 387-395.

63. White CW, Jackson JH, Abuchowski A, Kazo GM, Mimmack RF, Berger EM, Freeman BA, McCord JM, Repine JE. Polyethylene glycol-attached antioxidant enzymes decrease pulmonary oxygen toxicity in rats. J Appl Physiol 1989: 66(2): 584-590.

64. Brody JS, Lahiri S, Simpser M, Motoyama EK, Velasquez T. Lung elasticity and airway dynamics in Peruvian natives to high altitude. J Appl Physiol 1977: 42(2): 245-251.

65. Tenney SM, Remmers JE. Alveolar dimensions in the lungs of animals raised at high altitude. J Appl Physiol 1966: 21(4): 1328-1330.

66. Massaro GD, Olivier J, Dzikowski C, Massaro D. Postnatal development of lung alveoli: suppression by 13% O2 and a critical period. Am J Physiol 1990: 258(6 Pt 1): L321-327.

67. Massaro D, Massaro GD. Invited Review: pulmonary alveoli: formation, the "call for oxygen," and other regulators. Am J Physiol Lung Cell Mol Physiol 2002: 282(3): L345-358.

68. Mortola JP. How newborn mammals cope with hypoxia. Respir Physiol 1999: 116(2-3): 95-103.

69. Mortola JP, Matsuoka T, Saiki C, Naso L. Metabolism and ventilation in hypoxic rats: effect of body mass. Respir Physiol 1994: 97(2): 225-234.

70. Hogan J, Smith P, Heath D, Harris P. The thickness of the alveolar capillary wall in guinea-pigs at high and low altitude. J Comp Pathol 1986: 96(2): 217-226.

71. DeGraff AC, Jr., Grover RF, Johnson RL, Jr., Hammond JW, Jr., Miller JM. Diffusing capacity of the lung in Caucasians native to 3,100 m. J Appl Physiol 1970: 29(1): 71-76.

72. Clerch LB, Baras AS, Massaro GD, Hoffman EP, Massaro D. DNA microarray analysis of neonatal mouse lung connects regulation of KDR with dexamethasone-induced inhibition of alveolar formation. Am J Physiol Lung Cell Mol Physiol 2004: 286(2): L411-419.

73. Massaro GD, Radaeva S, Clerch LB, Massaro D. Lung alveoli: endogenous programmed destruction and regeneration. Am J Physiol Lung Cell Mol Physiol 2002: 283(2): L305-309.

74. Munch IC, Markussen NH, Oritsland NA. Resting oxygen consumption in rats during food restriction, starvation and refeeding. Acta Physiol Scand 1993: 148(3): 335-340.

75. Thet LA, Delaney MD, Gregorio CA, Massaro D. Protein metabolism by rat lung: influence of fasting, glucose, and insulin. J Appl Physiol 1977: 43(3): 463-467.

76. Massaro D, Massaro GD, Baras A, Hoffman EP, Clerch LB. Calorie-related rapid onset of alveolar loss, regeneration, and changes in mouse lung gene expression. Am J Physiol Lung Cell Mol Physiol 2004: 286(5): L896-906.

77. Massaro D, Alexander E, Reiland K, Hoffman EP, Massaro GD, Clerch LB. Rapid onset of gene expression in lung, supportive of formation of alveolar septa, induced by refeeding mice after calorie restriction. Am J Physiol Lung Cell Mol Physiol 2007: 292(5): L1313-1326.

78. Adamson TM, Brodecky V, Lambert TF, Maloney JE, Ritchie BC, Walker AM. Lung liquid production and composition in the "in utero" foetal lamb. Aust J Exp Biol Med Sci 1975: 53(1): 65-75.

79. Harding R, Sigger JN, Wickham PJ, Bocking AD. The regulation of flow of pulmonary fluid in fetal sheep. Respir Physiol 1984: 57(1): 47-59.

80. Wigglesworth JS, Desai R, Hislop AA. Fetal lung growth in congenital laryngeal atresia. Pediatr Pathol 1987: 7(5-6): 515-525.

81. Richards DS, Yancey MK, Duff P, Stieg FH. The perinatal management of severe laryngeal stenosis. Obstet Gynecol 1992: 80(3 Pt 2): 537-540.

82. Hashim E, Laberge JM, Chen MF, Quillen EW, Jr. Reversible tracheal obstruction in the fetal sheep: effects on tracheal fluid pressure and lung growth. J Pediatr Surg 1995: 30(8): 1172-1177.

83. Liao SL, Luks FI, Piasecki GJ, Wild YK, Papadakis K, De Paepe ME. Late-gestation tracheal occlusion in the fetal lamb causes rapid lung growth with type II cell preservation. J Surg Res 2000: 92(1): 64-70.

84. Benachi A, Chailley-Heu B, Delezoide AL, Dommergues M, Brunelle F, Dumez Y, Bourbon JR. Lung growth and maturation after tracheal occlusion in diaphragmatic hernia. Am J Respir Crit Care Med 1998: 157(3 Pt 1): 921-927.

85. Davey MG, Hedrick HL, Bouchard S, Mendoza JM, Schwarz U, Adzick NS, Flake AW. Temporary tracheal occlusion in fetal sheep with lung hypoplasia does not improve postnatal lung function. J Appl Physiol 2003: 94(3): 1054-1062.

86. De Paepe ME, Johnson BD, Papadakis K, Sueishi K, Luks FI. Temporal pattern of accelerated lung growth after tracheal occlusion in the fetal rabbit. Am J Pathol 1998: 152(1): 179-190.

87. Unbekandt M, del Moral PM, Sala FG, Bellusci S, Warburton D, Fleury V. Tracheal occlusion increases the rate of epithelial branching of embryonic mouse lung via the FGF10-FGFR2b-Sprouty2 pathway. Mech Dev 2008: 125(3-4): 314-324.

88. Seaborn T, Khan PA, Cloutier M, Maltais F, Piedboeuf B. Short-term response to tracheal occlusion during perinatal lung development in mice. Exp Lung Res 2007: 33(8-9): 441-457.

89. Bullard KM, Sonne J, Hawgood S, Harrison MR, Adzick NS. Tracheal ligation increases cell proliferation but decreases surfactant protein in fetal murine lungs in vitro. J Pediatr Surg 1997: 32(2): 207-211; discussion 211-203.

90. Sakurai MK, Greene AK, Wilson J, Fauza D, Puder M. Pneumonectomy in the mouse: technique and perioperative management. J Invest Surg 2005: 18(4): 201-205.

91. Cagle PT, Langston C, Thurlbeck WM. The effect of age on postpneumonectomy growth in rabbits. Pediatr Pulmonol 1988: 5(2): 92-95.

92. Hsia CC, Herazo LF, Fryder-Doffey F, Weibel ER. Compensatory lung growth occurs in adult dogs after right pneumonectomy. J Clin Invest 1994: 94(1): 405-412.

93. Fehrenbach H, Voswinckel R, Michl V, Mehling T, Fehrenbach A, Seeger W, Nyengaard JR. Neoalveolarisation contributes to compensatory lung growth following pneumonectomy in mice. Eur Respir J 2008: 31(3): 515-522.

94. Hsia CC. Signals and mechanisms of compensatory lung growth. J Appl Physiol 2004: 97(5): 1992-1998.

95. Voswinckel R, Motejl V, Fehrenbach A, Wegmann M, Mehling T, Fehrenbach H, Seeger W. Characterisation of post-pneumonectomy lung growth in adult mice. Eur Respir J 2004: 24(4): 524-532.

96. Hsia CC, Fryder-Doffey F, Stalder-Nayarro V, Johnson RL, Jr., Reynolds RC, Weibel ER. Structural changes underlying compensatory increase of diffusing capacity after left pneumonectomy in adult dogs. J Clin Invest 1993: 92(2): 758-764.

97. Takeda S, Hsia CC, Wagner E, Ramanathan M, Estrera AS, Weibel ER. Compensatory alveolar growth normalizes gas-exchange function in immature dogs after pneumonectomy. J Appl Physiol 1999: 86(4): 1301-1310.

98. Peters RM, Wilcox BR, Schultz EH, Jr. Pulmonary Resection in Children: Long-Term Effect on Function and Lung Growth. Ann Surg 1964: 159: 652-660.

99. Frenckner B, Freyschuss U. Pulmonary function after lobectomy for congenital lobar emphysema and congenital cystic adenomatoid malformation. A follow-up study. Scand J Thorac Cardiovasc Surg 1982: 16(3): 293-298.

100. Wu EY, Hsia CC, Estrera AS, Epstein RH, Ramanathan M, Johnson RL, Jr. Preventing mediastinal shift after pneumonectomy does not abolish physiological compensation. J Appl Physiol 2000: 89(1): 182-191.

101. Fernandez LG, Mehta CK, Kron IL, Laubach VE. Reinitiation of compensatory lung growth after subsequent lung resection. J Thorac Cardiovasc Surg 2007: 134(5): 1300-1305.

102. Kaza AK, Cope JT, Fiser SM, Long SM, Kern JA, Tribble CG, Kron IL, Laubach VE. Contrasting natures of lung growth after transplantation and lobectomy. J Thorac Cardiovasc Surg 2002: 123(2): 288-294.

103. Brown LM, Malkinson AM, Rannels DE, Rannels SR. Compensatory lung growth after partial pneumonectomy enhances lung tumorigenesis induced by 3-methylcholanthrene. Cancer Res 1999: 59(20): 5089-5092.

104. Brown LM, Welch DR, Rannels DE, Rannels SR. Partial pneumonectomy enhances melanoma metastasis to mouse lungs. Chest 2002: 121(3 Suppl): 28S-29S.

105. Brown LM, Welch DR, Rannels SR. B16F10 melanoma cell colonization of mouse lung is enhanced by partial pneumonectomy. Clin Exp Metastasis 2002: 19(5): 369-376.

106. R_Development_Core_Team. R: A language and environment for statistical computing. R Foundation for statistical computing, Vienna, Austria, 2007.

107. Smyth G. Limma: linear models for microarray data. In: Gentleman R CV, Dudoit S, Irizarry R, Huber W, ed. Bioinformatics and computational biology solutions using R and bioconductor. Springer, New York, 2005; pp. 397-420.

108. Gentleman RC, Carey VJ, Bates DM, Bolstad B, Dettling M, Dudoit S, Ellis B, Gautier L, Ge Y, Gentry J, Hornik K, Hothorn T, Huber W, Iacus S, Irizarry R, Leisch F, Li C, Maechler M, Rossini AJ, Sawitzki G, Smith C, Smyth G,

Tierney L, Yang JY, Zhang J. Bioconductor: open software development for computational biology and bioinformatics. Genome Biol 2004: 5(10): R80.

109. Edwards D. Non-linear normalization and background correction in one-channel cDNA microarray studies. Bioinformatics 2003: 19(7): 825-833.

110. Smyth GK, Speed T. Normalization of cDNA microarray data. Methods 2003: 31(4): 265-273.

111. Smyth GK. Linear models and empirical bayes methods for assessing differential expression in microarray experiments. Stat Appl Genet Mol Biol 2004: 3: Article3.

112. Ferkingstad E, Langaas M, Lindqvist B. Estimating the proportion of true null hypotheses, with application to DNA microarray data. Journal of the Royal Statistical Society Series B 2005: 67: 555-572.

113. Fink L, Stahl U, Ermert L, Kummer W, Seeger W, Bohle RM. Rat porphobilinogen deaminase gene: a pseudogene-free internal standard for laser-assisted cell picking. Biotechniques 1999: 26(3): 510-516.

114. Livak KJ, Schmittgen TD. Analysis of relative gene expression data using real-time quantitative PCR and the 2(-Delta Delta C(T)) Method. Methods 2001: 25(4): 402-408.

115. Corti M, Brody AR, Harrison JH. Isolation and primary culture of murine alveolar type II cells. Am J Respir Cell Mol Biol 1996: 14(4): 309-315.

116. Wolff JC, Wilhelm J, Fink L, Seeger W, Voswinckel R. Comparative gene expression profiling of post-natal and post-pneumonectomy lung growth. Eur Respir J 2010: 35(3): 655-666.

117. Mariani TJ, Reed JJ, Shapiro SD. Expression profiling of the developing mouse lung: insights into the establishment of the extracellular matrix. Am J Respir Cell Mol Biol 2002: 26(5): 541-548.

118. Foster JJ, Goss KL, George CL, Bangsund PJ, Snyder JM. Galectin-1 in secondary alveolar septae of neonatal mouse lung. Am J Physiol Lung Cell Mol Physiol 2006: 291(6): L1142-1149.

119. Boucherat O, Franco-Montoya ML, Thibault C, Incitti R, Chailley-Heu B, Delacourt C, Bourbon JR. Gene expression profiling in lung fibroblasts reveals new players in alveolarization. Physiol Genomics 2007: 32(1): 128-141.

120. Silva D, Venihaki M, Guo WH, Lopez MF. Igf2 deficiency results in delayed lung development at the end of gestation. Endocrinology 2006: 147(12): 5584-5591.

121. Quaggin SE, Schwartz L, Cui S, Igarashi P, Deimling J, Post M, Rossant J. The basic-helix-loop-helix protein pod1 is critically important for kidney and lung organogenesis. Development 1999: 126(24): 5771-5783.

122. Steiglitz BM, Keene DR, Greenspan DS. PCOLCE2 encodes a functional procollagen C-proteinase enhancer (PCPE2) that is a collagen-binding protein differing in distribution of expression and post-translational modification from the previously described PCPE1. J Biol Chem 2002: 277(51): 49820-49830.

123. Moreb JS, Baker HV, Chang LJ, Amaya M, Lopez MC, Ostmark B, Chou W. ALDH isozymes downregulation affects cell growth, cell motility and gene expression in lung cancer cells. Mol Cancer 2008: 7: 87.

124. Ding X, Kaminsky LS. Human extrahepatic cytochromes P450: function in xenobiotic metabolism and tissue-selective chemical toxicity in the respiratory and gastrointestinal tracts. Annu Rev Pharmacol Toxicol 2003: 43: 149-173.

125. Yildirim AO, Veith M, Rausch T, Muller B, Kilb P, Van Winkle LS, Fehrenbach H. Keratinocyte growth factor protects against Clara cell injury induced by naphthalene. Eur Respir J 2008: 32(3): 694-704.

126. Reynolds SD, Zemke AC, Giangreco A, Brockway BL, Teisanu RM, Drake JA, Mariani T, Di PY, Taketo MM, Stripp BR. Conditional stabilization of beta-catenin expands the pool of lung stem cells. Stem Cells 2008: 26(5): 1337-1346.

127. Kotton DN, Summer RS, Sun X, Ma BY, Fine A. Stem cell antigen-1 expression in the pulmonary vascular endothelium. Am J Physiol Lung Cell Mol Physiol 2003: 284(6): L990-996.

128. Sunil VR, Patel KJ, Nilsen-Hamilton M, Heck DE, Laskin JD, Laskin DL. Acute endotoxemia is associated with upregulation of lipocalin 24p3/Lcn2 in lung and liver. Exp Mol Pathol 2007: 83(2): 177-187.

129. Gwira JA, Wei F, Ishibe S, Ueland JM, Barasch J, Cantley LG. Expression of neutrophil gelatinase-associated lipocalin regulates epithelial morphogenesis in vitro. J Biol Chem 2005: 280(9): 7875-7882.

130. Meissner A, Zilles O, Varona R, Jozefowski K, Ritter U, Marquez G, Hallmann R, Korner H. CC chemokine ligand 20 partially controls adhesion of naive B cells to activated endothelial cells under shear stress. Blood 2003: 102(8): 2724-2727.

131. Ambrosini E, Columba-Cabezas S, Serafini B, Muscella A, Aloisi F. Astrocytes are the major intracerebral source of macrophage inflammatory protein-3alpha/CCL20 in relapsing experimental autoimmune encephalomyelitis and in vitro. Glia 2003: 41(3): 290-300.

132. Hamacher-Brady A, Brady NR, Gottlieb RA. The interplay between pro-death and pro-survival signaling pathways in myocardial ischemia/reperfusion injury: apoptosis meets autophagy. Cardiovasc Drugs Ther 2006: 20(6): 445-462.

133. Maruyama R, Goto K, Takemura G, Ono K, Nagao K, Horie T, Tsujimoto A, Kanamori H, Miyata S, Ushikoshi H, Nagashima K, Minatoguchi S, Fujiwara T, Fujiwara H. Morphological and biochemical characterization of basal and starvation-induced autophagy in isolated adult rat cardiomyocytes. Am J Physiol Heart Circ Physiol 2008: 295(4): H1599-1607.

134. Adamson ED, Mercola D. Egr1 transcription factor: multiple roles in prostate tumor cell growth and survival. Tumour Biol 2002: 23(2): 93-102.

135. O'Donovan KJ, Tourtellotte WG, Millbrandt J, Baraban JM. The EGR family of transcription-regulatory factors: progress at the interface of molecular and systems neuroscience. Trends Neurosci 1999: 22(4): 167-173.

136. Yan SF, Fujita T, Lu J, Okada K, Shan Zou Y, Mackman N, Pinsky DJ, Stern DM. Egr-1, a master switch coordinating upregulation of divergent gene families underlying ischemic stress. Nat Med 2000: 6(12): 1355-1361.

137. Sureban SM, Ramalingam S, Natarajan G, May R, Subramaniam D, Bishnupuri KS, Morrison AR, Dieckgraefe BK, Brackett DJ, Postier RG, Houchen CW, Anant S. Translation regulatory factor RBM3 is a proto-oncogene that prevents mitotic catastrophe. Oncogene 2008: 27(33): 4544-4556.

138. Adams D, Larman B, Oxburgh L. Developmental expression of mouse Follistatin-like 1 (Fstl1): Dynamic regulation during organogenesis of the kidney and lung. Gene Expr Patterns 2007: 7(4): 491-500.

139. Bonapace IM, Latella L, Papait R, Nicassio F, Sacco A, Muto M, Crescenzi M, Di Fiore PP. Np95 is regulated by E1A during mitotic reactivation of terminally differentiated cells and is essential for S phase entry. J Cell Biol 2002: 157(6): 909-914.

140. Erdogan M, Pozzi A, Bhowmick N, Moses HL, Zent R. Signaling pathways regulating TC21-induced tumorigenesis. J Biol Chem 2007: 282(38): 27713-27720.

141. Warburton D, Gauldie J, Bellusci S, Shi W. Lung development and susceptibility to chronic obstructive pulmonary disease. Proc Am Thorac Soc 2006: 3(8): 668-672.

142. Wendel DP, Taylor DG, Albertine KH, Keating MT, Li DY. Impaired distal airway development in mice lacking elastin. Am J Respir Cell Mol Biol 2000: 23(3): 320-326.

143. von Kodolitsch Y, Rybczynski M, Detter C, Robinson PN. Diagnosis and management of Marfan syndrome. Future Cardiol 2008: 4(1): 85-96.

144. Sers C, Emmenegger U, Husmann K, Bucher K, Andres AC, Schafer R. Growth-inhibitory activity and downregulation of the class II tumor-suppressor gene H-rev107 in tumor cell lines and experimental tumors. J Cell Biol 1997: 136(4): 935-944.

145. Rehn AP, Cerny R, Sugars RV, Kaukua N, Wendel M. Osteoadherin is upregulated by mature osteoblasts and enhances their in vitro differentiation and mineralization. Calcif Tissue Int 2008: 82(6): 454-464.

146. Lian RH, Maeda M, Lohwasser S, Delcommenne M, Nakano T, Vance RE, Raulet DH, Takei F. Orderly and nonstochastic acquisition of CD94/NKG2 receptors by developing NK cells derived from embryonic stem cells in vitro. J Immunol 2002: 168(10): 4980-4987.

147. Ota T, Takeda K, Akiba H, Hayakawa Y, Ogasawara K, Ikarashi Y, Miyake S, Wakasugi H, Yamamura T, Kronenberg M, Raulet DH, Kinoshita K, Yagita H, Smyth MJ, Okumura K. IFN-gamma-mediated negative feedback regulation of NKT-cell function by CD94/NKG2. Blood 2005: 106(1): 184-192.

148. Ramakrishnan SN, Lau P, Crowther LM, Cleasby ME, Millard S, Leong GM, Cooney GJ, Muscat GE. Rev-erb beta regulates the Srebp-1c promoter and mRNA expression in skeletal muscle cells. Biochem Biophys Res Commun 2009: 388(4): 654-659.

149. Liu AC, Tran HG, Zhang EE, Priest AA, Welsh DK, Kay SA. Redundant function of REV-ERBalpha and beta and non-essential role for Bmal1 cycling in transcriptional regulation of intracellular circadian rhythms. PLoS Genet 2008: 4(2): e1000023.

150. Roudkenar MH, Kuwahara Y, Baba T, Roushandeh AM, Ebishima S, Abe S, Ohkubo Y, Fukumoto M. Oxidative stress induced lipocalin 2 gene expression: addressing its expression under the harmful conditions. J Radiat Res (Tokyo) 2007: 48(1): 39-44.

151. Yang J, Goetz D, Li JY, Wang W, Mori K, Setlik D, Du T, Erdjument-Bromage H, Tempst P, Strong R, Barasch J. An iron delivery pathway mediated by a lipocalin. Mol Cell 2002: 10(5): 1045-1056.

152. Goetz DH, Holmes MA, Borregaard N, Bluhm ME, Raymond KN, Strong RK. The neutrophil lipocalin NGAL is a bacteriostatic agent that interferes with siderophore-mediated iron acquisition. Mol Cell 2002: 10(5): 1033-1043.

153. Miharada K, Hiroyama T, Sudo K, Nagasawa T, Nakamura Y. Lipocalin 2 functions as a negative regulator of red blood cell production in an autocrine fashion. FASEB J 2005: 19(13): 1881-1883.

154. Leng X, Ding T, Lin H, Wang Y, Hu L, Hu J, Feig B, Zhang W, Pusztai L, Symmans WF, Wu Y, Arlinghaus RB. Inhibition of lipocalin 2 impairs breast tumorigenesis and metastasis. Cancer Res 2009: 69(22): 8579-8584.

155. Leng X, Lin H, Ding T, Wang Y, Wu Y, Klumpp S, Sun T, Zhou Y, Monaco P, Belmont J, Aderem A, Akira S, Strong R, Arlinghaus R. Lipocalin 2 is required for BCR-ABL-induced tumorigenesis. Oncogene 2008: 27(47): 6110-6119.

156. Curran T, MacConnell WP, van Straaten F, Verma IM. Structure of the FBJ murine osteosarcoma virus genome: molecular cloning of its associated helper virus and the cellular homolog of the v-fos gene from mouse and human cells. Mol Cell Biol 1983: 3(5): 914-921.

157. Durchdewald M, Angel P, Hess J. The transcription factor Fos: a Janus-type regulator in health and disease. Histol Histopathol 2009: 24(11): 1451-1461.

158. Angel P, Karin M. The role of Jun, Fos and the AP-1 complex in cell-proliferation and transformation. Biochim Biophys Acta 1991: 1072(2-3): 129-157.

159. Rauscher FJ, 3rd, Sambucetti LC, Curran T, Distel RJ, Spiegelman BM. Common DNA binding site for Fos protein complexes and transcription factor AP-1. Cell 1988: 52(3): 471-480.

160. Acquaviva C, Bossis G, Ferrara P, Brockly F, Jariel-Encontre I, Piechaczyk M. Multiple degradation pathways for Fos family proteins. Ann N Y Acad Sci 2002: 973: 426-434.

161. Okada S, Wang ZQ, Grigoriadis AE, Wagner EF, von Ruden T. Mice lacking c-fos have normal hematopoietic stem cells but exhibit altered B-cell differentiation due to an impaired bone marrow environment. Mol Cell Biol 1994: 14(1): 382-390.

162. Shiozawa S, Tanaka Y, Fujita T, Tokuhisa T. Destructive arthritis without lymphocyte infiltration in H2-c-fos transgenic mice. J Immunol 1992: 148(10): 3100-3104.

163. Zhang J, Zhang D, McQuade JS, Behbehani M, Tsien JZ, Xu M. c-fos regulates neuronal excitability and survival. Nat Genet 2002: 30(4): 416-420.

164. Sunters A, Thomas DP, Yeudall WA, Grigoriadis AE. Accelerated cell cycle progression in osteoblasts overexpressing the c-fos proto-oncogene: induction of cyclin A and enhanced CDK2 activity. J Biol Chem 2004: 279(11): 9882-9891.

165. Gerdes MJ, Myakishev M, Frost NA, Rishi V, Moitra J, Acharya A, Levy MR, Park SW, Glick A, Yuspa SH, Vinson C. Activator protein-1 activity regulates epithelial tumor cell identity. Cancer Res 2006: 66(15): 7578-7588.

166. Reichmann E, Schwarz H, Deiner EM, Leitner I, Eilers M, Berger J, Busslinger M, Beug H. Activation of an inducible c-FosER fusion protein causes loss of epithelial polarity and triggers epithelial-fibroblastoid cell conversion. Cell 1992: 71(7): 1103-1116.

167. Warburton D, Bellusci S, De Langhe S, Del Moral PM, Fleury V, Mailleux A, Tefft D, Unbekandt M, Wang K, Shi W. Molecular mechanisms of early lung specification and branching morphogenesis. Pediatr Res 2005: 57(5 Pt 2): 26R-37R.

168. Pepicelli CV, Lewis PM, McMahon AP. Sonic hedgehog regulates branching morphogenesis in the mammalian lung. Curr Biol 1998: 8(19): 1083-1086.

169. Wagner KF, Hellberg AK, Balenger S, Depping R, Dodd OJ, Johns RA, Li D. Hypoxia-induced mitogenic factor has antiapoptotic action and is upregulated in the developing lung: coexpression with hypoxia-inducible factor-2alpha. Am J Respir Cell Mol Biol 2004: 31(3): 276-282.

170. Svaren J, Sevetson BR, Apel ED, Zimonjic DB, Popescu NC, Milbrandt J. NAB2, a corepressor of NGFI-A (Egr-1) and Krox20, is induced by proliferative and differentiative stimuli. Mol Cell Biol 1996: 16(7): 3545-3553.

171. Russo MW, Sevetson BR, Milbrandt J. Identification of NAB1, a repressor of NGFI-A- and Krox20-mediated transcription. Proc Natl Acad Sci U S A 1995: 92(15): 6873-6877.

172. Cui MZ, Parry GC, Oeth P, Larson H, Smith M, Huang RP, Adamson ED, Mackman N. Transcriptional regulation of the tissue factor gene in human epithelial cells is mediated by Sp1 and EGR-1. J Biol Chem 1996: 271(5): 2731-2739.

173. Silverman ES, Collins T. Pathways of Egr-1-mediated gene transcription in vascular biology. Am J Pathol 1999: 154(3): 665-670.

174. Topilko P, Schneider-Maunoury S, Levi G, Trembleau A, Gourdji D, Driancourt MA, Rao CV, Charnay P. Multiple pituitary and ovarian defects in Krox-24 (NGFI-A, Egr-1)-targeted mice. Mol Endocrinol 1998: 12(1): 107-122.

175. Lee SL, Tourtellotte LC, Wesselschmidt RL, Milbrandt J. Growth and differentiation proceeds normally in cells deficient in the immediate early gene NGFI-A. J Biol Chem 1995: 270(17): 9971-9977.

176. Yan YX, Nakagawa H, Lee MH, Rustgi AK. Transforming growth factor-alpha enhances cyclin D1 transcription through the binding of early growth response protein to a cis-regulatory element in the cyclin D1 promoter. J Biol Chem 1997: 272(52): 33181-33190.

177. Bae SK, Bae MH, Ahn MY, Son MJ, Lee YM, Bae MK, Lee OH, Park BC, Kim KW. Egr-1 mediates transcriptional activation of IGF-II gene in response to hypoxia. Cancer Res 1999: 59(23): 5989-5994.

178. Biesiada E, Razandi M, Levin ER. Egr-1 activates basic fibroblast growth factor transcription. Mechanistic implications for astrocyte proliferation. J Biol Chem 1996: 271(31): 18576-18581.

179. Lin WF, Chen CJ, Chang YJ, Chen SL, Chiu IM, Chen L. SH2B1beta enhances fibroblast growth factor 1 (FGF1)-induced neurite outgrowth through MEK-ERK1/2-STAT3-Egr1 pathway. Cell Signal 2009: 21(7): 1060-1072.

180. Thigpen AE, Cala KM, Guileyardo JM, Molberg KH, McConnell JD, Russell DW. Increased expression of early growth response-1 messenger ribonucleic acid in prostatic adenocarcinoma. J Urol 1996: 155(3): 975-981.

181. Kramer B, Meichle A, Hensel G, Charnay P, Kronke M. Characterization of an Krox-24/Egr-1-responsive element in the human tumor necrosis factor promoter. Biochim Biophys Acta 1994: 1219(2): 413-421.

182. Nair P, Muthukkumar S, Sells SF, Han SS, Sukhatme VP, Rangnekar VM. Early growth response-1-dependent apoptosis is mediated by p53. J Biol Chem 1997: 272(32): 20131-20138.

183. Skerka C, Decker EL, Zipfel PF. A regulatory element in the human interleukin 2 gene promoter is a binding site for the zinc finger proteins Sp1 and EGR-1. J Biol Chem 1995: 270(38): 22500-22506.

184. Silins G, Grimmond S, Egerton M, Hayward N. Analysis of the promoter region of the human VEGF-related factor gene. Biochem Biophys Res Commun 1997: 230(2): 413-418.

185. Mechtcheriakova D, Wlachos A, Holzmuller H, Binder BR, Hofer E. Vascular endothelial cell growth factor-induced tissue factor expression in endothelial cells is mediated by EGR-1. Blood 1999: 93(11): 3811-3823.

186. Liu C, Adamson E, Mercola D. Transcription factor EGR-1 suppresses the growth and transformation of human HT-1080 fibrosarcoma cells by induction of transforming growth factor beta 1. Proc Natl Acad Sci U S A 1996: 93(21): 11831-11836.

187. Hocevar BA, Howe PH. Analysis of TGF-beta-mediated synthesis of extracellular matrix components. Methods Mol Biol 2000: 142: 55-65.

188. Virolle T, Adamson ED, Baron V, Birle D, Mercola D, Mustelin T, de Belle I. The Egr-1 transcription factor directly activates PTEN during irradiation-induced signalling. Nat Cell Biol 2001: 3(12): 1124-1128.

189. Baron V, Adamson ED, Calogero A, Ragona G, Mercola D. The transcription factor Egr1 is a direct regulator of multiple tumor suppressors including TGFbeta1, PTEN, p53, and fibronectin. Cancer Gene Ther 2006: 13(2): 115-124.

190. Ruoslahti E. Fibronectin and its integrin receptors in cancer. Adv Cancer Res 1999: 76: 1-20.

191. Huang RP, Liu C, Fan Y, Mercola D, Adamson ED. Egr-1 negatively regulates human tumor cell growth via the DNA-binding domain. Cancer Res 1995: 55(21): 5054-5062.

192. Chen ZH, Kim HP, Sciurba FC, Lee SJ, Feghali-Bostwick C, Stolz DB, Dhir R, Landreneau RJ, Schuchert MJ, Yousem SA, Nakahira K, Pilewski JM, Lee JS, Zhang Y, Ryter SW, Choi AM. Egr-1 regulates autophagy in cigarette smoke-induced chronic obstructive pulmonary disease. PLoS One 2008: 3(10): e3316.

193. Ning W, Li CJ, Kaminski N, Feghali-Bostwick CA, Alber SM, Di YP, Otterbein SL, Song R, Hayashi S, Zhou Z, Pinsky DJ, Watkins SC, Pilewski JM, Sciurba FC, Peters DG, Hogg JC, Choi AM. Comprehensive gene expression profiles reveal pathways related to the pathogenesis of chronic obstructive pulmonary disease. Proc Natl Acad Sci U S A 2004: 101(41): 14895-14900.

194. Chen ZH, Kim HP, Ryter SW, Choi AM. Identifying targets for COPD treatment through gene expression analyses. Int J Chron Obstruct Pulmon Dis 2008: 3(3): 359-370.

195. Reynolds PR, Cosio MG, Hoidal JR. Cigarette smoke-induced Egr-1 upregulates proinflammatory cytokines in pulmonary epithelial cells. Am J Respir Cell Mol Biol 2006: 35(3): 314-319.

196. Ngiam N, Post M, Kavanagh BP. Early growth response factor-1 in acute lung injury. Am J Physiol Lung Cell Mol Physiol 2007: 293(5): L1089-1091.

197. Copland IB, Post M. Stretch-activated signaling pathways responsible for early response gene expression in fetal lung epithelial cells. J Cell Physiol 2007: 210(1): 133-143.

198. Bode W, Engh R, Musil D, Thiele U, Huber R, Karshikov A, Brzin J, Kos J, Turk V. The 2.0 A X-ray crystal structure of chicken egg white cystatin and its possible mode of interaction with cysteine proteinases. EMBO J 1988: 7(8): 2593-2599.

199. Keppler D. Towards novel anti-cancer strategies based on cystatin function. Cancer Lett 2006: 235(2): 159-176.

200. Rivenbark AG, Coleman WB. Epigenetic regulation of cystatins in cancer. Front Biosci 2009: 14: 453-462.

201. Scott DK, Lord R, Muller HK, Malley RC, Woods GM. Proteomics identifies enhanced expression of stefin A in neonatal murine skin compared with adults: functional implications. Br J Dermatol 2007: 156(6): 1156-1162.

202. Turk V, Bode W. The cystatins: protein inhibitors of cysteine proteinases. FEBS Lett 1991: 285(2): 213-219.

203. Takahashi M, Tezuka T, Katunuma N. Inhibition of growth and cysteine proteinase activity of Staphylococcus aureus V8 by phosphorylated cystatin alpha in skin cornified envelope. FEBS Lett 1994: 355(3): 275-278.

204. Dubin G. Proteinaceous cysteine protease inhibitors. Cell Mol Life Sci 2005: 62(6): 653-669.

205. Kopitar-Jerala N. The role of cystatins in cells of the immune system. FEBS Lett 2006: 580(27): 6295-6301.

206. van Eijk M, van Noorden CJ, de Groot C. Proteinases and their inhibitors in the immune system. Int Rev Cytol 2003: 222: 197-236.

207. van Eijk M, de Groot C. Germinal center B cell apoptosis requires both caspase and cathepsin activity. J Immunol 1999: 163(5): 2478-2482.

208. Chapman HA. Endosomal proteases in antigen presentation. Curr Opin Immunol 2006: 18(1): 78-84.

209. Mihelic M, Teuscher C, Turk V, Turk D. Mouse stefins A1 and A2 (Stfa1 and Stfa2) differentiate between papain-like endo- and exopeptidases. FEBS Lett 2006: 580(17): 4195-4199.

210. Verdot L, Lalmanach G, Vercruysse V, Hoebeke J, Gauthier F, Vray B. Chicken cystatin stimulates nitric oxide release from interferon-gamma-activated mouse

peritoneal macrophages via cytokine synthesis. Eur J Biochem 1999: 266(3): 1111-1117.

211. Leung-Tack J, Tavera C, Gensac MC, Martinez J, Colle A. Modulation of phagocytosis-associated respiratory burst by human cystatin C: role of the N-terminal tetrapeptide Lys-Pro-Pro-Arg. Exp Cell Res 1990: 188(1): 16-22.

212. Hartmann S, Kyewski B, Sonnenburg B, Lucius R. A filarial cysteine protease inhibitor down-regulates T cell proliferation and enhances interleukin-10 production. Eur J Immunol 1997: 27(9): 2253-2260.

213. Kuopio T, Kankaanranta A, Jalava P, Kronqvist P, Kotkansalo T, Weber E, Collan Y. Cysteine proteinase inhibitor cystatin A in breast cancer. Cancer Res 1998: 58(3): 432-436.

214. Mirtti T, Alanen K, Kallajoki M, Rinne A, Soderstrom KO. Expression of cystatins, high molecular weight cytokeratin, and proliferation markers in prostatic adenocarcinoma and hyperplasia. Prostate 2003: 54(4): 290-298.

215. Bianchi F, Hu J, Pelosi G, Cirincione R, Ferguson M, Ratcliffe C, Di Fiore PP, Gatter K, Pezzella F, Pastorino U. Lung cancers detected by screening with spiral computed tomography have a malignant phenotype when analyzed by cDNA microarray. Clin Cancer Res 2004: 10(18 Pt 1): 6023-6028.

216. Boike G, Lah T, Sloane BF, Rozhin J, Honn K, Guirguis R, Stracke ML, Liotta LA, Schiffmann E. A possible role for cysteine proteinase and its inhibitors in motility of malignant melanoma and other tumour cells. Melanoma Res 1992: 1(5-6): 333-340.

217. Li W, Ding F, Zhang L, Liu Z, Wu Y, Luo A, Wu M, Wang M, Zhan Q. Overexpression of stefin A in human esophageal squamous cell carcinoma cells inhibits tumor cell growth, angiogenesis, invasion, and metastasis. Clin Cancer Res 2005: 11(24 Pt 1): 8753-8762.

218. Obermajer N, Jevnikar Z, Doljak B, Kos J. Role of cysteine cathepsins in matrix degradation and cell signalling. Connect Tissue Res 2008: 49(3): 193-196.

219. Kuester D, Lippert H, Roessner A, Krueger S. The cathepsin family and their role in colorectal cancer. Pathol Res Pract 2008: 204(7): 491-500.

220. Shi GP, Villadangos JA, Dranoff G, Small C, Gu L, Haley KJ, Riese R, Ploegh HL, Chapman HA. Cathepsin S required for normal MHC class II peptide loading and germinal center development. Immunity 1999: 10(2): 197-206.

221. Roth W, Deussing J, Botchkarev VA, Pauly-Evers M, Saftig P, Hafner A, Schmidt P, Schmahl W, Scherer J, Anton-Lamprecht I, Von Figura K, Paus R,

Peters C. Cathepsin L deficiency as molecular defect of furless: hyperproliferation of keratinocytes and pertubation of hair follicle cycling. FASEB J 2000: 14(13): 2075-2086.

222. Saftig P, Hunziker E, Wehmeyer O, Jones S, Boyde A, Rommerskirch W, Moritz JD, Schu P, von Figura K. Impaired osteoclastic bone resorption leads to osteopetrosis in cathepsin-K-deficient mice. Proc Natl Acad Sci U S A 1998: 95(23): 13453-13458.

223. Berchem G, Glondu M, Gleizes M, Brouillet JP, Vignon F, Garcia M, Liaudet-Coopman E. Cathepsin-D affects multiple tumor progression steps in vivo: proliferation, angiogenesis and apoptosis. Oncogene 2002: 21(38): 5951-5955.

Appendices

A Declaration

"I declare that I have completed this dissertation single-handedly without the unauthorized help of a second party and only with the assistance acknowledged therein. I have appropriately acknowledged and referenced all text passages that are derived literally from or are based on the content of published or unpublished work of others, and all information that relates to verbal communications. I have abided by the principles of good scientific conduct laid down in the charter of the Justus Liebig University of Giessen in carrying out the investigations described in the dissertation."

_____

Jens-Christian Wolff, MD

B List of publications

MD thesis:

"Untersuchungen zur molekularen Expression des granulozytären Glykoproteins NB1 (CD177) bei Gesunden und ausgewählten Patienten-Kollektiven", **May 2005, *VVB Laufersweiler Verlag*; ISBN: 978-3896874368**

Peer-reviewed papers:

1. **Wolff J**, Brendel C, Fink L, Bohle RM, Kissel K, Bux J. Lack of NB1 GP (CD177/HNA-2a) gene transcription in NB1 GP- neutrophils from NB1 GP-expressing individuals and association of low expression with NB1 gene polymorphisms. ***Blood* 2003**: 102(2): 731-733.
2. Gohring K*, **Wolff J***, Doppl W, Schmidt KL, Fenchel K, Pralle H, Sibelius U, Bux J. Neutrophil CD177 (NB1 gp, HNA-2a) expression is increased in severe bacterial infections and polycythaemia vera. ***Br J Haematol* 2004**: 126(2): 252-254. * contributed equally
3. **Wolff JC**, Goehring K, Heckmann M, Bux J. Sex-dependent up regulation of CD 177-specific mRNA expression in cord blood due to different stimuli. ***Transfusion* 2006**: 46(1): 132-136.
4. Voswinckel R, Ahlbrecht K, **Wolff JC**, Weissmann N, Fehrenbach H, Yildirim AO, Grimminger F, Seeger W. [Pulmonary tissue regeneration -- a hope for the future]. ***Dtsch Med Wochenschr* 2006**: 131(16): 865-868.
5. Wolff S, Klatt S, **Wolff JC**, Wilhelm J, Fink L, Kaps M, Rosengarten B. Endotoxin-induced gene expression differences in the brain and effects of iNOS inhibition and norepinephrine. ***Intensive Care Med* 2009**: 35(4): 730-739.
6. Dierkes C, Kreisel M, Schulz A, Steinmeyer J, **Wolff JC**, Fink L. Catabolic properties of microdissected human endosteal bone lining cells. ***Calcif Tissue Int* 2009**: 84(2): 146-155.
7. Laumanns IP, Fink L, Wilhelm J, **Wolff JC**, Mitnacht-Kraus R, Graef-Hoechst S, Stein MM, Bohle RM, Klepetko W, Hoda MA, Schermuly RT, Grimminger F, Seeger W, Voswinckel R. The noncanonical WNT pathway is operative in idiopathic pulmonary arterial hypertension. ***Am J Respir Cell Mol Biol* 2009**: 40(6): 683-691.
8. **Wolff JC**, Wilhelm J, Fink L, Seeger W, Voswinckel R. Comparative gene expression profiling of post-natal and post-pneumonectomy lung growth. ***Eur Respir J* 2010**: 35(3): 655-666.

C Acknowledgements

First of all, I would like to cordially thank Prof. Dr. Ludger Fink and Dr. Robert Voswinckel for the competent supervision in this project and for productive discussions about methodological approaches as well as with regards to content. Additionally, I want to thank both of them and Prof. Dr. Werner Seeger for offering lab space, proper equipment and financial supplies and for giving me the opportunity to learn a lot about science in the lab and in the MBML graduate programme.

Next, I would like to thank Dr. Jochen Wilhelm, who did all of the statistical analyses for the project and with whom I had many fruitful discussions about numerous fascinating topics.

I always felt very comfortable in my old lab in pathology; acknowledging all of the team there, I would like to especially emphasize Dr. Grazyna Kwapiszewska-Marsh and Marlene Stein, who both were really helpful not only in technical aspects.

Many thanks to Ulrike Seay for introducing me into the field of cell culture and to Dr. Vandana Nikam, who supported me in flow cytometry experiments.

I would like to thank Prof. Dr. Oliver Eickelberg for giving me the opportunity and the equipment to perform cloning experiments in his lab; special thanks to Dr. Anna Zakrzewicz for teaching me the appropriate techniques!

Finally, I would like to cordially thank Diana Fuchs for her skilful technical support in the complicated field of in-situ hybridizations and Sven Becker for assisting me in hard- and software problems.

Der Lebenslauf wurde aus der elektronischen Version der Arbeit entfernt.

The curriculum vitae was removed from the electronic version of the paper.

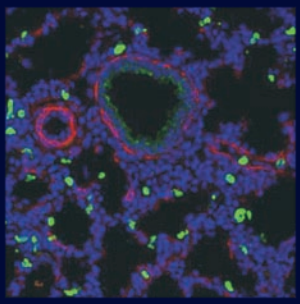

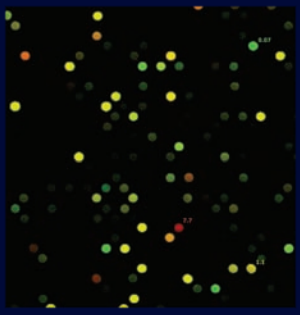

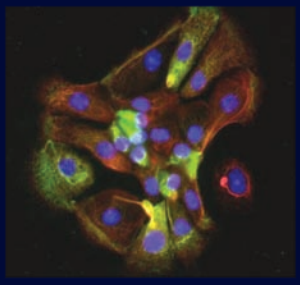

VVB LAUFERSWEILER VERLAG

VVB LAUFERSWEILER VERLAG
STAUFENBERGRING 15
D-35396 GIESSEN

Tel: 0641-5599888 Fax: -5599890
redaktion@doktorverlag.de
www.doktorverlag.de

ISBN: 978-3-8359-5611-7